KIT SCIENTIFIC REPORTS 7564

Modelling of Multi-Component Plasma for TOKES

Yuri Igitkhanov

KIT Scientific Publishing

Yuri Igitkhanov

Modelling of Multi-Component Plasma for TOKES

Karlsruhe Institute of Technology
KIT SCIENTIFIC REPORTS 7564

Modelling of Multi-Component Plasma for TOKES

by
Yuri Igitkhanov

KIT Scientific Publishing

Report-Nr. KIT-SR 7564

Impressum

Karlsruher Institut für Technologie (KIT)
KIT Scientific Publishing
Straße am Forum 2
D-76131 Karlsruhe
www.ksp.kit.edu

KIT – Universität des Landes Baden-Württemberg und nationales
Forschungszentrum in der Helmholtz-Gemeinschaft

KIT Scientific Publishing 2011
Print on Demand

ISSN 1869-9669

Table of content

Abstract

The transport models in multi-component tokamak plasma with various impurity ions are discussed here for implementation in the tokamak integrated code TOKES. Impurity transport in the core and boundary plasma of a tokamak is a crucial issue for a fusion reactor device like ITER and DEMO. In steady state reactor operation the tokamak bulk plasma can be contaminated by intrinsic impurities, which can considerably affect the confinement time and bring about the burning plasma dilution. The impurities are originated due to erosion of plasma-facing components and, particularly, during the transient processes like repetitive ELMs, small disruptions etc. Mitigation of ELMs can relax the power loading on PSCs and the problem of core plasma contamination. However, it is still remains unclear to which extend these ELMs must be reduced in order to have a moderate erosion of divertor plates due to physical sputtering during the long-pulse reactor operation to avoid intolerable accumulation of impurities in the core. Impurities, originated at the plate can migrate through the SOL and penetrate through pedestal region into balk plasma. Effect of impurity screening due to ELMs repulsive force (entraining effect) can protect balk plasma from impurities.

The transport features in tokamak plasma in the presence of arbitrary concentration of various impurity species in different charge state are investigated. Impurity behaviour in the balk and boundary plasma can be simulated in the frame of the integrated code TOKEs. Recently the code was considerably updated [1]. The neoclassical and anomalous transport coefficients where implemented in balk plasma and the pedestal region together with ELM model. The SOL and divertor region were elaborated. These improvements and the impurity transport models, described here will enable a self-consistent simulation of impurity dynamic in muli-component complex plasma, where impurity ions dominate and determine the transport properties.

The various transport models for multi-component plasma have been reviewed and proper equations, describing a multi-component plasma transport have been suggested for implementation in the integrated code TOKES.

In the frame of the Contract the following tasks have been completed:

- Analytical models of the multi-fluid 1D impurity equations (in the frame of Grad and the Chapmen-Enscog methods) are derived and analysed. The models describe the dynamic of impurity ions of arbitrary charge state in the SOL and divertor region.
- The Reduce Charge State procedure was elaborate to decrease the number of fluid equations in the SOL for impurity ions of each charge state to the equations of only nucleus. Source of impurity ions due to the plasma flux impinging the tungsten divertor plates can be self-consistently calculated.
- Boundary conditions for impurity ions flows at the separatrix and at the chamber wall are formulated and can easily be implemented into the code.
- Simulation of drifts in transport equations is introduced. Drifts can affect the spatial distribution of extrinsic impurities, lunched into plasma for disruption mitigation.
- The modelling of neutral atoms in tokamak boundary plasma is suggested in the frame of fluid approximation.
- Sputtering of the first wall and divertor plates in multi-component plasma in the presence of impurity ions and the secondary electron emission is self-consistently described.

Zusamenfassung

Thema dieser Arbeit ist die Betrachtung von Transportmodellen für Multi-Komponenten-Plasmen mit verschiedenen Verunreinigungen zur Implementierung im Tokamak-Simulationsprogramm TOKES. The Verunreinigungstransport im zentralen Plasma und im Plasma-Randbereich ist von entscheidender Bedeutung für Fusionsreaktoren wie ITER und DEMO. Intrinsische Verunreinigungen im zentralen Plasma eines Tokamaks können bei stationärem Betrieb signifikant die Einschlusszeit beeinflussen und führen zur Verdünnung des Fusionsbrennstoffes. Diese Verunreinigungen werden durch Erosion an den dem Plasma zugewandten Materialoberflächen gebildet. Dabei können transiente Prozesse wie die sich wiederholenden ELMs und kleine Disruptionen eine bedeutende Rolle spielen. Eine Abschwächung der ELMs kann den Leistungseintrag auf die Erste Wand und das Problem der Plasmaverunreinigung verringern. Es ist aber noch nicht klar, wie stark diese Abschwächung und Reduzierung der ELMs erfolgen müssen, damit die physikalische Zerstäubung auf den Divertorplatten unter Langpuls-Bedingungen akzeptabel bleibt und nichttolerierbare Verunreinigungskonzentrationen im zentralen Plasma vermieden werden können. Verunreinigungen, die von den Divertorplatten erodiert werden, können durch die SOL und die Piedestal-Region in das zentrale Plasma gelangen. Der Abschirmungseffekt durch die abstoßenden Kräfte der sich regelmäßig wiederholenden ELMs (Mitnahme-Effekt) kann das zentrale Plasma vor den Verunreinigungen bewahren.

Die besonderen Transportprozesse in einem Tokamak-Plasma bei Vorhandensein beliebiger Konzentrationen verschiedener Verunreinigungs-Spezies in unterschiedlichen Ladungszuständen wurden untersucht. Das Verhalten der Verunreinigungen im zentralen Plasma und im Plasma-Randbereich kann mit Hilfe des Programms TOKES simuliert werden. Dieses Programm wurde kürzlich bedeutend erweitert [1]. Neoklassische und anomale Transportkoeffizienten wurden für das zentrale Plasma und das Randschichtplasma implementiert und ein ELM Model integriert. Insbesondere wurden die SOL und der Divertor-Bereich untersucht. Diese hier beschriebenen Verbesserungen erlauben eine selbstkonsistente Simulation der Verunreinigungs-Dynamik in einem Multi-Komponenten-Plasma, in dem die Verunreinigungsionen die Transportprozesse dominieren.

Die verschiedenen Transportmodelle für ein Multi-Komponenten-Plasma wurden analysiert und geeignete Gleichungen zur Implementierung in das Programm TOKES entwickelt.

Im Rahmen des Vertrags wurden die folgenden Aufgaben abgeschlossen.

- Analytische Modelle der 1D Mehrflüssigkeitsgleichungen der Verunreinigungen wurden abgeleitet und analysiert (mit Hilfe der Grad- und Chapmen-Enscog Methoden). Die Modelle beschreiben die Dynamik der Verunreinigungen beliebigen Ladungszustandes in der SOL und im Divertor-Bereich.
- Die Prozedur der Ladungszustands-Reduktion wurde angewandt, um die Anzahl der Gleichungen im Mehrflüssigkeitsbild der Verunreinigungen mit vielen Ladungszuständen auf die Gleichungen für nur jeweils unterschiedliche Verunreinigungselemente zu reduzieren. Die Verunreinigungsquelle aufgrund der Zerstäubung der Divertorplatten aus Wolfram kann selbstkonsistent berechnet werden.
- Die Randbedingungen für die Verunreinigungsionen an der Separatrix und an den Materialoberflächen der ersten Wand wurden formuliert und sind einfach im Programm zu implementieren.
- Simulationen von Driften in den Transportgleichungen sind eingeführt worden. Diese Driften können die räumliche Verteilung von Verunreinigungen beeinflussen, die z.B. für die Abschwächung und Verhinderung von Disruptionen von außen eingebracht werden.
- Die Modellierung von neutralen Atomen im Randschichtplasma eines Tokamaks wird im Rahmen der Flüssigkeits-Betrachtung vorgeschlagen.
- Die Zerstäubung an den Materialoberflächen der ersten Wand und der Divertorplatten in einem Multi-Komponenten-Plasma und bei Berücksichtigung von Sekundär-Elektronenemission ist selbstkonsistent beschrieben.

Introduction

In the field of plasma-edge modeling, there has been much resent interest in obtaining various transport models which adequately account for the effects of impurities in contamination of fusion plasma and mitigation of disruption events in reactor plasma. During the transient processes like ELM and pre-emptive disruption mitigation by intensive gas puffing the boundary plasma becomes strongly mixed with neutral atoms and impurity ions of different species in various charge states. This multi-component mixture reviles its own specific properties, which require a special description. Below two approaches for multi-component plasma are suggested for the SOL and bulk plasma region as a possible approach for numerical implementation in integrated code TOKES [2-5]. There are two types of equations: for each charge state of species and the equations, describing plasma as a whole. For partial quantities, it is convenient to work in the coordinate system of reference where the whole plasma does not move.

The two-dimensional transport equations are presented to simulate multi-species plasma in curvilinear configuration. The equations are a direct extension of Braginskii equations for electrons and single ionic species to a multiple case. The equations are of Navier-Stokes form as regards the parallel flow along B and of a diffusive form in the radial direction.

The transport equations and corresponding kinetic coefficients for multi-component plasma in 1-D can be written in the moment approximation directly related to the 21-moment Grad method, which can be naturally generalized to the plasma with many impurity species in different charge states. Here we will derive the 21-moment equations, which being equivalent to Braginskii ones, but having an advantage to be the first order differential equations. Moreover, this system is inherently can be generalized to account for the kinetic effects in the SOL region.

The Braginskii equations are based on Chapman-Enscogo approximation. In this approximation the equations for coefficients are truncated by some iteration procedure, where all coefficients (or moments) the higher order are expressed through the low moments n_α, u, T_α and its partial derivatives.

In the Grad method the equations for coefficients are truncated based on assumption that for each system of equation of the order k the distribution function can be approximated in series, where the coefficients of higher order than k assumed to be zero. This allows one to close the system of equations. The difference in results obtained by these two methods for multi-component

plasma becomes negligible in the case when the 21-moments approach is used. The difference between the Chapman-Enscogo and the Grad methods is also in the choice of reference coordinate system. The moment equations in Grad method are derived in a centre of mass frame of reference, which has an advantage of having a simplified evolution of the collision integral. Braginskii uses a multiple set of velocity reference frames, one for each species, corresponding to the mean mass velocity of each species. This has an advantage of reducing the number of terms in the fluid equations, but complicates a rigorous calculation of the collisional terms, along with relationships of energy conservation due to collisions.
Both sets of equations are presented here for implementation in TOKEs.

The presence of several different multiply charged ions in the divertor plasma increases immensely the number of equation to be solved. The fluid equations for separate charge states of a given isotope can be replaced by a set of averaged equations representing an effective single reduced charge state. These equations are fewer in number than the original equations for the individual ions by a factor of $Z_{\max}$ for each species α. This Reduce Charge State approach, suggested here for implementation in TOKES, was incorporated into B2 Code allowing one to simulate divertor and the SOL plasmas with multiple ion species plasma without excessive time consumption.

Classical particle drifts across the magnetic field can play an important role in tokamak edge-plasma transport. The relative influence of these terms is important for self-consistent simulations by including them, together with anomalous diffusion transport, in a 2-D fluid model of edge-plasma transport for the tokamak geometry. The drifts cause asymmetries in the plasma equilibrium which depend on the direction of the magnetic field, B. Here transport equations are complemented by drifts and some results are presented, showing how drifts modifying plasma density and temperature distribution near the divertor plates.

In this report the sheath potential formation at the divertor plates in the presence of impurity ions and of secondary electron emission is self-consistently considered. This is important for simulation of boundary plasma in the case of multi-component species at the vicinity to the divertor plate. It is shown that the sputtering at the plate or limiter can increase the potential drop, when impurities cause strong increases of electron upstream density. Impurity flux to the target as far as the secondary electron emission (SEE) from the target can only reduce the potential drop. The SEE yield saturates due to space charge limitations and cannot be used to reduce completely the unfavourable effect on sputtering yield of the acceleration by the potential drop even when a dilution effect of positive impurity ions is taken into account.

It is now recognized that the lifetime of a tokamak reactor is determined by damage of structural elements facing the plasma (e.g. the first wall and divertor plates). For this reason, it is important to

obtain the most accurate estimates of erosion rates for these elements. Available experimental data applied to steady state or long pulse operation indicate that the first wall erosion rate is due mainly to charge exchange neutral sputtering, and that fuel and impurity ion physical sputtering (particularly self-sputtering) determines the erosion rate of divertor plates. The sputtering yields averaged over the distribution function and over the projectile incident angle have been obtained for some candidate target materials (C, Al, Ti, Fe, MO, W) and incident deuterium and tritium ions. It is shown here that the sputtering yield increases if the sheath potential is taken into account and that the usual estimation of the sputtering yield at energy $E = 3.5Z_j T_e$ is underestimates the yield value.

The effect of neutral atoms is not included in standard tokamak transport treatments. However, it is clear that neutral atoms in the tokamak edge can influence global confinement by affecting the transition from low to high confinement. The physical mechanism by which this occurs is not yet clearly identified, but it is well known that neutrals influence ion dynamics through charge-exchange interactions. Furthermore, the radial neutral flux of toroidal angular momentum can modify or even determine the edge radial electric field and plasma rotation. The radial localization of the neutrals also introduces a shear in the flow that may affect edge turbulence. Neutral atoms play an essential role in momentum transfer from the plasma to the wall, thereby facilitating the transition from attached to detach operation regime with increasing input power. They can also play an important role in mitigation of ELMs and runaway electrons. In this report several models of neutral atoms transport in boundary plasma and in the SOL is considered.

Some additional issues were also considered in this report and are presented in attachments. These concerns the derivation of frictional and thermal forces in complex plasma, expressions for Coulomb collision frequencies in multi-species plasma, the origin of plasma rotation in poloidal direction, the quasi-dynamic transport across B, the explanation of the origin of 5/2 term in the energy balance equation in the case of current-less plasma, compendium of atomic data for Ar and Ne, needed for our tacks and, finally, the numerical program written in FORTRAN for neutral atoms.

I. Transport in complex plasma-main definitions and transport equations

We start first with the basic definitions and conservation equations. The main assumption hereafter is that the fluid approach is justified in the relative cold and dense plasma of interest. We will consider a reactor plasma of electrons and arbitrary number of ion species α, β of different mass m_α, m_β and in different charge states, Z and ξ, correspondingly. These ion species include atoms ($Z, \xi = 0$) and deuterium and tritium hydrogen isotopes. The former can be taken in equal proportion (deuterons). The kinetic equation for α species in Z charge stage reads:

$$\frac{\partial f_{\alpha z}}{\partial t} + (V_{\alpha z}\nabla) f_{\alpha z} + \frac{(F_{\alpha z}\nabla_V f_{\alpha z})}{m_\alpha} = \sum_{\beta,\xi} St_{\alpha z,\beta\xi}\,, \tag{I.1}$$

where

∇_V is the gradient in velocity space, $St_{\alpha z,\beta\xi}$ is the collisional term and $F_{\alpha z}$ is the force

$$F_{\alpha z} = eZ(E + [VB]) \tag{I.2}$$

We introduce the current velocity, c, and diffusive velocities:

$$w_{\alpha z} = u_{\alpha z} - u_\alpha \quad \text{and} \quad w_\alpha = u_\alpha - u \tag{I.3}$$

We will distinguish the macroscopic parameters of each particular component in its charge state, the species and the plasma as a whole.

Densities:

$$n_{\alpha z} = \int f_{\alpha z} d\mathrm{V}\,, \qquad n_\alpha = \sum_z n_{\alpha z} \qquad \text{and} \qquad n = \sum_\alpha n_\alpha\,, \tag{I.4}$$

$$\rho_{\alpha z} = m_\alpha n_{\alpha z}\,, \qquad \rho_\alpha = m_\alpha n_\alpha \qquad \text{and} \qquad \rho = \sum_\alpha \rho_\alpha \tag{I.5}$$

Velocities:

$$\mathrm{u}_{\alpha z} = \frac{1}{n_{\alpha z}} \int \mathrm{V} f_{\alpha z} d\mathrm{V}\,, \quad \mathrm{u}_\alpha = \frac{1}{\rho_\alpha} \sum_z \rho_{\alpha z} \mathrm{u}_{\alpha z} \quad \text{and} \quad \mathrm{u} = \frac{1}{\rho} \sum_\alpha \rho_\alpha \mathrm{u}_\alpha\,, \tag{I.6}$$

Temperatures:

$$\frac{3}{2} n_{\alpha z} T_{\alpha z} = \frac{m_\alpha}{2} \int (\mathrm{V} - \mathrm{u})^2 f_{\alpha z} d\mathrm{V}\,, \qquad n_\alpha T_\alpha = \sum_z n_{\alpha z} T_{\alpha z} \quad \text{and} \quad nT = \sum_\alpha n_\alpha T_\alpha \tag{I.7}$$

The mass flow:

$$m_\alpha \Gamma_{\alpha z} = \rho_{\alpha z} w_{\alpha z} = m_\alpha \int c f_{\alpha z} dV\,, \qquad m_\alpha \Gamma_\alpha = \rho_\alpha w_\alpha \tag{I.8}$$

From definition of mass average velocity, u it follows that

$$\sum_z \rho_{\alpha z} w_{\alpha z} = \sum_z \rho_{\alpha z} (u_{\alpha z} - u_\alpha) = 0\,, \qquad \sum_\alpha \rho_\alpha w_\alpha = \sum_\alpha \rho_\alpha (u_\alpha - u) = 0 \tag{I.9}$$

Partial and total pressure tensor(r,s components):

$$P_{\alpha z}^{rs} = m_\alpha \int c_r c_s f_{\alpha z} dV \quad , \quad P_\alpha^{rs} = \sum_z P_{\alpha z}^{rs} \quad \text{and} \quad P^{rs} = \sum_\alpha P_\alpha^{rs} \tag{I.10}$$

$$P_{\alpha z}^{rs} = p_{\alpha z}\delta_{rs} + \pi_{\alpha z}^{rs} , \qquad P_\alpha^{rs} = p_\alpha \delta_{rs} + \pi_\alpha^{rs} \quad \text{and} \quad P^{rs} = p\ \delta_{rs} + \pi^{rs} \tag{I.11}$$

Pressure:

$$p_{\alpha z} = n_{\alpha z} T_{\alpha z} = \frac{m_\alpha}{2}\int c^2 f_{\alpha z} dV , \quad p_\alpha = n_\alpha T_\alpha \quad \text{and} \quad p = \sum_\alpha n_\alpha T_\alpha = nT \tag{I.12}$$

Viscosity:

$$\pi_{\alpha z}^{rs} = m_\alpha \int (c_r c_s - \frac{1}{3}\delta_{rs} c^2) f_\alpha d\ V, \qquad \pi_\alpha^{rs} = \sum_z \pi_{\alpha z}^{rs} \quad \text{and} \quad \pi^{rs} = \sum_\alpha \pi^{rs} \tag{I.13}$$

Partial and total heat flues:

$$q_{\alpha z} = \frac{m_\alpha}{2}\int c c^2 f_{\alpha z} dV , \qquad q_\alpha = \sum_z q_{\alpha z} \quad \text{and} \quad q = \sum_\alpha q_\alpha \tag{I.14}$$

I.1 The partial equations for arbitrary species and charge states

There are two types of equations: the partial equations for each charge state of species and the equations, describing plasma as a whole. For partial quantities, it is convenient to work in the coordinate system of reference where the whole plasma does not move. For this purpose it is convenient to present the current velocity of specie, c, as $\mathrm{c} = \mathrm{V} - \mathrm{u}$, so that an average of $\langle \mathrm{c} \rangle$ equals zero ($\langle \mathrm{u} \rangle = \mathrm{V}$). In this variable kinetic equation reads:

$$\frac{\partial f_{\alpha z}}{\partial t} + (c_{\alpha z}\nabla) f_{\alpha z} + \frac{\left(F_{\alpha z} - \dfrac{d\mathrm{u}}{dt}\right)}{m_\alpha}\nabla_V f_{\alpha z} - c_{\alpha z}^s \frac{\partial f_{\alpha z}}{\partial c_r}\frac{\partial f_{\alpha z}}{\partial c_s} = \sum_{\beta,\xi} St_{\alpha z,\beta\xi} \tag{I.15}$$

The fluid equations for macroscopic plasma parameters can be derived from the kinetic equation by multiplying it on some dynamic variable $\psi_\alpha(\mathrm{V},\mathrm{r},t))$ and integrating over the velocity space. For α type specie in Z charge state the fluid transport equation reads [6]:

$$\left(\frac{\partial}{\partial t} + \mathrm{u}\nabla\right) n_{\alpha z}\langle \psi_{\alpha z}\rangle + n_{\alpha z}\langle \psi_{\alpha z}\rangle \nabla \mathrm{u} + \nabla n_{\alpha z}\langle \psi_{\alpha z}\mathrm{c}\rangle - n_{\alpha z}\Sigma_{\alpha z} = \sum_{\beta,\xi}\int \psi_{\alpha z} St_{\alpha z,\beta\xi} d\mathrm{c} \tag{I.16}$$

where

$$\Sigma_{\alpha z} \equiv \left\{\left\langle \frac{\partial \psi_{\alpha z}}{\partial t}\right\rangle + \langle \mathrm{c}\nabla\psi_{\alpha z}\rangle + \left\langle \left(F_{\alpha z}/m_{\alpha z} - \left(\frac{\partial}{\partial t} + \mathrm{u}\nabla\right)\mathrm{u}\right)\nabla\psi_{\alpha z} - \left\langle c_s \frac{\partial \psi_{\alpha z}}{\partial c_r}\right\rangle \frac{\partial u_r}{\partial c_s}\right\rangle\right\} \tag{I.17}$$

Here $\langle \psi_{\alpha z}\rangle$ indicates the averaging procedure

$$n_{\alpha z}\langle \psi_{\alpha z}\rangle = \int \psi_{\alpha z} f_{\alpha z} d\mathrm{c} \tag{I.18}$$

and $f_{\alpha z}$ is the distribution function of α species in Z charge state, chosen as a Maxwellian one. Choosing in conservation equation above $\psi_{\alpha z} = m_\alpha,\quad m_\alpha \mathrm{c}$ and $(m_\alpha c^2/2)$ correspondingly, we coming to the partial equations for arbitrary specie α in arbitrary charge state Z.

- *particle continuity:*

$$\frac{d\rho_{\alpha z}}{dt} + \rho_{\alpha z}\frac{\partial u_\alpha^r}{\partial x_r} + \frac{\partial \rho_{\alpha z} w_{\alpha z}^r}{\partial x_r} = S_{\alpha z} \qquad or \qquad \frac{d\rho_{\alpha z}}{dt} + \rho_{\alpha z} div(\mathrm{u}_\alpha) + div\left(\rho_{\alpha z}\mathrm{w}_{\alpha\xi}\right) = S_{\alpha z} \tag{I.19}$$

- *momentum*

$$\frac{d\rho_{\alpha z} w_{\alpha z}^r}{dt} + \rho_{\alpha z}\frac{du_\alpha^r}{dt} + \rho_{\alpha z} w_{\alpha z}^r \frac{\partial u^s}{\partial x_s} + \rho_{\alpha z} w_{\alpha z}^s \frac{\partial u^r}{\partial x_s} + \frac{\partial P_{\alpha z}^{rs}}{\partial x_s} - n_{\alpha z} eZ(E^r + [\mathrm{u}_{\alpha z}\mathrm{B}]_r) = R_{\alpha z}^r \tag{I.20}$$

or

$$\frac{d\rho_{\alpha z} w_{\alpha z}^r}{dt} + \rho_{\alpha z}\frac{du_\alpha^r}{dt} + \rho_{\alpha z} w_{\alpha z}^r div(\mathrm{u}) + \rho_{\alpha z}\left(\mathrm{w}_{\alpha z}\nabla\right)u^r + \frac{\partial P_{\alpha z}^{\alpha z}}{\partial x_s} - n_{\alpha z} eZ(E^r + [\mathrm{u}_{\alpha z}\mathrm{B}]_r) = R_{\alpha z}^r \tag{I.13}$$

- *energy*

$$\frac{3}{2}\left(\frac{dp_{\alpha z}}{dt} + p_{\alpha z}\frac{\partial u_\alpha^r}{\partial x_r}\right) + P_{\alpha z}^{rs}\frac{\partial u_\alpha^r}{\partial x_s} + \frac{\partial q_{\alpha z}^r}{\partial x_r} - n_{\alpha z}\left\langle \mathrm{cF}_{\alpha z}^*\right\rangle = Q_{\alpha z} \tag{I.14}$$

or

$$\frac{3}{2}\left(\frac{dp_{\alpha z}}{dt} + p_{\alpha z} div(u_\alpha)\right) + P_{\alpha z}^{rs}\frac{\partial u_\alpha^r}{\partial x_s} + div(q_{\alpha z}) - n_{\alpha z}\left\langle \mathrm{cF}_{\alpha z} - \rho_{\alpha z}\frac{d\mathrm{u}_\alpha}{dt}\right\rangle = Q_{\alpha z} \tag{I.15}$$

Here $\frac{d}{dt} = \frac{\partial}{\partial t} + (\mathrm{u}\nabla)$ and the repetitive Latin indexes indicate summation.

$$R_{\alpha z}^r = \sum_{\beta\xi}\int m_\alpha c_r St_{\alpha z,\beta\xi} d\mathrm{c} \qquad\qquad Q_{\alpha z} = \sum_{\beta\xi}\int m_\alpha c_r St_{\alpha z,\beta\xi} d\mathrm{c} \tag{I.16}$$

$$n_{\alpha\xi}\left\langle \mathrm{F}_{\alpha z}^*\right\rangle \equiv n_{\alpha\xi}\left\langle \mathrm{F}_{\alpha z}\right\rangle - \rho_{\alpha z}\frac{d}{dt}\mathrm{u}_\alpha \qquad\qquad \left\langle \mathrm{F}_{\alpha z}\right\rangle \equiv eZ\left(\mathrm{E} + [\mathrm{uB}]\right) \tag{I.17}$$

Equations for pure "nucleus" e.g. for quantities $n_\alpha = \sum_z n_{\alpha z}$, T_α and u_α can be obtained after summation over charge states Z the equations for partial quantities presented above

- *particle continuity:*

$$\frac{d\rho_\alpha}{dt} + \rho_\alpha div(\mathrm{u}) + div\left(\rho_\alpha \mathrm{w}_\alpha\right) = m_\alpha \dot{n}_\alpha \tag{I.18}$$

or

$$\frac{dn_\alpha}{dt} + div\left(n_\alpha\left(\mathrm{u} + \mathrm{w}_\alpha\right)\right) = \dot{n}_\alpha \tag{I.19}$$

- *momentum*

$$\frac{d\rho_\alpha w_\alpha^r}{dt} + \rho_\alpha \frac{du^r}{dt} + \rho_\alpha w_\alpha^r div(\mathrm{u}) + \rho_\alpha (\mathrm{w}_\alpha \nabla) u^r + \frac{\partial P_\alpha^{rs}}{\partial x_s} - n_\alpha e_\alpha (E_\mathrm{r} + [\mathrm{u}_{\alpha\mathrm{z}} \mathrm{B}]_r) = R_\alpha^r \qquad \text{(I.20)}$$

or

$$\rho_\alpha \left(\frac{\partial u_\alpha^r}{\partial t} + u_\alpha^r \frac{\partial u_\alpha^r}{\partial x_r} \right) + \frac{\partial P_\alpha^{rs}}{\partial x_s} - \frac{\partial}{\partial x_s} \left(\rho_\alpha w_\alpha^r w_\alpha^s \right) - n_\alpha e_\alpha (E_\mathrm{r} + [\mathrm{u}_{\alpha\mathrm{z}} \mathrm{B}]_r) = R_\alpha^r \qquad \text{(I.21)}$$

- *energy*

$$\frac{3}{2} \left(\frac{dp_\alpha}{dt} + p_\alpha div(u\ ) \right) + P_\alpha^{rs} \frac{\partial u^r}{\partial x^s} + div(q_\alpha) - n_\alpha \left\langle \mathrm{cF}_\alpha - \rho_\alpha \frac{d\mathrm{u}}{dt} \right\rangle = Q_\alpha \qquad \text{(I.22)}$$

or

$$\frac{3}{2} n_\alpha \frac{dT_\alpha}{dt} + p_\alpha div(\mathrm{u}) + \pi_{rs} \frac{\partial u_r}{\partial x_s} + div(\mathrm{q}) - \frac{3}{2} \sum_\alpha div(n_\alpha w_\alpha) - \mathrm{j}(\mathrm{E} + [\mathrm{uB}]) = Q_{rad} \qquad \text{(I.23)}$$

Here $\frac{d}{dt} = \frac{\partial}{\partial t} + (\mathrm{u}\nabla)$ and the repetitive Latin indexes indicate summation.

$$R_\alpha^r = \sum_z R_{\alpha z}^r \qquad Q_\alpha = \sum_z Q_{\alpha z} \qquad \text{(I.24)}$$

$$n_\alpha \left\langle \mathrm{F}_\alpha^* \right\rangle \equiv n_\alpha \left\langle \mathrm{F}_\alpha \right\rangle - \rho_\alpha \frac{d}{dt} \mathrm{u} \qquad \left\langle \mathrm{F}_\alpha \right\rangle \equiv eZ(\mathrm{E} + [\mathrm{uB}]) \qquad \text{(I.25)}$$

One can note, that S_α term in the continuity equation turns to zero after summation over α and β particles in the case of pure elastic collisions. But in the case of ionization or recombination $S_\alpha = m_\alpha \dot{n}_\alpha$, where $\dot{n}_\alpha$ is rate of α particles production.

If further sum up over α the equations for "nucleus ", then the right hand side terms in the rest equations will also tern to zero, since

$$\sum_\alpha \mathrm{R}_\alpha = 0 \qquad \sum_\alpha \mathrm{Q}_\alpha = 0 \qquad \text{(I.26)}$$

I.2 The conservation equations for entire mixture

Finally, summing up the last equations over Z and α one gets finally the equations for entire mixture:

- *continuity equation*

$$\frac{d\rho}{dt} + \rho \cdot div(\mathrm{u}) = \sum_{\alpha,\beta} m_\alpha \dot{n}_\alpha \quad or \quad \frac{dn}{dt} + div(n\mathrm{u}) + \sum_\alpha div(n w_\alpha) = \sum_\alpha m_\alpha \dot{n}_\alpha \qquad \text{(I.27)}$$

- *momentum*

$$\rho\frac{du_r}{dt}+\frac{\partial P_{rs}}{\partial x_s}-\sum_\alpha n_\alpha\left\langle F_\alpha^r\right\rangle = R_{c-ex} \quad or \quad \rho\frac{d\mathrm{u}}{dt}+\mathrm{grad}(p)+div\pi-[\mathrm{jB}]=R_{c-ex} \tag{I.28}$$

- *energy*

$$\frac{3}{2}\left(\frac{dp}{dt}+p\ div(\mathrm{u}\ )\right)+P_{rs}\frac{\partial u_r}{\partial x_s}+div(\mathrm{q})-\sum_\alpha n_\alpha\left\langle \mathrm{cF}_\alpha\right\rangle = Q_{rad} \tag{I.29}$$

Here R_{c-ex} is the momentum source due to charge exchange collisions with neutral atoms and Q_{rad} are the radiation energy losses.

Using the definition for the current density

$$\mathrm{j}=\sum_\alpha e_\alpha n_\alpha \mathrm{w}_\alpha \tag{I.30}$$

and quasi-neutrality, $\sum e_\alpha n_\alpha = 0$, it is easy to see that

$$\sum_\alpha n_\alpha\left\langle \mathrm{F}_\alpha\right\rangle = [\mathrm{jB}] \tag{I.31}$$

and

$$\sum_\alpha n_\alpha\left\langle \mathrm{cF}_\alpha\right\rangle = \mathrm{j(E}+[\mathrm{uB}]) \tag{I.32}$$

Now, the **equation of motion of entire plasma** (*momentum equation*) can be written as:

$$\rho\frac{d\mathrm{u}}{dt}+\mathrm{grad}(p)+div\pi-[\mathrm{jB}]=R_{c-ex} \tag{I.33}$$

As far as the energy equation concerns, it can be presented in variety forms:

- *temperature equation for α species*

$$\frac{3}{2}n_\alpha\frac{dT}{dt}+p\ div(\mathrm{u})+\pi_{rs}\frac{\partial u_r}{\partial x_s}+div(\mathrm{q})-\frac{3}{2}\sum_\alpha div(n_\alpha w_\alpha)-\mathrm{j(E}+[\mathrm{uB}])=Q_{rad} \tag{I.34}$$

- *energy balance of entire plasma*

$$\frac{\partial}{\partial t}\varepsilon_t+div\left((\varepsilon_t+p)\mathrm{u}+\pi_{\mathrm{rs}}u_s+\mathrm{q}\right)=\mathrm{jE}, \qquad \text{where} \qquad \varepsilon_t\equiv\frac{\rho\cdot u^2}{2}+\frac{3}{2}p \tag{I.35}$$

In quasi-hydrodynamic approximation, when $|\mathrm{w}_\alpha| << V_{T\alpha}$, the distribution function for αz particles can be written as $f_{\alpha z}=f_{\alpha z}^0(1+\gamma_{\alpha z}\mathrm{w}_{\alpha z}\mathrm{c})$,

where $f_{\alpha z}^0=n_{\alpha z}\left(\frac{\gamma_{\alpha z}}{2\pi}\right)^{3/2}\exp(-\gamma_{\alpha z}c^2/2)$ and $\gamma_{\alpha z}=m_\alpha/T_{\varepsilon z}$, $\mathrm{c}=\mathrm{V}-\mathrm{u}$.

Notice, that in this case the thermal conductivity and viscosity can be ignored and

$$\mathrm{R}_\alpha = -n_\alpha \sum_\beta \mu_{\alpha\beta}\tau_{\alpha\beta}^{-1}\left(\mathrm{w}_\alpha - \mathrm{w}_\beta\right), \qquad \mu_{\alpha\beta} = \frac{m_\alpha m_\beta}{m_\alpha + m_\beta} \tag{I.36}$$

$$Q_\alpha = -3\sum_\beta n_\alpha [\mu_{\alpha\beta}/(m_\alpha + m_\beta)]\tau_{\alpha\beta}^{-1}\left(T_\alpha - T_\beta\right) \tag{I.37}$$

$$\tau_{\alpha\beta}^{-1} = \sum_{z,\xi} \nu_{\alpha z\beta\xi} = \frac{4\sqrt{2\pi}}{3} e^4 \lambda \frac{n_\beta \overline{\xi^2} Z^2}{T_{\alpha\beta}^{3/2}} \frac{\sqrt{\mu_{\alpha\beta}}}{m_\alpha}, \qquad n_\beta \overline{\xi^2} = \sum_\xi n_{\beta\xi}\xi^2 \tag{I.38}$$

$$\nu_{\alpha z\beta\xi} = \frac{4\sqrt{2\pi}}{3} e_\alpha^2 e_\beta^2 \lambda \frac{n_{\beta\xi}}{T_{\alpha\beta}^{3/2}} \frac{\sqrt{\mu_{\alpha\beta}}}{m_\alpha} = \frac{4\sqrt{2\pi}}{3} e^4 \lambda \frac{n_{\beta\xi} Z^2 \xi^2}{T_{\alpha\beta}^{3/2}} \frac{\sqrt{\mu_{\alpha\beta}}}{m_\alpha} \tag{I.39}$$

In this approximation the closed system of equations for n_α, u_α and T_α of a particular species α reads:

$$\frac{d_\alpha n_\alpha}{dt} + div\left(n_\alpha\left(\mathrm{u} + \mathrm{w}_\alpha\right)\right) = \dot{n}_\alpha \tag{I.40}$$

$$\rho_\alpha \frac{d_\alpha \mathrm{u}_\alpha}{dt} + \nabla p_\alpha - n_\alpha e_\alpha(\mathrm{E} + [\mathrm{u}_\alpha \mathrm{B}]) = -n_\alpha \sum_\beta \mu_{\alpha\beta}\tau_{\alpha\beta}^{-1}\left(\mathrm{w}_\alpha - \mathrm{w}_\beta\right) \tag{I.41}$$

$$\frac{3}{2} n_\alpha \frac{dT_\alpha}{dt} + p_\alpha div(\mathrm{u}_\alpha) + \mathrm{w}_\alpha \mathrm{R}_\alpha = -3n_\alpha \sum_\beta [\mu_{\alpha\beta}/(m_\alpha + m_\beta)]\tau_{\alpha\beta}^{-1}\left(T_\alpha - T_\beta\right) + Q_{rad} \tag{I.42}$$

I.3 The equations for diffusive velocities

Equations for diffusive velocities can be obtained from the momentum equation by replacing $\frac{d_\alpha \mathrm{u}_\alpha}{dt} ==> \frac{d\mathrm{u}_\alpha}{dt}$, that corresponds to the situation, when the terms $\frac{d_\alpha \mathrm{w}_\alpha}{dt}$ are disregarded in compare with the terms of the order $\tau_{\alpha\beta}^{-1}\mathrm{w}_\alpha$ in the r.h.s. of the equation. Then the equation of motion can be recast so:

$$n_\alpha \sum_\beta \mu_{\alpha\beta}\tau_{\alpha\beta}^{-1}\left(\mathrm{w}_\alpha - \mathrm{w}_\beta\right) = n_\alpha e_\alpha(\mathrm{E} + [\mathrm{uB}] + [\mathrm{w}_\alpha \mathrm{B}]) - \nabla p_\alpha - \rho_\alpha \frac{d\mathrm{u}}{dt} \tag{I.43}$$

It also can be written as

$$n_\alpha \sum_\beta \mu_{\alpha\beta}\tau_{\alpha\beta}^{-1}\left(\mathrm{w}_\alpha - \mathrm{w}_\beta\right) = n_\alpha e_\alpha(\mathrm{E} + [\mathrm{uB}] + [\mathrm{w}_\alpha \mathrm{B}]) - \left(\nabla p_\alpha - \frac{\rho_\alpha}{\rho}\nabla p\right) - \frac{\rho_\alpha}{\rho}[\mathrm{jB}] \tag{I.44}$$

if one replaces term $\rho\frac{d\mathrm{u}}{dt}$ by $\rho\frac{d\mathrm{u}}{dt} = [\mathrm{jB}] - \mathrm{grad}(p)$, neglect the viscosity term. The two equations presented above allow one to find diffusive velocities, w by keeping in mind, that $\mathrm{j} = \sum_\alpha e_\alpha n_\alpha \mathrm{w}_\alpha$ and $\sum_\alpha \rho_\alpha \mathrm{w}_\alpha = 0$. The explicit solution of these equations against w_α can be written as [6]:

$$\mathrm{w}_\alpha = \mathrm{x}_\alpha - \sum_{\gamma=1}^{\mathrm{N}} \left(\frac{\rho_\gamma}{\rho} \right) \cdot \mathrm{x}_\gamma \,, \tag{I.45}$$

where

$$\mathrm{x}_\alpha = \left|c'\right|^{-1} \sum_{\beta \neq k}^{N} \left|c'\right|_{\beta\alpha} \cdot \varepsilon_{\beta //} + \left|a'\right|^{-1} \sum_{\beta \neq k}^{N} \left|a'\right|_{\beta\alpha} \cdot \varepsilon_{\beta\perp} + \left|a'\right|^{-1} \sum_{\beta,\gamma \neq k}^{N} \chi_{\gamma\beta} \left|a'\right|_{\beta\alpha} \cdot \left[\varepsilon_\beta \mathrm{h}\right] \tag{I.46}$$

Here the following definitions are used. Index k is for the arbitrary chosen component of initial equations, which is omitted and not considered. One should keep in mind, that system of equations for w_α is linear dependent; therefore the actual number of equations needed for solution must be in one equation smaller, $N-1$, where N is the total number of components in mixture; $\mathrm{x}_\alpha \equiv \mathrm{w}_\alpha - \mathrm{w}_\beta$, $\mathrm{h} = \mathrm{B}/|\mathrm{B}|$ and

$$\varepsilon_\alpha \equiv n_\alpha e_\alpha (\mathrm{E} + [\mathrm{uB}]) - \left(\nabla p_\alpha - \frac{\rho_\alpha}{\rho} \nabla p \right);$$

$$\varepsilon_{\alpha //} = \mathrm{h}(\mathrm{h}\varepsilon_\alpha); \qquad c_{\alpha\beta} = n_\alpha \mu_{\alpha\beta} \tau_{\alpha\beta}^{-1}; \; c_{\alpha\alpha} = -\sum_{\gamma \neq \alpha}^{N} n_\alpha \mu_{\alpha\gamma} \tau_{\alpha\gamma}^{-1}; \; \left|c'\right| = \det(c'_{\alpha\beta}) \text{ and } c'_{\alpha\beta} \text{ is the } c_{\alpha\beta} \text{ matrix,}$$

where the k line and k column are removed; the (α, β) cofactor (minor) of that determinant matrix is $\left|c'\right|_{\alpha\beta}$.

The equations obtained above allow one to calculate diffusion of arbitrary particles both along and across the magnetic field as well as. For magnetized plasma $\omega_\alpha \tau_{\alpha\beta} >> 1$ equation () can be recast as:

$$\sum_\beta \left(\omega_\alpha \tau_{\alpha\beta}\right)^{-1} \left(\mu_{\alpha\beta} / m_\alpha\right) \left(\mathrm{w}_\alpha - \mathrm{w}_\beta\right) = [\mathrm{w}_\alpha \mathrm{h}] + \frac{1}{(\rho_\alpha \omega_\alpha)} \left(n_\alpha e_\alpha \mathrm{E}' - \nabla p_\alpha - \rho_\alpha \frac{d\mathrm{u}}{dt} \right) \tag{I.47}$$

where $\mathrm{E}' = \mathrm{E} + [\mathrm{uB}]$, $\omega_\alpha = e_\alpha |\mathrm{B}| / m_\alpha$ and $\tau_{\alpha\beta}^{-1} = \frac{4\sqrt{2\pi}}{3} e^4 \lambda \frac{n_\beta \overline{\xi^2} Z^2}{T_{\alpha\beta}^{3/2}} \frac{\sqrt{\mu_{\alpha\beta}}}{m_\alpha}$

In zero approximation over the small parameter $\left(\omega_\alpha \tau_{\alpha\beta}\right)^{-1}$ the last term on the r.h. side can be dropped and after substitution of zero order solution into the r.h. side term the first approximation can be obtained. As a result $w_{\alpha\perp} = w_{\alpha\perp}^0 + w_{\alpha\perp}^1$, where

$$w_{\alpha\perp}^0 = \frac{1}{B}[\mathrm{E}'\mathrm{h}] + \frac{1}{\rho_\alpha \omega_\alpha}[\mathrm{h}\nabla p] + \frac{1}{\omega_\alpha}[\mathrm{h}\frac{\mathrm{du}}{\mathrm{dt}}] \tag{I.48}$$

and

$$w_{\alpha\perp}^1 = -\frac{1}{(m_\alpha \omega_\alpha)^2} \sum_\alpha \mu_{\alpha\beta} \tau_{\alpha\beta}^{-1} \left\{ \left(\frac{\nabla_\perp p_\alpha}{n_\alpha} - \frac{Z_\alpha}{Z_\beta} \frac{\nabla_\perp p_\beta}{n_\beta} \right) + \left(m_\alpha - \frac{Z_\alpha}{Z_\beta} m_\beta \right) \frac{\mathrm{du}_\perp}{\mathrm{dt}} \right\} \tag{I.49}$$

Keeping in mind, that $\mathrm{j} = \sum_{\alpha} e_{\alpha} n_{\alpha} \mathrm{w}_{\alpha}$, easy to obtain:

$$\mathrm{j}_{\perp} = \frac{1}{B}[\mathrm{h}\nabla p] + \frac{\rho}{B}[\mathrm{h}\frac{\mathrm{du}}{\mathrm{dt}}] \qquad \text{(I.50)}$$

or by substituting the time derivative in the last term: here $\mathrm{E}'_{\perp} = \mathrm{E}_{\perp} + [\mathrm{uB}]$, and

$$\left\langle \frac{Z}{m} \right\rangle^{-1} = \sum_{\alpha} \left(m_{\alpha} \rho_{\alpha} / \rho Z_{\alpha} \right) \qquad \langle p \rangle = \sum_{\alpha} \left(m_{\alpha} p_{\alpha} / \rho Z_{\alpha} \right) / \langle m / Z \rangle \qquad \text{(I.51)}$$

Equations above allow one to conclude, that the relative diffusion of plasma components across the magnetic field line in case of electrons and background ions occurs with the rate of penetration ~ $D_m \left(4\pi p / B^2 \right) / L$, where $D_m = c^2 / 4\pi\sigma$ is the diffusion of the magnetic field through plasma:

$$u_{er} = u_{ir} = \frac{c^2}{\sigma B^2} \frac{\partial p}{\partial r} = D_m \beta \frac{\partial p}{p \partial r} \qquad \text{(I.52)}$$

where $\beta = 4\pi n T / B^2$. However, in the case of multi-species the mutual diffusion of different species occurs in $\left(m_i / m_e \right)^{1/2}$ times quicker than the magnetic field penetration rate. Therefore, in time scale much smaller then the penetration time impurity ions can come in equilibrium in radial direction: $Z_{\alpha} n_{\alpha Z} w^r_{\alpha z} = -Z_{\beta} n_{\beta \xi} w^r_{\beta \xi}$.

In the case of $\alpha = i$, $\beta = I$

$$Z_i n_{iZ} w^r_{iz} = -Z_I n_{I\xi} w^r_{I\xi} = \frac{\mu_{i,I} \tau_{i,I}}{Z_i B^2} \left(\frac{\partial p_i}{\partial r} - \frac{Z_i n_i}{Z_I n_I} \frac{\partial p_I}{\partial r} \right) \qquad \text{(I.53)}$$

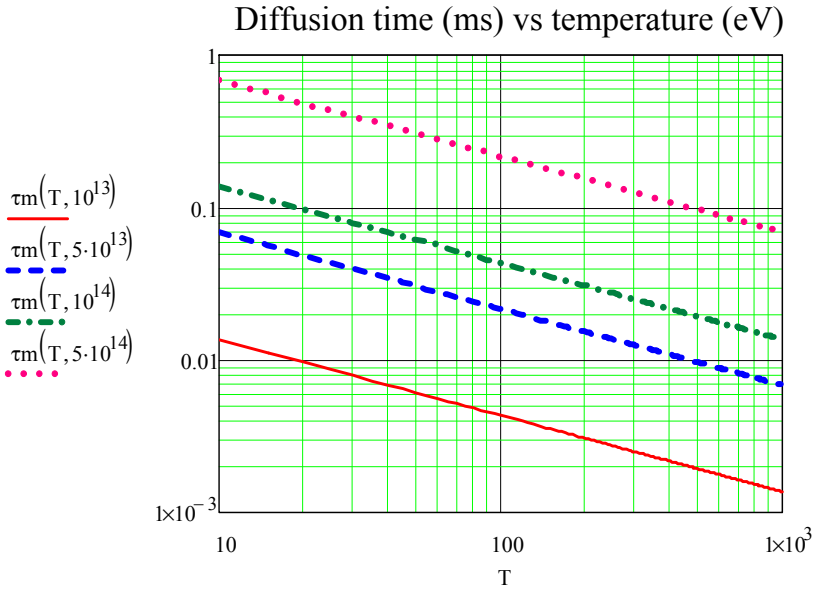

Fig. (I.1) Diffusion time of impurities vs. temperature for different density.

$(n = 10^{13}, 5 \cdot 10^{13}, 10^{14}, 5 \cdot 10^{14}\, cm^{-3})$

this brings to the Boltzmann type radial distribution of impurities in time scale

$$\tau_m = D_m\left(4\pi p / B^2\right)/ L\,. \qquad \text{(I.54)}$$

For $L \sim a$ and typical values for ITER parameters $a = 2m,\ B = 5T$ diffusion time is shown in Fig. (I.1) for different density values $\sim 10^{13}, 5\cdot 10^{13}, 10^{14}, 5\cdot 10^{14}\, cm^{-3}$.

II. Transport equations for the multi-component tokamak plasma

The two-dimensional transport equations are presented to simulate multi-species plasma in curvilinear configuration with the *x*-axis in radial direction and the *y*-axis in poloidal direction. The plasma inside the separatrix is assumed to be quite dense and relative cold, allowing one the fluid description. The present equations are a direct extension of Braginskii equations for electrons and single ionic species to a multiple case. The equations are of Nervier-Stokes form as regards the parallel flow along B and of a diffusive form in the radial direction.

II.1 The 2D multi-species transport model based on the Chapmen-Enscog approach

Specifically, we suggest for TOKES the following system of N transport equations for each ionic species a, $(1 \le a \le N,$ *and* where $a = 1$ corresponds to background ions):

Continuity of species a:

$$\frac{\partial n_a}{\partial t} + \frac{1}{\sqrt{g}}\frac{\partial}{\partial x}\left(\frac{\sqrt{g}}{h_x} n_a V_{a,x}\right) + \frac{1}{\sqrt{g}}\frac{\partial}{\partial y}\left(\frac{\sqrt{g}}{h_y} n_a V_{a,y}\right) = nN\left\langle \sigma V \right\rangle_{ion} \tag{II.1.1}$$

$$n_a V_{a,x} = -\frac{D_a}{h_x}\frac{\partial n_a}{\partial x} \tag{II.1.2}$$

Momentum balance of species a $(1 \le a \le N)$

$$\begin{aligned} &\frac{\partial}{\partial t}\left(m_a n_a V_{a,//}\right) + \frac{1}{\sqrt{g}}\frac{\partial}{\partial y}\left\{\frac{\sqrt{g}}{h_y} m_a n_a V_{a,//} V_{a,y} - \frac{\sqrt{g}}{h_y^2}\eta_{a,y}\frac{\partial V_{a,//}}{\partial y}\right\} + \\ &+ \frac{1}{\sqrt{g}}\frac{\partial}{\partial x}\left\{\frac{\sqrt{g}}{h_x} m_a n_a V_{a,//} V_{a,x} - \frac{\sqrt{g}}{h_x^2}\eta_{a,x}\frac{\partial V_{a,//}}{\partial x}\right\} = \\ &= \frac{b_\theta}{h_y}\left\{-\frac{\partial p_a}{\partial y} - \frac{Z_a n_a}{n_e}\frac{\partial p_e}{\partial y} + R_{a,e}^{T_e} + R_{a,i}^{T_i}\right\} + \sum_{b=1}^{N} R^F{}_{a,b} + S_a^{mu} \end{aligned} \tag{II.1.3}$$

Electron energy balance:

$$\begin{aligned} &\frac{\partial}{\partial t}\left(\varepsilon_e\right) + \frac{1}{\sqrt{g}}\frac{\partial}{\partial x}\left\{\frac{\sqrt{g}}{h_x}\left(\left(\varepsilon_e + p_e\right)V_{e,x} - \frac{\sqrt{g}}{h_x^2}\chi_{e,x}\frac{\partial T_e}{\partial x}\right)\right\} + \\ &+ \frac{1}{\sqrt{g}}\frac{\partial}{\partial y}\left\{\frac{\sqrt{g}}{h_y}\left(\varepsilon_e + p_e\right)V_{e,y} - \frac{\sqrt{g}}{h_y^2}\chi_{e,y}\frac{\partial T_e}{\partial y}\right\} = \frac{V_{e,x}}{h_x}\frac{\partial p_e}{\partial x} + \frac{V_{e,y}}{h_y}\frac{\partial p_e}{\partial y} + Q_{ea} + S_{\varepsilon,e} \end{aligned} \tag{II.1.4}$$

Ion energy balance:

$$\frac{\partial}{\partial t}(\varepsilon_a)+\frac{1}{\sqrt{g}}\frac{\partial}{\partial x}\left\{\frac{\sqrt{g}}{h_x}\left((\varepsilon_a+p_a)V_{a,x}+q_{a,x}+\pi_{a,x}\right)\right\}+ \\ +\frac{1}{\sqrt{g}}\frac{\partial}{\partial y}\left\{\frac{\sqrt{g}}{h_y}\left((\varepsilon_a+p_a)V_{a,y}+q_{a,y}+\pi_{a,y}\right)\right\}=-\frac{V_{e,x}}{h_x}\frac{\partial p_e}{\partial x}-\frac{V_{e,y}}{h_y}\frac{\partial p_e}{\partial y}+Q_{ae}+S_\varepsilon^i \tag{II.1.5}$$

Here:

$$n_\alpha=\sum_j n_{\alpha_j} \qquad n_e=\sum_a Z_a n_a \qquad n_e = n_i + \sum_j n_{\alpha_j} z_j \approx n_i + z\cdot n_\alpha \tag{II.1.6}$$

$$V_{e,x}=\sum_a Z_a n_a V_{a,x}/n_e \qquad V_{e,y}=\sum_a Z_a n_a V_{a,y}/n_e \qquad V_{a,y,//}=\frac{B}{B_\theta}V_{a,y}=\frac{1}{b_\theta}V_{a,y} \tag{II.1.7}$$

$$V_{i,//}\Rightarrow V_{i,//}+V_{pol\,rot}/b_\theta \qquad V_{pol\,rot}=\rho_i V_{Ti}\left(\frac{1}{n_i}\frac{\partial n_i}{\partial r}-2.7\frac{1}{T_i}\frac{\partial T_i}{\partial r}\right) \tag{II.1.8}$$

$$z=\sum_j Z_j n_{\alpha,j}/n_\alpha \qquad Z_{eff}=\frac{n_i+\sum_j n_{\alpha_j} z_j^2}{n_e} \tag{II.1.9}$$

$$\varepsilon_e=\frac{3}{2}p_e, \qquad p_a=n_a T_i, \qquad \varepsilon_a=\frac{3}{2}p_a+\frac{1}{2}\sum_N \rho_a V_{a,y,//}^2 \tag{II.1.10}$$

$$Q_{e\beta}=3n_e\sum_\beta \frac{m_e}{m_\beta}\nu_{e,\beta\xi}\left(T_\beta-T_e\right) \qquad \nu_{e,\beta\xi}=\nu_0\cdot\xi^2\frac{n_{\beta\xi}}{T_e^{3/2}}\frac{1}{\sqrt{m_e}} \tag{II.1.11}$$

Where the coefficients and forces are:

$$R_{a,e}^{T_e}=\alpha_e n_a\frac{Z_a^2}{Z_{eff}}\frac{\partial T_e}{\partial y} \qquad \alpha_e\approx 2.2Z_{eff}\frac{\left(1+0.52Z_{eff}\right)}{\left(1+2.65Z_{eff}\right)\left(1+0.285Z_{eff}\right)} \tag{II.1.12}$$

$$R_{a,i}^{T_i}=\alpha_i n_a\frac{Z_a^2\sqrt{2}}{1+\sqrt{2}Z_0}\frac{\partial T_i}{\partial y} \qquad \alpha_i=\frac{1.56\cdot\left(1+\sqrt{2}Z_0\right)\cdot\left(1+0.52Z_0\right)}{\left(1+2.65Z_0\right)\cdot\left(1+0.285Z_0\right)} \tag{II.1.13}$$

$$R_{a,b}^{F_e}=-c_{a,b}^{(1)}\cdot m_a n_a \nu_{a,b}\cdot\left(V_{a,//}-V_{b,//}\right) \qquad c_{a,b}^{(1)}=\frac{\left(1+0.24Z_0\right)\cdot\left(1+0.93Z_0\right)}{\left(1+2.65Z_0\right)\cdot\left(1+0.285Z_0\right)} \tag{II.1.14}$$

$$q_{a,x}=-\frac{\chi_x^i}{h_x}\frac{\partial T_i}{\partial x}, \qquad q_{a,y}=-\frac{\chi_y^i}{h_y}\frac{\partial T_i}{\partial y} \qquad \pi_{a,x}=-\frac{\eta_x^a}{2h_x}\frac{\partial V_{a,//}^2}{\partial x} \qquad \pi_{a,y}=-\frac{\eta_y^a}{2h_y}\frac{\partial V_{a,//}^2}{\partial x} \tag{II.1.15}$$

$$Q_{a,e} = 3n_e \sum_{\alpha} \frac{m_e}{m_\alpha} \nu_{a,e} \left(T_e - T_\alpha\right) \qquad \nu_{a,e} = \frac{\nu_0}{T_e^{3/2}} \frac{\sqrt{m_e}}{m_\alpha} n_e Z_{eff} \tag{II.1.16}$$

The external momentum source due to e.g. plasma rotation in poloidal direction:

$$S_\alpha^{mv} = m_\alpha n_\alpha V_{\alpha,y}^0 / \tau_0 \tag{II.1.17}$$

In these equations

x - is the radial axis,

y - is the poloidal axis,

$\sqrt{g} = h_x h_y r$, h_y - metric coefficients, (the coordinate system is orthogonal curvilinear)

B_θ, B - poloidal and total magnetic fields,

Z_a, m_a - charge number and mass of an ion of species a,

$S_{a,n}$, $S_{a,mv}$ - volume sources of ions and momentum for species a,

$S_{\varepsilon,e}$, $S_{\varepsilon,i}$ - volume sources of electrons and ion energy,

$\eta_{a,y}$, $\eta_{a,x}$ - poloidal and radial viscosity coefficients for species a,

$R^F{}_{a,b}$ - friction force on ion species a due to species b,

$R_{a,e}^{T_e}$, $R_{a,i}^{T_i}$ - thermal forces for electrons and ions,

$D_n^{a_e}$, D_p^a - diffusion coefficients for species a,

χ_x^{e,i_e}, $\chi_y^{e,i}$ - heat conduction coefficients,

$V_{a,y}$ - velocity in poloidal direction

$V_{a,y,//}$ - velocity along B, $V_{a,y} = \frac{B_\theta}{B} V_{a,y,//}$

The other definitions are summarized here:

$$n_i = \sum_a n_a$$

$$n_e = \sum_a Z_a n_a$$

$$\rho_a = m_a n_a$$

$$p_a = n_a T_a$$

$$p_e = n_e T_e$$

$$V_{a,y,//} = \frac{B}{B_\theta} V_{a,y} = \frac{1}{b_\theta} V_{a,y}$$

$$V_{a,y} = \frac{B_\theta}{B} V_{a,y,//}$$

$$V_{e,y} = \sum_a Z_a n_a V_{a,y} / n_e$$

$$V_{e,x} = \sum_a Z_a n_a V_{a,x} / n_e$$

$$Z_{eff} = \sum_a Z_a^2 n_a / n_e$$

$$\varepsilon_i = \frac{3}{2} nT + \sum_a \frac{1}{2} \rho_a V^2{}_{a,y,//}$$

$$\chi_{e,SH} = 3.16 \frac{n_e T_e \tau_e}{m_e} \frac{\sum_a Z_a n_a}{\sum_b Z_b^2 n_b}$$

$$\chi_{i,SH} = 3.16 \frac{n_i T_i \tau_{ii}}{m_i} \frac{\sum_a Z_a^{-1} n_a}{\sum_b Z_b^2 n_b \sqrt{\mu_{ab}}}$$

$$\mu_{ab} = m_a m_b / (m_a + m_b)$$

$$Q_{ea} = -Q_{ae} = \frac{3}{2} m_e n_e \sum_a Z_a^2 n_a \frac{(T_e - T_a)}{m_a \tau_e}$$

$$Q = -Q_{rad} - I_i n N_0 \langle \sigma V \rangle_{ion} - (\alpha_{rec} + n\beta_{rec}) n^2$$

$$\eta_{a,y} = \left(\frac{B_\theta}{B} \right)^2 \eta_{a,//}$$

$$\chi_{e,y} = \left(\frac{B_\theta}{B} \right)^2 \chi_{e,//}$$

$$\chi_{i,y} = \left(\frac{B_\theta}{B} \right)^2 \chi_{i,//}$$

$$\chi_{e,//} = \chi_{e,SH} \cdot \left(1 + \left| \frac{q_{SH}}{q_{FL}} \right|^\gamma \right)^{-1/\gamma}$$

$$q_{e,SH} = -\chi_{e,//SH} \frac{\partial T_e}{\partial y}$$

$$q_{e,FL} = 0.12 n_e T_e \sqrt{T_e / 2m_e} \qquad \gamma \propto 1$$

$$q_{a,x} = \frac{1}{h_x} \chi_{a,x} \frac{\partial T_a}{\partial x}$$

$$q_{a,y} = \frac{1}{h_y} \chi_{a,y} \frac{\partial T_a}{\partial y}$$

$$\eta_{a,//} = 0.96 n_a T_a \tau_{ii} \frac{m_a}{\sqrt{2\mu_{ab} / m_i}}$$

$$R_{\alpha,e}^{T_e} = \alpha_e \frac{z^2}{z_{eff}} n_\alpha \frac{\partial T_e}{\partial y}$$

$$\alpha_e \approx 2.2 Z_{eff} \frac{(1 + 0.52 Z_{eff})}{(1 + 2.65 Z_{eff})(1 + 0.285 Z_{eff})}$$

$$R_{\alpha,i}^{T} = \alpha_i n_\alpha \frac{z^2 \sqrt{2}}{1 + \sqrt{2} Z_0} \frac{\partial T_i}{\partial y}$$

$$\alpha_i = \frac{1.56 \cdot (1 + \sqrt{2} Z_0) \cdot (1 + 0.52 Z_0)}{(1 + 2.65 Z_0) \cdot (1 + 0.285 Z_0)}$$

- Correspondence to original TOKES equations and definitions is shown below.

Here x - is the radial axis, y - is the poloidal axis,

$w = \Psi$ -is the poloidal flux $\Psi(r) = (2\pi)^{-1}\int\left(\vec{\nabla}\theta\cdot\vec{B}\right)d\vec{r}$

$G = h_y / B_y$

$rh_x h_y = \sqrt{g}$

$S = h_x h_y = \sqrt{g}/r, \quad r = h_\varsigma \qquad \vec{B} = (0, B_y, B_\xi) \qquad B_y = -\Psi_r'(r)/rh_x$

$u = V_y / B_y$

$\frac{\partial}{\partial y} = h_y \frac{\partial}{\partial \theta}$, therefore the continuity Eq. in TOKES can be written as

$$G\frac{\partial\rho}{\partial t} + \frac{\partial}{\partial y}(\rho u) = 0 \qquad \Rightarrow \quad \frac{\partial n}{\partial t} + \frac{B_y}{h_y}\frac{\partial}{\partial y}(nV_y / B_y) \Rightarrow \frac{\partial n_a}{\partial t} + \frac{1}{\sqrt{g}}\frac{\partial}{\partial y}\left(\frac{\sqrt{g}}{h_y} n_a V_{a,y}\right)$$

this coincides with the equation:

$$\frac{\partial n_a}{\partial t} + \frac{1}{\sqrt{g}}\frac{\partial}{\partial y}\left(\frac{\sqrt{g}}{h_y} n_a V_{a,y}\right) + \frac{1}{\sqrt{g}}\frac{\partial}{\partial x}\left(\frac{\sqrt{g}}{h_x} n_a V_{a,x}\right) - nN\langle\sigma V\rangle_{ion} = 0$$

II.2 Impurity simulation in the SOL plasma: the Grad 21 moment approach

The transport equations and corresponding kinetic coefficients for multi-component plasma in 1-D can be written in the moment approximation directly related to the 21-moment Grad method which can be naturally generalized to the plasma with many impurity species in different charge states [7-9]. Here we will derive the 21-moment equations, which being equivalent to Braginskii ones [10], but having an advantage to be the first order differential equations. Moreover, this system is inherently can be generalized to account for the kinetic effects in the SOL region. To derive the system of equations for the moments of distribution function and to determine the diffusion velocities and heat flows in multi-component plasma we use the distribution function in the form of an expansion in irreducible Hermit polynomials **[6]**

$$f_{\alpha z} = f_{\alpha z}^0 = \sum_{n,m=0}^{\infty} \frac{(2m+1)!(m+n)!}{n!(m!)^2(2n+2m+1)!}\, \mathrm{a}_{\alpha z}^{mn} \cdot \mathrm{H}^{mn}\left(\left(\mathrm{V}-\mathrm{u}\right)\sqrt{\frac{m_\alpha}{T_{\alpha z}}}\right) \qquad \text{(II.2.1)}$$

where

$f_{\alpha z}^0 = n_{\alpha z}\left(\frac{m_\alpha}{2\pi T_{\alpha z}}\right)^{3/2} \exp\left(-\frac{m_\alpha}{2T_{\alpha z}}(\mathrm{V}-\mathrm{u})^2\right)$ is the local Maxwell distribution function, V is the current velocity and u is the mean-mass velocity of the mixture, m_α is the mass of the particles, and

$n_{\alpha z}$ and $T_{\alpha z}$ are the density and temperature of the particles of sort α and charge z. In this expansion m represents the rank of the tensor, while n represents the degree of the polynomial.
In general case substitution of the expansion (II.1.1) into the kinetic equation leads, after integration over the velocity with weight H^{mn}, to a system of non-linear differential equations for the coefficients $\mathrm{a}_{\alpha z}^{\mathrm{mn}}$ [10]. The latter can be simplified by assuming that the macroscopic parameters of the plasma vary only slightly at the distances of the order of the effective mean free pass and in the time of the order of the time between collisions between the plasma particles. When these conditions are satisfied one can neglect the derivatives of the coefficients $\mathrm{a}_{\alpha z}^{\mathrm{mn}}$ and the nonlinear terms in equations. Finally, one arrives to a linear system of algebraic equations for $\mathrm{a}_{\alpha z}^{\mathrm{mn}}$ [6]. For a fairly accurate calculation of the transfer coefficients it is necessary to use not less than three terms with $m = 1$ in expansion (II.2.1). These coefficients $\mathrm{a}_{\alpha z}^{10}$, $\mathrm{a}_{\alpha z}^{11}$, $\mathrm{a}_{\alpha z}^{12}$ are related to the moments of density

$$\rho_{\alpha z} = m_{\alpha} n_{\alpha z}, \tag{II.2.2}$$

relative (diffusive) velocity,

$$\mathrm{w}_{\alpha} = \mathrm{u}_{\alpha z} - \mathrm{u} \tag{II.2.3}$$

conductive heat flux

$$\mathrm{h}_{\alpha z} = \mathrm{q}_{\alpha z} - 5\mathrm{p}_{\alpha z}\mathrm{w}_{\alpha z}/2 \tag{II.2.4}$$

in addition, additional moment of higher order $\mathrm{r}_{\alpha z}$ and $\sigma_{\alpha z rs}$ as given by the relations:

$$\mathrm{r}_{\alpha z} = \frac{m_{\alpha}}{4}\int \left(c^4 - 14c^2/\gamma_{\alpha z} + 35/\gamma_{\alpha z}^2\right)\mathrm{c} f_{\alpha z} d\mathrm{c} \tag{II.2.5}$$

$$\sigma_{\alpha z rs} = \frac{m_{\alpha}}{2}\int \left(c_r c_s - \frac{\delta_{rs}}{3}c^2\right)\left(c^2 - 7/\gamma_{\alpha z}\right) f_{\alpha z} d\mathrm{c} \tag{II.2.6}$$

$$\mathrm{a}_{\alpha z}^{10} = \rho_{\alpha z}\mathrm{w}_{\alpha z}/p_{\alpha z}\sqrt{\gamma_{\alpha z}}, \tag{II.2.7}$$

$$\mathrm{a}_{\alpha z}^{11} = 2\mathrm{h}_{\alpha z} p_{\alpha z}\sqrt{\gamma_{\alpha z}} \tag{II.2.8}$$

$$\mathrm{a}_{\alpha z}^{12} = 4\mathrm{r}_{\alpha z}\sqrt{\gamma_{\alpha z}^3}/p_{\alpha z} \tag{II.2.9}$$

where $u_{\alpha z}$ and $q_{\alpha z}$ are the velocity and heat flux of particles of sort α and charge z, $p_{\alpha z} = n_{\alpha z} T_{\alpha z}$, $\gamma_{\alpha z} = m_\alpha / T_{\alpha z}$. The distribution function in terms these moments then reds as:

$$f_{\alpha z} = f_{\alpha z}^0 \left\{ \begin{array}{l} 1 + \gamma_{\alpha z} w_{\alpha z} c + \frac{\gamma_{\alpha z}^2 h_{\alpha z}}{5 p_{\alpha z}} c\left(c^2 - 5/\gamma_{\alpha z}\right) + \frac{\gamma_{\alpha z}^4 h_{\alpha z}}{70 p_{\alpha z}} c\left(c^4 - 14 c^2/\gamma_{\alpha z} + 35/\gamma_{\alpha z}^2\right) + \\ + \frac{\gamma_{\alpha z}}{2} \frac{\pi_{\alpha z rs}}{p_{\alpha z}} \left(c_r c_s - \frac{\delta_{rs}}{3} c^2\right) + \frac{\gamma_{\alpha z}^3 \sigma_{\alpha z rs}}{14 p_{\alpha z}} \left(c_r c_s - \frac{\delta_{rs}}{3} c^2\right)\left(c^2 - 7/\gamma_{\alpha z}\right) \end{array} \right\} \qquad \text{(II.2.10)}$$

The general number of independent moments is equal twelve; therefore, the distribution function above corresponds to 12-moment approximation. Seven equations are required for the 21-moment approximation. These constitute equations of change for twenty-one moments of the distribution function $f_{\alpha z}$ for particles type α of mass m_α and charge eZ_α. The particle velocities c_α have chosen in a centre of mass frame reference

$$c_\alpha = V_\alpha - u_\alpha, \qquad \text{(II.2.11)}$$

Where V_α is the velocity of species α, and

$$u_{\alpha z} = \frac{\sum_{\alpha z} \int m_\alpha v_{\alpha z} f_{\alpha z}}{\sum_{\alpha z} m_\alpha n_{\alpha z}} \qquad \text{(II.2.12)}$$

$c_{\alpha z}$ is the particle velocity. The rest quantities of interest are defined as (dropping particle subscripts for ease of notation):

$\rho_\alpha = m_\alpha n_\alpha$, for mass density species α

$p = nT = \frac{1}{3}\rho\langle w^2 \rangle$, for thermal pressure

$u = \langle w \rangle$, for drift velocity

Then, the equations read:

$$\frac{\partial \rho_\alpha}{\partial t} + \nabla \rho_\alpha (w_\alpha + u) = S_\alpha \qquad \text{(II.2.13)}$$

The equations for $w_{\alpha z}$, $h_{\alpha z}$ and $r_{\alpha z}$ can then be written in the form:

$$\rho_{\alpha z}\left(\frac{d\mathrm{u}}{dt}-\frac{\mathrm{F}_{\alpha z}}{m_\alpha}\right)+\nabla p_{\alpha z}-\rho_{\alpha z}\omega_{\alpha z}[\mathrm{w}_{\alpha z}\mathrm{b}]=$$

$$=\sum_{\beta,\xi}\left\{G^{(1)}_{\alpha z,\beta\xi}(\mathrm{w}_{\alpha z}-\mathrm{w}_{\beta\xi})+\frac{\mu_{\alpha\beta}}{T_{\alpha\beta}}G^{(2)}_{\alpha z,\beta\xi}\left(\frac{\mathrm{h}_{\alpha z}}{\rho_{\alpha z}}-\frac{\mathrm{h}_{\beta\xi}}{\rho_{\beta\xi}}\right)+\frac{\mu^2_{\alpha\beta}}{T^2_{\alpha\beta}}G^{(3)}_{\alpha z,\beta\xi}\left(\frac{\mathrm{r}_{\alpha z}}{\rho_{\alpha z}}-\frac{\mathrm{r}_{\beta\xi}}{\rho_{\beta\xi}}\right)\right\} \tag{II.2.14}$$

$$-\omega_{\alpha z}[\mathrm{h}_{\alpha z}\mathrm{b}]+\frac{5}{2}\frac{p_{\alpha z}}{m_\alpha}\nabla T_{\alpha z}=$$

$$=\frac{T_{\alpha\beta}}{m_\alpha}\sum_{\beta,\xi}\left\{\frac{5}{2}\frac{\mu_{\alpha\beta}}{m_\alpha}G^{(2)}_{\alpha z,\beta\xi}\left(\mathrm{w}_{\alpha z}-\mathrm{w}_{\beta\xi}\right)+G^{(4)}_{\alpha z,\beta\xi}\frac{\mathrm{h}_{\alpha z}}{\rho_{\alpha z}}-G^{(5)}_{\alpha z,\beta\xi}\frac{\mathrm{h}_{\beta\xi}}{\rho_{\beta\xi}}+\frac{\mu_{\alpha\beta}}{T_{\alpha\beta}}(G^{(6)}_{\alpha z,\beta\xi}\frac{\mathrm{r}_{\alpha z}}{\rho_{\alpha z}}-G^{(7)}_{\alpha z,\beta\xi}\frac{\mathrm{r}_{\beta\xi}}{\rho_{\beta\xi}})\right\} \tag{II.2.15}$$

$$-\omega_{\alpha z}[\mathrm{r}_{\alpha z}\mathrm{b}]=\left(\frac{T_{\alpha\beta}}{m_\alpha}\right)^2 x$$

$$x\sum_{\beta,\xi}\left\{\frac{35}{2}\left(\frac{\mu_{\alpha\beta}}{m_\alpha}\right)^2 G^{(3)}_{\alpha z,\beta\xi}\left(\mathrm{w}_{\alpha z}-\mathrm{w}_{\beta\xi}\right)+\frac{7\mu_{\alpha\beta}}{m_\alpha}\left(G^{(6)}_{\alpha z,\beta\xi}\frac{\mathrm{h}_{\alpha z}}{p_{\alpha z}}-G^{(7)}_{\alpha z,\beta\xi}\frac{\mathrm{h}_{\beta\xi}}{p_{\beta\xi}}\right)+G^{(8)}_{\alpha z,\beta\xi}\frac{m_\alpha}{T_{\alpha\beta}}\frac{\mathrm{r}_{\alpha z}}{p_{\alpha z}}-G^{(9)}_{\alpha z,\beta\xi}\frac{m_\beta}{T_{\alpha\beta}}\frac{\mathrm{r}_{\beta\xi}}{p_{\beta\xi}}\right\} \tag{II.2.16}$$

where

$$\mathrm{F}_{\alpha z}=eZ(\mathrm{E}+[\mathrm{uB}]/c)+\mathrm{X}_\alpha, \tag{II.2.17}$$

X_α are forces of non-electromagnetic origin, $\omega_{\alpha z}=ezB/m_\alpha c$,

$$\mu_{\alpha\beta}=m_\alpha m_\beta/(m_\alpha+m_\beta),\ \mathrm{b}=\mathrm{B}/|B| \tag{II.2.18}$$

The coefficients $G^{(n)}_{\alpha z,\beta\xi}$ taking into account the relationship between the irreducible Hermit polynomials H^{ik} and the Sonin polynomials $S^k_{3/2}$:

$$\mathrm{H}^{\mathrm{ik}}(u)=(-2)^k k!\,S^k_{3/2}(\frac{u^2}{2})\mathrm{u} \tag{II.2.19}$$

can be expressed in terms of the integral brackets of the Sonin polynomials. In the case of completely ionized plasma the later calculations leads to the following results:

$$G^{(1)}_{\alpha z,\beta\xi}=-W_{\alpha z\beta\xi} \tag{II.2.20}$$

$$G^{(2)}_{\alpha z,\beta\xi}=\frac{3}{5}W_{\alpha z\beta\xi} \tag{II.2.21}$$

$$G^{(3)}_{\alpha z,\beta\xi}=-\frac{3}{14}W_{\alpha z\beta\xi} \tag{II.2.22}$$

$$G^{(4)}_{\alpha z,\beta\xi} = -\left(\frac{13}{10}\frac{m_\beta}{m_\alpha} + \frac{8}{5} + 3\frac{m_\alpha}{m_\beta}\right)\chi_{\alpha\beta}W_{\alpha z\beta\xi} \tag{II.2.23}$$

$$G^{(5)}_{\alpha z,\beta\xi} = -\frac{27}{10}\chi_{\alpha\beta}W_{\alpha z\beta\xi} \tag{II.2.24}$$

$$G^{(6)}_{\alpha z,\beta\xi} = \frac{3}{5}\left(\frac{23}{28}\frac{m_\beta}{m_\alpha} + \frac{8}{7} + 3\frac{m_\alpha}{m_\beta}\right)\chi_{\alpha\beta}W_{\alpha z\beta\xi} \tag{II.2.25}$$

$$G^{(7)}_{\alpha z,\beta\xi} = -\frac{45}{28}\chi_{\alpha\beta}W_{\alpha z\beta\xi} \tag{II.2.26}$$

$$G^{(8)}_{\alpha z,\beta\xi} = -\left(\frac{433}{280}\left(\frac{m_\beta}{m_\alpha}\right)^2 + \frac{139}{35}\frac{m_\beta}{m_\alpha} + \frac{459}{35} + \frac{32}{5}\frac{m_\alpha}{m_\beta} + 5\left(\frac{m_\alpha}{m_\beta}\right)^2\right)\chi^2_{\alpha\beta}W_{\alpha z\beta\xi} \tag{II.2.27}$$

$$G^{(9)}_{\alpha z,\beta\xi} = -\frac{75}{8}\chi^2_{\alpha\beta}W_{\alpha z\beta\xi} \tag{II.2.28}$$

where $\chi_{\alpha\beta} = \dfrac{m_\alpha m_\beta}{(m_\alpha + m_\beta)^2}$ and $W_{\alpha z\beta\xi} = W_{\beta\xi\alpha z} = n_{\alpha z}m_\alpha\nu_{\alpha z\beta\xi}$

$$\nu_{\alpha z\beta\xi} = \frac{4\sqrt{2\pi}}{3}e^4\lambda\frac{n_{\beta\xi}Z^2\xi^2}{T^{3/2}_{\alpha\beta}}\frac{\sqrt{\mu_{\alpha\beta}}}{m_\alpha} \tag{II.2.29}$$

and λ is the Coulomb logarithm, which due to weak dependence on the parameters, is used to be approximately the same for all sorts of species.

The system of linear algebraic equations (II.1.13-16) with coefficients $G^{(n)}_{\alpha z,\beta\xi}$ enables one to determine the velocity of diffusion and the heat fluxes in multi-component plasma for arbitrary values of $\omega\tau$. In the case of electron-ion plasma the solution of this system in the limit, when $m_e / m_i << 1$ leads to the Braginskii result obtained by using the Chapmen-Enscog method [11, 12].

Now we can derive the parallel (along B) friction forces and heat fluxes. The friction forces and heat fluxes along the B-field can be derived from equation (II.1.16) by taking $\omega_c = 0$. In this case, only the last two equations will in fact remain, while the first serves merely to determine the forces of friction in terms of the velocity and temperature gradient of the components. This quite complex system describes diffusion and heat transfer in plasma with species of arbitrary mass, which can

fortunately differ sensationally. This, in particular, helps to separate particles, whose masses are considerable less than the masses of the remaining particles. First of all, it concerns electrons. In addition, the masses of ions of one species but in different charge states are equal. The later fact enables one to calculate the longitudinal components in two stages: first to determine the mean values of the quantities for the particles of one sort, and then to obtain the difference between the partial and average values. Using this approach, the general expressions for the force of friction, thermal force and heat flux can be written in the following way:

$$\mathrm{R}_{\alpha z,//} = -\frac{n_{\alpha z} m_\alpha z^2}{\overline{z_\alpha^2}} \left\{ \sum_\beta \left[\frac{c_{\alpha\beta}^{(1)}}{\tau_{\alpha\beta}} \left(w_{\alpha z,//} - \overline{w}_{\beta,//} \right) - c_{\alpha\beta}^{(2)} \frac{\tau_\beta}{\tau_{\alpha\beta}} \frac{\nabla_{//} T_\beta}{m_\beta} \right] + \frac{\overline{z_\alpha^2}}{z^2} c_\alpha^{(5)} \frac{\nabla_{//} T_{\alpha z}}{m_\alpha} \right\} \qquad \text{(II.2.30)}$$

$$\mathrm{h}_{\alpha z,//} = p_{\alpha z} \tau_{\alpha z} \left\{ \sum_\beta \left[\frac{c_{\beta\alpha}^{(2)}}{\tau_{\alpha\beta}} \left(w_{\alpha z,//} - \overline{w}_{\beta,//} \right) - c_{\alpha\beta}^{(3)} \frac{\tau_\beta}{\tau_{\alpha\beta}} \frac{\nabla_{//} T_\beta}{m_\beta} \right] - \frac{\overline{z_\alpha^2}}{z^2} c_\alpha^{(6)} \frac{\nabla_{//} T_{\alpha z}}{m_\alpha} \right\} \qquad \text{(II.2.31)}$$

where $\tau_\alpha^{-1} = \sum_\beta \tau_{\alpha\beta}^{-1}$. The numerical coefficients $c_{\alpha\beta}^{(n)}$ are found from the solution of the set of equations for the mean values, while $c_\alpha^{(n)}$ is found from the equations for the difference between the partial and mean values. In this case the relation between them reads:

$$c_{\alpha\beta}^{(1)} = c_{\beta\alpha}^{(1)}, \qquad \sum_\beta \frac{c_{\alpha\beta}^{(1)}}{\tau_{\alpha\beta}} = \frac{c_\alpha^{(4)}}{\tau_\alpha}, \qquad \sum_\beta \frac{c_{\beta\alpha}^{(21)}}{\tau_{\alpha\beta}} = \frac{c_\alpha^{(5)}}{\tau_\alpha}, \qquad c_{\alpha\beta}^{(31)} = c_{\beta\alpha}^{(3)} \qquad \text{(II.2.32)}$$

the summation here is carried out only over the different sorts of species.

Hence, the problem now is reduced to finding the coefficients $c_{\alpha\beta}^{(n)}$ and $c_\alpha^{(n)}$ for components with different particle masses. The general expressions for these quantities are quite cumbersome, however for light particles (at list one sort of such particles (electrons) always present in plasma) an explicit form of the coefficients can be obtained using an expansions with respect to small parameter m_k / m_α (the index k relates to the light particles). In the zero approximation to that parameter the set of equations for these coefficients splits into two independent equations for the light component and for the heavy one with $m_\alpha >> m_k$. For the light component one has:

$$c_{k\alpha}^{(1)} = \frac{\left(1 + 0.24 z_k^*\right)\left(1 + 0.93 z_k^*\right)}{\Delta_k}, \qquad \text{(II.2.33)}$$

$$c_{k\alpha}^{(2)} = 0,$$

$$c_{\alpha k}^{(2)} = 1.56\frac{\left(1+\sqrt{2}z_k^*\right)\left(1+0.52z_k^*\right)}{\Delta_k}, \qquad c_{k\alpha}^{(3)} = 0\,, \tag{II.2.34}$$

$$c_k^{(5)} - c_{kk}^{(2)}\frac{\tau_k}{\tau_{kk}} = 2.2z_k^*\frac{\left(1+0.52z_k^*\right)}{\Delta_k}, \tag{II.2.35}$$

$$c_k^{(6)} + c_{kk}^{(3)}\frac{\tau_k}{\tau_{kk}} = 3.9z_k^*\frac{\left(1+\sqrt{2}z_k^*\right)\left(1+1.7z_k^*\right)}{\Delta_k} \tag{II.2.36}$$

where $\Delta_k = \left(1+2.65z_k^*\right)\left(1+0.285z_k^*\right)$ and $z_k^* = \sum_\alpha n_\alpha \overline{z_\alpha^2} / n_k \overline{z_k^2}$.

The summation here is carried out over all the sorts of particles α for which $m_\alpha >> m_k$. Here was also assumed that in majority of cases the light particles are those particles with only one possible charge state, so that $c_{kk}^{(n)}$ and $c_k^{(n)}$ occur in (II.2.30) and (II.2.31) in only certain combinations. Note, that if the condition $T_k / m_k >> T_\alpha / m_\alpha$ is satisfied, the separation of the equation for the light particles is also possible, if their temperature differs from the temperature of remaining components. In this case it is necessary to use their own temperatures in the coefficients of the expressions for the friction force and the heat flux for the light particles. Obviously, this procedure of separation of lightest particles can be further extended, because in plasma remains again a component for which $m_i << m_\alpha$, where $\alpha \neq i,k$ (e.g. hydrogen isotopes in a plasma with heavy impurities). The coefficients $c_{\alpha\beta}^{(n)}$ and $c_\alpha^{(n)}$ for the heavy particles and masses that are not too different, remaining in the result of the last separation all the light components. These coefficients for two heavy impurities were calculated and the result can be presented as:

$$c = P_1 + P_2 /\left(Z_{iI} + P_3\right) \tag{II.2.37}$$

where $Z_{iI} = n_I \overline{Z_I^2} / n_i \overline{Z_i^2}$. The index I corresponds to the heaviest component of the plasma. The values of the constant P_n (for any pair from the set carbon, oxygen, iron and tungsten) are given in Table 1.

The viscosity tensor for parallel moment transfer reads as:

$$\pi_{ij} = -\frac{3}{2}\eta^{(0)}\left(\delta_{ik}^{//} - \frac{1}{3}\delta_{ik}\right)\left(\delta_{kl}^{//} - \frac{1}{3}\delta_{kl}\right)W_{kl} \tag{II.2.38}$$

where $\delta_{ik}^{//} = \begin{pmatrix} 0 & 0 & 0 \\ 0 & 0 & 0 \\ 0 & 0 & 1 \end{pmatrix}$ and $W_{kl} = \frac{\partial V_k}{\partial x_l} + \frac{\partial V_l}{\partial x_k} - \frac{2}{3}\delta_{ik}\frac{\partial V_k}{\partial x_k}$. (II.2.39)

The parallel viscosity coefficient can be presented as:

$$\eta_{\alpha z}^{(0)} = p_\alpha \tau_\alpha \left(\sum_\beta c_{\alpha\beta} \tau_\beta \tau_{\alpha\beta}^{-1} + c_\alpha \frac{\overline{z_\alpha^2}}{z^2} \right) \quad \text{(II.2.40)}$$

Now the calculation of parallel viscosity coefficients for each charge state of ion is reduced to calculation of $c_{\alpha\beta}$ and c_α for different sorts of ions. For the light particles

$$c_k + \frac{\tau_k}{\tau_{kk}} c_{kk} = 0.96 \frac{\left(1+\sqrt{2}z_k^*\right)^2}{\left(1+1.8z_k^*\right)\left(1+0.6z_k^*\right)} \quad \text{and} \quad c_{k\alpha} = 0 \quad \text{(II.2.41)}$$

For definition of these coefficients in the case of several heavy ions with arbitrary masses the numerical calculations are needed. However, for the heaviest component these coefficients can be found analytically:

$$c_{\alpha\alpha} = 0.167 \qquad c_\alpha = 0.793 \quad \text{(II.2.42)}$$

in the case of two heavy components these coefficients can be estimated numerically
(See **Tab. I**)

- Transport coefficients and forces for light particles (e.g. electrons and protons) in multi-component plasma can be easily obtained from (II.2.30-31). The light components are those whose masses are satisfied the following chain of inequalities:
  $m_1 << m_2 << m_3 << ...$ and so on. Let's define them by index k, and then the particle, heat and viscous fluxes can be written as:

$$\mathrm{R}_{k,//} = -\frac{e_k^2 n_k^2}{\sigma_{k,//}} \mathrm{u}_{//} - \gamma_{k,//} \frac{\nabla_{//} T_k}{T_k}, \quad \text{(II.2.43)}$$

$$\mathrm{h}_{k,//} = -\gamma_{k,//} \mathrm{u}_{//} - \chi_{k,//} \nabla_{//} T_k \quad \text{(II.2.44)}$$

$$h_{k,//} = q_{k,//} - \frac{5}{2} p_{k,//} V_{k,//} \tag{II.2.45}$$

$$R_{k,\perp} = -\frac{e_k^2 n_k^2}{\sigma_{k,//}} u_\perp - \frac{e_k^2 n_k^2}{\sigma_{k,//}} [b u_\perp] - \gamma_{k,\perp} \frac{\nabla_\perp T_k}{T_k} - \gamma_{k,\Lambda} \frac{[b \nabla T_k]}{T_k} \tag{II.2.46}$$

$$h_{k,\perp} = -\gamma_{k,\perp} u_\perp - \gamma_{k,\Lambda} [b u] - \chi_{k,\perp} \nabla_\perp T_k - \chi_{k,\Lambda} [b \nabla T_k], \tag{II.2.47}$$

where

$$\sigma_{k,//} = \sigma_{//} \frac{0.51}{(1+1.8 z_k^*)(1+0.93 z_k^*) z_k^*}, \quad \sigma_{k,\perp} = \sigma_\perp / z_k^* \quad , \quad \sigma_{k,\Lambda} = \sigma_\Lambda / (z_k^*)^2 \tag{II.2.48}$$

$$\gamma_{k,//} = \gamma_{//} \frac{3.09 z_k^* (1+0.52 z_k^*)}{(1+2.65 z_k^*)(1+0.285 z_k^*)}, \quad \gamma_{k,\perp} = \gamma_\perp z_k^* (1+0.745 z_k^*), \quad \gamma_{k,\Lambda} = \gamma_\Lambda z_k^* \tag{II.2.49}$$

$$\chi_{k,//} = \chi_{//} \frac{1.74(1+1.7 z_k^*)}{(1+2.65 z_k^*)(1+0.285 z_k^*)}, \quad \chi_{k,\perp} = \chi_\perp (0.3+0.7 z_k^*), \quad \chi_{k,\Lambda} = \chi_\Lambda \tag{II.2.50}$$

Table I (i – the light impurity ion, I – the heavy impurity ion)

	C - O	Fe -W	O -Fe	C -Fe	O -W	C -W
m_i/m_I	**0,750**	**0,304**	**0,286**	**0,214**	**0,087**	**0,065**
$c_{ii}^{(1)}$ P_1	0,74	0,83	0,63	0,63	0,62	0,62
P_2	0,09	0,11	0,11	0,10	0,09	0,09
P_3	0,86	0,53	0,53	0,49	0,45	0,45
$c_{iI}^{(1)}$ P_1	0,77	0,55	0,54	0,48	0,38	0,36
P_2	0,10	0,27	0,27	0,29	0,30	0,31
P_3	0,87	0,63	0,62	0,57	0,50	0,49
$c_{II}^{(1)}$ P_1	0,84	0,84	0,84	0,84	0,84	0,84
P_2	0,12	0,36	0,36	0,38	0,33	0,31
P_3	0,88	0,65	0,63	0,58	0,49	0,48
$c_{ii}^{(2)}$ P_1		0,38	0,38	0,40	0,47	0,49
P_2	0,51	0,11	0,10	0,01	0,01	0,01
P_3	0,07	0,55	0,51	0,10	0,10	0,10
	0,92					
$c_{iI}^{(2)}$ P_1	0,37	-0,07	-0,08	-0,12	-0,11	-0,09
P_2	0,07	0,27	0,27	0,27	0,18	0,14
P_3	1,00	1,16	1,15	1,15	1,12	1,10
$c_{Ii}^{(2)}$ P_1	0,75	1,14	1,16	1,28	1,29	1,29
P_2	0,04	0,02	0,02	0,01	0,00	0,00
P_3	0,80	0,10	0,10	0,08	0,00	0,00
$c_{II}^{(2)}$ P_1	0,59	0,58	0,59	0,59	0,58	0,58
P_2	0,04	-0,12	-0,45	-0,30	-0,32	-0,31
P_3	0,86	13,00	8,00	2,90	1,40	1,2
$c_i^{(5)}$ P_1	0,75	1,17	1,19	1,26	1,37	1,39
P_2	-0,17	-0,78	-0,78	-0,95	-1,19	-1,26
P_3	1,09	1,38	1,37	1,48	1,56	1,59
$c_I^{(5)}$ P_1	0,59	0,58	0,58	0,58	0,57	0,57
P_2	-0,15	-0,52	-0,53	-0,56	-0,50	-0,46
P_3	1,09	1,26	1,25	1,21	0,95	0,86
$c_{ii}^{(3)}$ P_1	1,54	2,57	2,69	3,41	6,79	8,00
P_2	-0,31	-4,00	-4,65	-8,80	-38,00	-52,00
P_3	1,28	3,10	3,29	4,10	6,80	7,64
$c_{iI}^{(3)}$ P_1	1,35	0,64	0,56	0,20	-0,50	-0,55
P_2	-0,28	-0,17	-0,07	1,20	4,00	4,50
P_3	1,26	1,48	1,90	6,00	6,00	6,60
$c_{iI}^{(3)}$ P_1	1,29	1,29	1,29	1,29	1,27	1,28
P_2	-0,30	-1,67	-1,74	-2,02	-2,10	-1,96
P_3	1,25	2,02	2,05	2,16	2,00	1,84
$c_i^{(6)}$ P_1	3,17	5,32	5,49	6,30	8,85	9,55
P_2	-0,64	-5,05	-5,53	-8,11	-19,10	-23,00
P_3	1,16	1,87	1,93	2,20	3,10	3,31
$c_I^{(6)}$ P_1	2,61	2,81	2,61	2,61	2,80	2,80
P_2	-0,53	-2,13	-2,21	-2,47	-2,51	-2,36
P_3	1,15	1,83	1,65	1,70	1,53	1,41

$$\eta_k^{(0)} = \eta^{(0)} \frac{1.86\left(1+\sqrt{2}z_k^*\right)}{\left(1+1.8z_k^*\right)\left(1+0.6z_k^*\right)}, \tag{II.2.51}$$

$$\eta_k^{(1,2)} = \eta^{(1,2)}\left(0.3+0.42z_k^* - 0.28 z_k z_k^*/z_I\right),\ \eta_k^{(3,4)} = \chi^{(3,4)} \tag{II.2.52}$$

and values without indexes are the electron coefficients for pure hydrogen plasma:

$$\sigma_{//} = 1.96\frac{e^2 n_e \tau_{ep}}{m_e},\quad \sigma_{\perp} = \frac{e^2 n_e \tau_{ep}}{m_e},\quad \sigma_{\Lambda} = -0.59\frac{e^2 n_e \tau_{ep}}{m_e}\left(\omega_e \tau_{ep}\right) \tag{II.2.53}$$

$$\gamma_{//} = 0.75 n_e T_e,\qquad \gamma_{\perp} = 5.1\frac{n_e T_e}{\left(\omega_e \tau_{ep}\right)^2},\qquad \gamma_{\Lambda} = -1.5\frac{n_e T_e}{\omega_e \tau_{ep}} \tag{II.2.54}$$

$$\chi_{//} = 3.16\frac{T_e n_e \tau_{ep}}{m_e},\quad \chi_{\perp} = 4.66\frac{T_e n_e \tau_{ep}}{m_e\left(\omega_e \tau_{ep}\right)^2},\quad \chi_{\Lambda} = -2.5\frac{n_e T_e}{m_e \omega_e} \tag{II.2.55}$$

$$\eta^{(0)} = 0.73 T_e n_e \tau_{ep},\quad \eta^{(1)} = 0.71 T_e n_e \tau_{ep}/\left(\omega_e \tau_{ep}\right)^2,\quad \eta^{(3)} = \frac{n_e T_e}{2\omega_e} \tag{II.2.56}$$

For electron coefficients in plasma with impurities in the above given formulas z_k^* must be replaced by z_{eff}, and for light ions - $z_i^* = \sum_I n_I \overline{z_I^2}/n_i z_i^2$, where the index I corresponds to ions with $m_I >> m_i$. In the case of hydrogen ions all indexes e in formulas must be replicated by i (at that ω_i changes the sign) and τ_{ep} must be replaced by $\tau_{ii}/\sqrt{2}$.

For electron thermal and friction force along B one has:

$$R_{e,//} = -c_{e\beta}^{(1)}\frac{m_e n_e}{\tau_{e\beta}}\left(V_e - \overline{V_\beta}\right) - \beta n_e \nabla_{//} T_e = e n_e j_e/\sigma_{//} - \beta n_e \nabla_{//} T_e, \tag{II.2.57}$$

where

$$j = -e n_e\left(V_e - \overline{V_\beta}\right),\qquad \overline{V_\beta} = \frac{\sum_j n_{\beta Z_j} Z_j^2 V_{Z_j}}{n_e Z_{eff}} \tag{II.2.58}$$

$$\sigma_{//} = \frac{1.96 e^2 n_e \tau_e^*}{m_e}\left\{\frac{0.51\Delta\left(Z_{eff}\right)}{\left(1+0.24Z_{eff}\right)\left(1+0.93Z_{eff}\right)Z_{eff}}\right\} \tag{II.2.59}$$

$$\Delta(Z_{eff}) = (1+0.265Z_{eff})(1+0.285Z_{eff}) \tag{II.2.60}$$

$$\tau_e^* = 1/\left(\frac{4\sqrt{2\pi}}{3} \cdot \frac{e^2 \ln\Lambda}{\sqrt{m_e} T_e^{3/2}} n_e Z_{eff} \right) \qquad \text{(II.2.61)}$$

and $$\beta = 0.71 \left[\frac{3.09 Z_{eff}(1 + 0.52 Z_{eff})}{\Delta(Z_{eff})} \right] \qquad \text{(II.2.62)}$$

Therefore at high Z_{eff} conductivity increases almost twice (1.72 times) compare with pure plasma. The thermal force coefficient increases from 0.71 to 1.51 (~2.1 times)

II.3 The Reduce Charge State approach for impurity transport along B.

The presence of several different multiply charged ions in the divertor plasma increases immensely the number of equation to be solved. The fluid equations for separate charge states of a given isotope can be replaced by a set of averaged equations representing an effective single reduced charge state [8, 9]. These equations are fewer in number than the original equations for the individual ions by a factor of $Z_{\max}$ for each species α. This Reduce Charge State approach was incorporated into B2 Code allowing one to simulate divertor and the SOL plasmas with multiple ion species plasma without excessive time consumption. Based on the fact, that charge number enters in collision term symmetrically for each pair of multiply ionised ions, one can find the following property of coefficients, entering in Esq. (II.I.14-17):

$$G^{(n)}_{\alpha z \beta \xi} = I_{\alpha z} I_{\beta \xi} \overline{G^{(n)}_{\alpha\beta}}, \qquad \text{(II.3.57)}$$

where $I_{\alpha z} = \frac{n_{\alpha z} z^2}{n_\alpha \overline{z^2_\alpha}}$, $\quad \overline{G^{(n)}_{\alpha\beta}} = \sum_{z,\xi} G^{(n)}_{\alpha z \beta \xi}$, $\quad n_\alpha = \sum_z n_{\alpha,z}$, $\quad \overline{z^2_\alpha} = \frac{\sum_z n_{\alpha z} z^2}{n_\alpha}$ $\qquad \text{(II.3.58)}$

Summing up equations (II.1.14-17) in the case of $\omega_{\alpha z} = 0$ over the charge state ξ and using above shown properties of the coefficients, one can come to reduced number of equation (equal to the number of nucleus) for some average values:

$$\frac{5}{2} n_{\alpha z} \nabla_{//} T_{\alpha z} =$$
$$= I_{\alpha z} \sum_\beta \left\{ \frac{5}{2} \frac{\mu_{\alpha\beta}}{m_\alpha} \overline{G^{(2)}_{\alpha\beta}} \left(\mathrm{w}_{\alpha z} - \overline{\mathrm{w}_\beta} \right) + \overline{G^{(4)}_{\alpha\beta}} \frac{\mathrm{h}_{\alpha z}}{p_{\alpha z}} - \overline{G^{(5)}_{\alpha\beta}} \frac{\mathrm{h}_\beta}{p_\beta} + \frac{\mu_{\alpha\beta}}{T_{\alpha\beta}} \left(\overline{G^{(6)}_{\alpha\beta}} \frac{\mathrm{r}_{\alpha z}}{p_{\alpha z}} - \overline{G^{(7)}_{\alpha\beta}} \frac{\overline{\mathrm{r}_\beta}}{p_\beta} \right) \right\} \qquad \text{(II.3.59)}$$

$$0 = I_{\alpha z}\sum_{\beta}\left\{\frac{35}{2}\left(\frac{\mu_{\alpha\beta}}{m_\alpha}\right)^2\overline{G^{(3)}_{\alpha\beta}}\left(\mathrm{w}_{\alpha z}-\overline{\mathrm{w}_\beta}\right)+\frac{7\mu_{\alpha\beta}}{m_\alpha}\left(\overline{G^{(6)}_{\alpha\beta}}\frac{\mathrm{h}_{\alpha z}}{p_{\alpha z}}-G^{(7)}_{\varepsilon\beta}\frac{\mathrm{h}_\beta}{p_\beta}\right)+\overline{G^{(8)}_{\alpha\beta}}\frac{m_\alpha}{T_{\alpha\beta}}\frac{\mathrm{r}_{\alpha z}}{p_{\alpha z}}-\overline{G^{(9)}_{\alpha\beta}}\frac{m_\beta}{T_{\alpha\beta}}\frac{\overline{\mathrm{r}_\beta}}{p_\beta}\right\} \qquad \text{(II.3.60)}$$

where $\overline{\mathrm{w}_\alpha}=\sum_z I_{\alpha z}\mathrm{w}_{\alpha z}$, $\overline{\mathrm{h}_\alpha}=p_\alpha\sum_z I_{\alpha z}\mathrm{h}_{\alpha z}/p_{\alpha z}$, $\overline{\mathrm{r}_\alpha}=p_\alpha\sum_z I_{\alpha z}\mathrm{r}_{\alpha z}/p_{\alpha z}$ are the mean value of the quantities $\mathrm{w}_{\alpha z}$, $\mathrm{h}_{\alpha z}$ and $\mathrm{r}_{\alpha z}$ for α species. Summing now the above equations over z, we arrive at the following set of equations:

$$\frac{5}{2}n_\alpha\nabla_{//}T_\alpha=\sum_\beta\left\{\frac{5}{2}\frac{\mu_{\alpha\beta}}{m_\alpha}\overline{G^{(2)}_{\alpha\beta}}\left(\overline{\mathrm{w}_\alpha}-\overline{\mathrm{w}_\beta}\right)+\overline{G^{(4)}_{\alpha\beta}}\frac{\bar{\mathrm{h}}_\alpha}{p_\alpha}-\overline{G^{(5)}_{\alpha\beta}}\frac{\mathrm{h}_\beta}{p_\beta}+\frac{\mu_{\alpha\beta}}{T_{\alpha\beta}}\left(\overline{G^{(6)}_{\alpha\beta}}\frac{\bar{\mathrm{r}}_\alpha}{p_\alpha}-\overline{G^{(7)}_{\alpha\beta}}\frac{\overline{\mathrm{r}_\beta}}{p_\beta}\right)\right\} \qquad \text{(II.3.61)}$$

$$0=\sum_\beta\left\{\frac{35}{2}\left(\frac{\mu_{\alpha\beta}}{m_\alpha}\right)^2\overline{G^{(3)}_{\alpha\beta}}\left(\overline{\mathrm{w}_\alpha}-\overline{\mathrm{w}_\beta}\right)+\frac{7\mu_{\alpha\beta}}{m_\alpha}\left(\overline{G^{(6)}_{\alpha\beta}}\frac{\bar{\mathrm{h}}_\alpha}{p_\alpha}-G^{(7)}_{\varepsilon\beta}\frac{\bar{\mathrm{h}}_\beta}{p_\beta}\right)+\overline{G^{(8)}_{\alpha\beta}}\frac{m_\alpha}{T_{\alpha\beta}}\frac{\bar{\mathrm{r}}_\alpha}{p_\alpha}-\overline{G^{(9)}_{\alpha\beta}}\frac{m_\beta}{T_{\alpha\beta}}\frac{\overline{\mathrm{r}_\beta}}{p_\beta}\right\} \qquad \text{(II.3.62)}$$

The number of obtained equations after summation over charge states is considerable reduced to the number of nucleus, equal α and β. The formal solution of these equations enables one to express $\bar{\mathrm{r}}_\alpha$ and $\bar{\mathrm{h}}_\alpha$ in terms of $\overline{\mathrm{w}}_\alpha$ and $\nabla_{//}T_\alpha$. Substituting these quantities into the right side of equation

$$\rho_{\alpha z}\left(\frac{d\mathrm{u}}{dt}-\frac{\mathrm{F}_{\alpha z}}{m_\alpha}\right)+\nabla p_{\alpha z}-\rho_{\alpha z}\omega_{\alpha z}[\mathrm{w}_{\alpha z}\mathrm{b}]=$$
$$=\sum_{\beta,\xi}\left\{G^{(1)}_{\alpha z,\beta\xi}(\mathrm{w}_{\alpha z}-\mathrm{w}_{\beta\xi})+\frac{\mu_{\alpha\beta}}{T_{\alpha\beta}}G^{(2)}_{\alpha z,\beta\xi}\left(\frac{\mathrm{h}_{\alpha z}}{\rho_{\alpha z}}-\frac{\mathrm{h}_{\beta\xi}}{\rho_{\beta\xi}}\right)+\frac{\mu^2_{\alpha\beta}}{T^2_{\alpha\beta}}G^{(3)}_{\alpha z,\beta\xi}\left(\frac{\mathrm{r}_{\alpha z}}{\rho_{\alpha z}}-\frac{\mathrm{r}_{\beta\xi}}{\rho_{\beta\xi}}\right)\right\} \qquad \text{(II.3.63)}$$

(which must be beforehand sum up over charge states z,ξ), one can determine $\overline{\mathrm{w}}_\alpha$ values.

Apart the average mean values, the partial values for each charge state can be calculate in the next step. In order to determine these properties we will divide Esq. (II.3.59) into $I_{\alpha z}$ and subtract from equation (II.3.62). As a result, we have

$$\frac{5}{2}n_\alpha\left(\nabla_{//}T_\alpha-\frac{\overline{z^2_\alpha}}{z^2}\nabla_{//}T_{\alpha z}\right)=\left(\overline{\mathrm{w}_\alpha}-\mathrm{w}_\alpha\right)S^{(2)}_\alpha+\left(\frac{\bar{\mathrm{h}}_\alpha}{p_\alpha}-\frac{\mathrm{h}_{\alpha z}}{p_{\alpha z}}\right)S^{(1)}_\alpha+\left(\frac{\bar{\mathrm{r}}_\alpha}{p_\alpha}-\frac{\mathrm{r}_{\alpha z}}{p_{\alpha z}}\right)\frac{m_\alpha}{T_{\alpha\beta}}S^{(6)}_\alpha \qquad \text{(II.3.64)}$$

$$0=\left(\overline{\mathrm{w}}_\alpha-\mathrm{w}_{\alpha z}\right)S^{(3)}_\alpha+7\left(\frac{\bar{\mathrm{h}}_\alpha}{p_\alpha}-\frac{\mathrm{h}_{\alpha z}}{p_{\alpha z}}\right)S^{(6)}_\alpha+\left(\frac{\bar{\mathrm{r}}_\alpha}{p_\alpha}-\frac{\mathrm{r}_{\alpha z}}{p_{\alpha z}}\right)\frac{m_\alpha}{T_{\alpha\beta}}S^{(8)}_\alpha \qquad \text{(II.3.65)}$$

where $S^{(2)}_\alpha=\frac{5}{2}\sum_\beta\mu_{\alpha\beta}\overline{G}^{(2)}_{\alpha\beta}/m_\alpha$, $\quad S^{(4)}_\alpha=\sum_\beta\overline{G}^{(4)}_{\alpha\beta}$, $\quad S^{(3)}_\alpha=\frac{35}{2}\sum_\beta\left(\frac{\mu_{\alpha\beta}}{m_\alpha}\right)^2\overline{G}^{(3)}_{\alpha\beta}$

$$S_\alpha^{(6)} = \sum_\beta \mu_{\alpha\beta} \overline{G}_{\alpha\beta}^{(6)} / m_\alpha \,, \quad S_\alpha^{(8)} = \sum_\beta \overline{G}_{\alpha\beta}^{(8)} \tag{II.3.66}$$

Solution of equation (II.3.64) for $\frac{\overline{\mathrm{h}}_\alpha}{p_\alpha} - \frac{\mathrm{h}_{\alpha z}}{p_{\alpha z}}$ can be written in the form:

$$\frac{\mathrm{h}_{\alpha z}}{p_{\alpha z}} = -\frac{\overline{\mathrm{h}}_\alpha}{p_\alpha} + c_\alpha^{(6)} \left(\mathrm{w}_{\alpha z} - \overline{\mathrm{w}}_\alpha \right) + \frac{\tau_\alpha}{\tau_{\alpha\alpha}} c_\alpha^{(5)} n_\alpha \left(\frac{\overline{z}_\alpha^2}{z^2} \nabla_{//} T_{\alpha z} - \nabla_{//} T_\alpha \right), \tag{II.3.67}$$

where

$$c_\alpha^{(5)} = \frac{5}{2} \frac{S_\alpha^{(2)}}{D_\alpha} \frac{\tau_{\alpha\alpha}}{\tau_\alpha}, \quad c_\alpha^{(6)} = \frac{S_\alpha^{(2)} S_\alpha^{(8)} - S_\alpha^{(3)} S_\alpha^{(6)}}{D_\alpha}, \quad D_\alpha = S_\alpha^{(4)} S_\alpha^{(8)} - 7 \left(S_\alpha^{(6)} \right)^2 \tag{II.3.68}$$

$$c_\alpha^{(4)} = 1 - \frac{2}{5} \frac{\left[\left(S_\alpha^{(2)} \right)^2 S_\alpha^{(8)} - 2 S_\alpha^{(2)} S_\alpha^{(3)} S_\alpha^{(6)} + \left(S_\alpha^{(3)} \right)^2 S_\alpha^{(6)} / 7 \right]}{D_\alpha \tau_{\alpha\alpha}} \tag{II.3.69}$$

This solution together with solution for $\overline{\mathrm{h}}_\alpha$ brings to expressions for $\mathrm{R}_{\alpha z,//}$ and $\mathrm{h}_{\alpha z,//}$:

$$\mathrm{R}_{\alpha z,//} = -\frac{n_{\alpha z} m_\alpha z^2}{\overline{z_\alpha^2}} \left\{ \sum_\beta \left[\frac{c_{\alpha\beta}^{(1)}}{\tau_{\alpha\beta}} \left(w_{\alpha z,//} - \overline{w}_{\beta,//} \right) - c_{\alpha\beta}^{(2)} \frac{\tau_\beta}{\tau_{\alpha\beta}} \frac{\nabla_{//} T_\beta}{m_\beta} \right] + \frac{\overline{z_\alpha^2}}{z^2} c_\alpha^{(5)} \frac{\nabla_{//} T_{\alpha z}}{m_\alpha} \right\}$$

$$\mathrm{h}_{\alpha z,//} = p_{\alpha z} \tau_{\alpha z} \left\{ \sum_\beta \left[\frac{c_{\beta\alpha}^{(2)}}{\tau_{\alpha\beta}} \left(w_{\alpha z,//} - \overline{w}_{\beta,//} \right) - c_{\alpha\beta}^{(3)} \frac{\tau_\beta}{\tau_{\alpha\beta}} \frac{\nabla_{//} T_\beta}{m_\beta} \right] - \frac{\overline{z_\alpha^2}}{z^2} c_\alpha^{(6)} \frac{\nabla_{//} T_{\alpha z}}{m_\alpha} \right\}$$

II.4 Analysis of impurity transport parallel to the magnetic field lines

The force acting on impurity ions of charge *Z* parallel to the magnetic field *B* is

$$F_{total} \cong -\nabla_{//} p_j + e Z_j n_j E_{//} + F_j^D + F_j^T \quad , \tag{II.4.70}$$

where the thermal and friction forces $F_j^D + F_j^T = R_{\alpha z,//}$ and

$$\mathrm{R}_{\alpha z,//} = -\frac{n_{\alpha z} m_\alpha z^2}{\overline{z_\alpha^2}} \left\{ \sum_\beta \left[\frac{c_{\alpha\beta}^{(1)}}{\tau_{\alpha\beta}} \left(w_{\alpha z,//} - \overline{w}_{\beta,//} \right) - c_{\alpha\beta}^{(2)} \frac{\tau_\beta}{\tau_{\alpha\beta}} \frac{\nabla_{//} T_\beta}{m_\beta} \right] + \frac{\overline{z_\alpha^2}}{z^2} c_\alpha^{(5)} \frac{\nabla_{//} T_{\alpha z}}{m_\alpha} \right\} \tag{II.4.71}$$

Assuming that impurity ion $\alpha \sim j,$ in average charge state denote as Z , then:

$$F_j^D == -\frac{n_{\alpha z} m_\alpha z^2}{\overline{z_\alpha^2}} \left\{ \sum_\beta \left[\frac{c_{\alpha\beta}^{(1)}}{\tau_{\alpha\beta}} \left(w_{\alpha z,//} - \overline{w}_{\beta,//} \right) \right] \right\} \cong m_Z n_j \nu_{j,i} (V_i - V_j) \approx n_j Z_j^2 V_i \qquad \text{(II.4.72)}$$

$$F_j^T = \frac{n_{\alpha z} m_\alpha z^2}{\overline{z_\alpha^2}} \left\{ \sum_\beta \left[c_{\alpha\beta}^{(2)} \frac{\tau_\beta}{\tau_{\alpha\beta}} \frac{\nabla_{//} T_\beta}{m_\beta} \right] - \frac{\overline{z_\alpha^2}}{z^2} c_\alpha^{(5)} \frac{\nabla_{//} T_{\alpha z}}{m_\alpha} \right\} \cong n_j \frac{Z_j^2}{1+\sqrt{2}Z_0} \nabla_{//} T_i + \beta n_j \frac{Z_j^2}{Z_{eff}} \nabla_{//} T_e$$

(II.4.73)

$$F_\alpha^{\ T} \sim \frac{m_\alpha n_\alpha V_\alpha}{\tau_{\alpha,\beta}} \frac{\lambda}{T} \frac{\partial T}{\partial x} \qquad \lambda \sim \tau_\alpha = \tau_{\alpha\alpha} + \tau_{\alpha\beta} \quad \alpha \neq \beta \qquad \text{(II.4.74)}$$

Three cases can be distinguished: low concentration level, intermediate and strong.

- In trace approximation, when $n_z << n_i \approx n_e$, in steady state: $F_j^T = 0$

$$en_e E_{//} = -\nabla_{//} p_e - \beta n_e \nabla_{//} T_{e,} \quad p \approx const., \; T \approx T_e \approx T_i$$

and impurity ions follow the electron temperature profile:

$n_{Z_j} = T^{k_j}$, where $k = k(n_e, Z_{eff}, Z_0)$

In multi-component plasma, effect of impurities on plasma behaviour depends on impurity content in the mixture and is determined by three parameters, electron density, Z_{eff} and Z_0:

$$n_e = n_i + \sum_z n_{\alpha z} Z, \qquad Z_{eff} \equiv \left(n_i + \sum_z n_{\alpha z} Z^2 \right) / n_e$$

$$Z_0 \equiv \sum_z n_{\alpha z} Z^2 / n_i$$

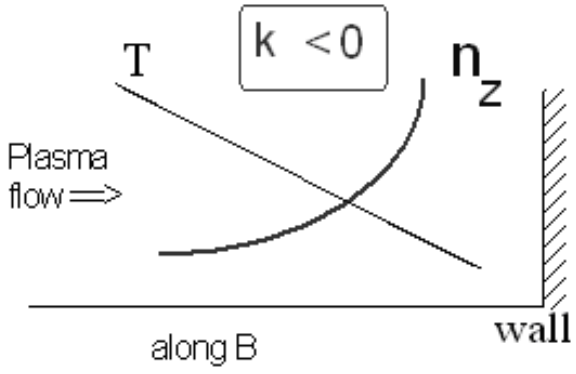

Fig. II.1 Impurity distribution at strong friction $(k < 0)$

- Almost "pure" plasma (trace concentration): $Z_{eff} \cong 1$

$$\sum_z n_{\alpha z} Z^2 << n_i \cong n_e \qquad \text{(II.4.75)}$$

Impurities affect only the energy balance, not the main plasma.

$$\sum n_{Z_j} = n_Z \cong T^{\mathrm{k}} \qquad \text{(II.4.76)}$$

$k \equiv -1 + \beta\left(\frac{\overline{Z^2}}{Z_{eff}} - \bar{Z}\right) + c\frac{\overline{Z^2}}{1+\sqrt{2}Z_0}(1-\eta)$	$\eta \equiv \frac{Friction\ \ force}{Ion\ \ thermal\ \ force} \equiv \frac{q^C_{//}(convective)}{q^T_{//}(conductive)}$

where

- $\eta > 1$

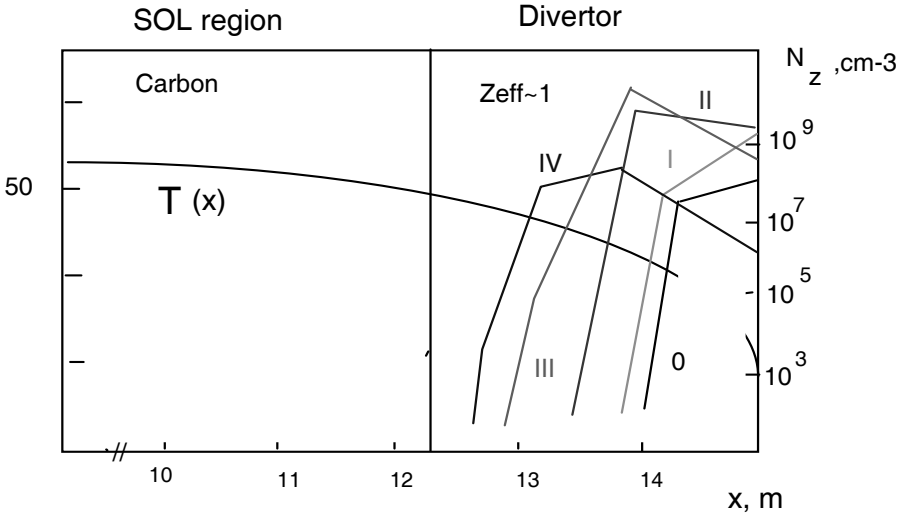

- $\eta < 1$

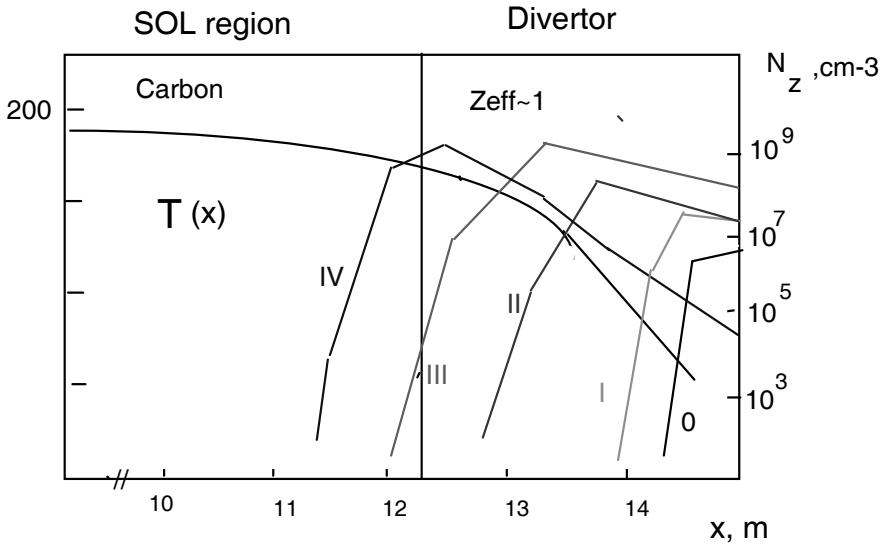

- Special distribution of the various impurity ions is strongly dependent on their charge state.

- High impurity concentration level:

$$\nu_{i,Z} / \nu_{i,i} \cong Z_0 \equiv \frac{\sum Z_j^2 n_j}{n_i} >> 1 \qquad \text{(II.4.77)}$$

$$n_e \approx \sum Z_j n_j \quad \Rightarrow \quad n_i / n_Z \to 0$$

- In this case the electric field effect is cancelled by the electron thermal force:

$$Z_{eff} \equiv (n_i + \sum n_j Z_j^2) / n_e \approx \sum n_j Z_j^2 / \sum n_j Z_j \approx \bar{Z} \qquad \text{(II.4.78)}$$

$$\boxed{k \equiv -1 + \beta\left(\frac{\overline{Z^2}}{Z_{eff}} - \bar{Z}\right) + C\frac{\overline{Z^2}}{1+\sqrt{2}Z_0}(1-\eta)}$$

- the ion thermal force becomes:

weakly dependent on charge state Z, and becomes small compared with drag force

$$n_z >> n_i$$

$$Z_0 \equiv \frac{n_Z}{n_i}(\sum n_Z Z_j^2 / n_Z) \approx \frac{n_i}{n_Z}\overline{Z^2} \qquad \text{(II.4.79)}$$

$$F_j^T \cong n_j \frac{Z_j^2}{1+\sqrt{2}Z_0}\nabla_{//}T_i \cong \frac{n_i}{n_Z}\nabla_{//}T_i \Rightarrow 0$$

$$F_j^D \sim m_Z n_j Z_j^2 \; V_i$$

- The distribution of impurity ions along B becomes weakly dependent on their charge state.
- Ion heat conduction in the case of high Zeff:

$$q_T \approx -\frac{\tau_{ii} n_i T_i}{m_i}\frac{\nu_{i,Z}}{\nu_Z}\nabla_{//}T_i \cong -\frac{\tau_{ii} n_i T_i}{m_i}\frac{1}{1+\sqrt{2}Z_0}\nabla_{//}T_i \qquad \text{(II.4.80)}$$

$$\nabla_{//}T_i \sim q_T Z_0$$

- the dependence of the ion thermal force on Z^2 can recover if ion heat flux remains the same at high impurity concentration.

- at low (or moderate) concentration of impurities the spatial impurity distribution depends on their charge states, whereas at high Z_{eff} the impurity distribution becomes weakly dependent on Z
- in the extreme case of high impurity concentration, the unfavourable thermal forces become less important, thus improving the retention. Both the impurity transport and the background plasma parameters are strongly coupled in this case and must be considered simultaneously.
- in the 2D case impurities can re-circulate in the SOL because the temperature gradient along the magnetic field lines in the inner part of the SOL is higher than in the outer part (cold). The impurity ions move upstream in the inner part of the SOL (by thermal force) and diffuse across the cold outer part where they are swept back by friction with background ions.
- the flow reversal of the background plasma can strongly deteriorate the impurity retention (upstream of the cushion in detached regimes) and helium exhaust

II.5 Classical transport in multi-species plasma in radial direction.

The necessity to use an additional equations for higher moments r_α and σ_α is required due to not sufficient accuracy in calculation of the parallel transport coefficients. In practical case of highly magnetized plasma the necessity in taking into account the higher moments for calculation of radial transport coefficients is unnecessary. Therefore, for estimation of radial transport coefficients it is sufficient a 13 moment approximation. In this case we employing the low order variables $\rho_\alpha, \mathrm{u}_\alpha, T_\alpha$ and the higher order variables $\pi_{\alpha rs}$ and q_α. As long as the tensor $\pi_{\alpha rs}$ is symmetric and its spur equals zero, it is defined by five independent components. The general number of variables in this case is equal $13N$ (where N is the number of plasma components). The corresponding system of closed equations can be presented as:

$$\frac{\partial \rho_\alpha}{\partial t} + \rho_\alpha \frac{\partial u_r}{\partial x_r} + \frac{\partial \rho_\alpha w_{\alpha r}}{\partial x_r} = 0 \qquad \text{(II.5.1)}$$

$$\rho \frac{\partial u_r}{\partial t} + \frac{\partial p}{\partial x_r} + \frac{\partial \pi_{rs}}{\partial x_s} = \sum_\alpha n_\alpha \langle F_{\alpha r} \rangle \qquad \text{(II.5.2)}$$

$$\frac{3}{2}\frac{\partial p_\alpha}{\partial t} + \frac{5}{2} p_\alpha \frac{\partial u_r}{\partial x_r} + \frac{\partial q_{\alpha r}}{\partial x_r} + \pi_{\alpha rs} \frac{\partial u_r}{\partial x_s} - n_\alpha w_{\alpha r} \langle F^*_{\alpha r} \rangle = R^{01}_\alpha \qquad \text{(II.5.3)}$$

$$\frac{\partial \rho_\alpha w_{\alpha r}}{\partial t} + \rho_\alpha w_{\alpha s} \frac{\partial u_r}{\partial x_s} + \rho_\alpha w_{\alpha s} \frac{\partial u_{\alpha r}}{\partial x_s} + \frac{\partial p_\alpha}{\partial x_r} + \frac{\partial \pi_{\alpha rs}}{\partial x_s} - n_\alpha \langle F^*_{\alpha r} \rangle = R^{10}_{\alpha r} \qquad \text{(II.5.4)}$$

$$\frac{\partial \pi_{\alpha rs}}{\partial t}+\pi_{\alpha rs}\frac{\partial u_l}{\partial x_l}+2\left\{\pi_{\alpha rl}\frac{\partial u_s}{\partial x_l}\right\}+\frac{4}{5}\left\{\frac{\partial q_{\alpha r}}{\partial x_s}\right\}+2p_\alpha\varepsilon_{rs}-2\left\{n_\alpha w_{\alpha r}\left\langle F^*_{\alpha s}\right\rangle\right\}-2\frac{e_\alpha}{m_\alpha}\left\{\left[\hat{\pi}_\alpha \mathrm{B}\right]_{rs}\right\}=R^{20}_{\alpha rs} \tag{II.5.5}$$

$$\frac{\partial h_{\alpha r}}{\partial t}+\frac{7}{5}h_{\alpha r}\frac{\partial u_r}{\partial x_s}+\frac{2}{5}h_{\alpha s}\frac{\partial u_s}{\partial x_r}+\frac{7}{5}h_{\alpha r}\frac{\partial u_l}{\partial x_l}+\frac{5}{3}p_\alpha w_{\alpha r}\frac{\partial u_l}{\partial x_l}+2p_\alpha w_{\alpha s}\varepsilon_{rs}+\frac{T_\alpha}{m_\alpha}\frac{\partial \pi_{\alpha rs}}{\partial x_s}+$$
$$+\frac{7\pi_{\alpha rs}}{2m_\alpha}\frac{\partial T_\alpha}{\partial x_s}+\frac{5p_\alpha}{2m_\alpha}\frac{\partial T_\alpha}{\partial x_r}+\frac{5p_\alpha}{2T_\alpha}w_{\alpha r}\frac{\partial T_\alpha}{\partial t}-\frac{\pi_{\alpha rs}}{m_\alpha}\left\langle F^*_{\alpha s}\right\rangle-\frac{e_\alpha}{m_\alpha}\left[\mathrm{h}_\alpha \mathrm{B}\right]_r=R^{11}_{\alpha r} \tag{II.5.6}$$

Here we use for shortening the following notations:

$$\{a_r b_s\}=\frac{1}{2}\left(a_r b_s+b_r a_s\right)-\frac{1}{3}a_l b_l \delta_{rs} \tag{II.5.7}$$

$$\varepsilon_{rs}=\left\{\frac{\partial u_r}{\partial x_s}\right\} \qquad \left[\pi_\alpha \mathrm{B}\right]_{rs}=\pi_{\alpha lr}\varepsilon_{slm}B_m\,, \tag{II.5.8}$$

where ε_{slm} is the permutation tensor. Note, that equations (II.5.3) and (II.5.4) are the conservation equations of energy and momentum for the α component of plasma. For all that

$$n_\alpha\left\langle \mathrm{F}^*_\alpha\right\rangle=n_\alpha\left(\mathrm{F}_\alpha\right)-\rho_\alpha\frac{\partial \mathrm{u}}{\partial \mathrm{t}} \tag{II.5.9}$$

$$\left\langle \mathrm{F}_\alpha\right\rangle=e_\alpha(\mathrm{E}+\left[\mathrm{u}_\alpha \mathrm{B}\right]/c)+\mathrm{X}_\alpha\,, \tag{II.5.10}$$

where X_α are forces of non-electromagnetic origin, e.g. gravitational force $m_\alpha \mathrm{g}$,

$$R^{10}_{\alpha r}=R_{\alpha r}=\sum_\beta G^{(1)}_{\alpha\beta}\left(w_{\alpha r}-w_{\beta r}\right)+\sum_\beta \gamma_{\alpha\beta}G^{(2)}_{\alpha\beta}\left(\frac{h_{\alpha r}}{\gamma_\alpha p_\alpha}-\frac{h_{\beta r}}{\gamma_\beta p_\beta}\right) \tag{II.5.11}$$

$$R^{01}_{\alpha r}=Q_\alpha=3\sum_\beta G^{(1)}_{\alpha\beta}\frac{\left(T_\alpha-T_\beta\right)}{m_\alpha+m_\beta}; \tag{II.5.12}$$

$$R^{20}_{\alpha rs}=\sum_\beta \frac{1}{\gamma_\alpha+\gamma_\beta}\left(G^{(3)}_{\alpha\beta}\frac{\pi_{\alpha rs}}{p_\alpha}+G^{(4)}_{\alpha\beta}\frac{\pi_{\beta rs}}{p_\beta}\right) \tag{II.5.13}$$

$$R^{11}_{\alpha r}=\frac{1}{\gamma_\alpha}\sum_\beta\left(w_{\alpha r}-w_{\beta r}\right)+\sum_\beta\left[G^{(5)}_{\alpha\beta}\frac{h_{\alpha r}}{p_\alpha}+G^{(6)}_{\alpha\beta}\frac{h_{\beta r}}{p_\beta}+\frac{5}{2}\frac{\gamma_{\alpha\beta}}{\gamma_\alpha}G^{(7)}_{\alpha\beta}\left(w_{\alpha r}-w_{\beta r}\right)+5\theta_{\alpha\beta}G^{(1)}_{\alpha\beta}w_{\alpha r}\right] \tag{II.5.14}$$

For these values the following conditions are obviously satisfied:

$$\sum_\alpha \mathrm{R}_\alpha=0 \quad \text{and} \quad \sum_\alpha Q_\alpha=0 \tag{II.5.15}$$

The coefficients $G_{\alpha\beta}^{(n)}$ are the linear combination of the Chapman-Cowling's integrals generalized for different temperatures of plasma species (see expressions above).

The equations (II.5.1-6) can be considerably simplified in the case of small gradients and proximity to the local equilibrium [13]. In that case all second order terms in equations can be omitted and the coefficients in the right hand side of equations $G_{\alpha\beta}^{(n)} \approx -n_\alpha \mu_{\alpha\beta} \tau_{\alpha\beta}^{-1}$.

III. Boundary conditions in the multi-component plasma.

III.1 Sheath potential in the presence of impurity ions

In this paragraph, the sheath potential formation at the divertor plates in the presence impurity ions (sputtered from the plates or injected into plasma) and of secondary electron, emission is self-consistently considered. This is important for simulation of boundary plasma in the case of multi-component species at the vicinity to the divertor plate. It is shown that the sputtering at the plate or limiter (hereafter named in general as a target) can increase the potential drop, when impurities cause strong increases of electron upstream density. Impurity flux to the target as far as the secondary electron emission (SEE) from the target can only reduce the potential drop. The SEE yield saturates due to space charge limitations and cannot reduce completely the unfavourable effect on sputtering yield due to the acceleration by the potential drop even when a dilution effect of positive impurity ions is taken into account. The comparison of two types of carbon (with different SEE) shows considerably different values of potential drop and eventually results in different sputtering yields. For materials such as tungsten with a high electron emissivity the effect of SEE prevails over the effect of sputtering and leads to a substantial decrease of the potential drop. The sputtering (and self-sputtering) of tungsten starts to be significant at some critical electron temperature (which depends on the level of impurity recycling at the target). At a temperature higher than this critical temperature, self-sputtering above one can occur. The exact value will depend also on details of the impurity orbits in the sheath electric field. Further, the energy transmission coefficients for the different species (electrons, plasma ions, impurity ions) have been calculated.

III.2 Model and assumptions

A schematic of the plasma flow to the target is shown in Fig. III.1. we consider a steady state1-D model with only four species. The background electrons are assumed a truncated Maxwellian, so for primary electron density one has:

$$n_e(\phi) = \frac{\sqrt{\pi}}{v_{Te}} j_e e^{\phi} Erf(-\sqrt{\phi}), \qquad Erf(x) \equiv \frac{2}{\sqrt{\pi}} \int_x^{\infty} e^{-t^2} dt \tag{III.1}$$

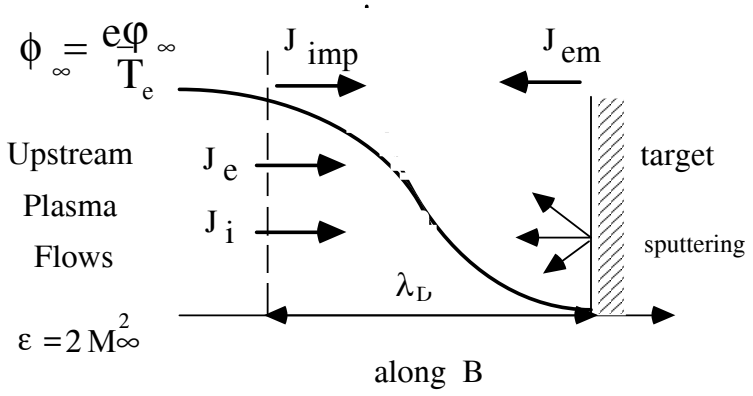

Fig. III.1: Chart of plasma flow near the target

where $\phi = e\varphi / T_e$. For background ions we assume a monoenergetic distribution, which Implies:

$$n_i(\phi) = j_i \,/ v_{Ti}\sqrt{\alpha}\sqrt{\varepsilon + (\phi_\infty - -\phi)}, \qquad \varepsilon \equiv {mv^2}/{2T_i}, \qquad \alpha \equiv \frac{T_e}{T_i} \tag{III.2}$$

Here v_{Ti}; notes the ion thermal speed and £ -the kinetic energy of incident ions upstream to the target. The secondary electrons emitted from the target are assumed with zero thermal energy, e.g.:

$$n_{em}(\phi) = j_{em} \,/ v_{Te}\sqrt{\phi}, \tag{III.3}$$

while $n_{em} \to \infty$ at the surface, this singularity is removable (see below). For impurities, sputtered from the target (ions of the target materials) we use a statistically average ion model [25]. This approach gives an average impurity ion density and charge number as function of plasma temperature. Additionally, a monoenergetic distribution of impurity ions incident to the target is assumed:

$$n_Z(\phi) = j_Z \,/ v_{Ti}\sqrt{\alpha/\mu_{Z,i}}\sqrt{\varepsilon_Z + Z(\phi_\infty - \phi)}, \qquad \mu_{Z,i} = m_Z/m_i \quad \varepsilon_z = Z\varepsilon \tag{III.4}$$

We are interesting in floating potential, so the total current at the target must vanish:

$$J \equiv j_i + j_{em} + j_{imp} - j_e = 0 \tag{III.5}$$

Here we take into account the plasma ion current, j_i, the plasma electron current, j_e the current of SE from the target, j_{em}, and the current of the impurity ions of the target materials which (according to our model) are returning from the plasma to the target in one "average" charge state. We also postulate the quasineutrality conditions in upstream region $(\varphi = \varphi_\infty)$ in interface between the plasma and the charge layer at the target:

$$n_e + n_{em} - Zn_Z - n_i = 0 \qquad \text{(III.6)}$$

To get a monotonic transition of the potential from the presheath area to the sheath region the Bohm condition must be fulfilled at the entrance to the sheath, which implies the existence of the positive charged sheath layer:

$$\rho(\varphi) = \rho(\varphi_\infty) + (\varphi - \varphi_\infty)\left.\frac{\partial \rho}{\partial \varphi}\right|_{\varphi=\varphi_\infty} + \ldots > 0 \quad \text{and} \quad \frac{\partial}{\partial \varphi}(n_e + n_{em} - Zn_Z - n_i) > 0 \qquad \text{(III.7)}$$

Further, we consider the case when all the SE enters the plasma. This implies a monotonic potential between plasma and target with zero value of electric field at the target. In this case, the governing equation for potential – the Poisson equation can be easily integrated from upstream region, where we also assume that ion saturation current is a maximum available positive current extracted from the plasma region, and the region at the target:

$$\Delta\varphi = -4\pi e\rho(\varphi), \quad \left.\left(\frac{\partial \varphi}{\partial x}\right)^2\right|_0^\infty = -4\pi\int_0^\varphi \rho(\varphi)d\varphi, \quad \int_0^\varphi (n_i + Zn_Z - n_e - n_{em})d\varphi = 0 \qquad \text{(III. 8)}$$

We assume below only the SEE and introducing the SEE yield, (see [26]) as

$$j_{em} = \gamma(T_e)\cdot j_e, \qquad \text{(III.9)}$$

The impurity ions flowing back to the target can cause the self-sputtering of the material surface, S_{Self}, additional to the sputtering caused by background plasma ions, S_i. The effective sputtering yield can be introduced simply as:

$$\mathbf{j_Z} = ZS_{eff}\ \mathbf{j_i}, \qquad S_{eff} = \frac{S_i(T_e)}{1-\eta\, S_{Self}(T_e)} \tag{III 10}$$

where η is fraction of impurities returning to the surface. The potential dependence of sputtering and self sputtering yields is taken into account. Corresponding values was used from [27].

These nine equations contain nine unknown variables, $\phi, \gamma_{\max}, \varepsilon, j_i, j_e, j_Z, n_e^{\infty}, n_i^{\infty}, n_{em}^{\infty}$

They solved as function of electron temperature *Te* at given input parameters or functions $\gamma(T_e), \varepsilon\, S_i, S_{Self}, \alpha = 1$

III.3 The generalised transmission coefficient and sheath potential drop.

The previous equations can be reduced to three main equations, which can be simply analysed. The relationship between currents and potential drop (current-voltage characteristic)

$$\mathbf{j_e}\left\{\sqrt{\pi}e^{\phi}\mathrm{Erf}(-\sqrt{\phi}) - \sqrt{\pi} - 2(1-\gamma)\sqrt{\phi}\right\} = \mathbf{j_i}\left\{2\sqrt{\varepsilon\mu_{ie}}\left(\sqrt{1+\frac{\phi}{\varepsilon}}-1\right)\right\} + \\ + 2Z^2\mathbf{j_Z}\sqrt{\varepsilon\mu_{ie}\mu_{iz}}\left(\sqrt{1+\frac{Z\phi}{\varepsilon}}-1\right) \tag{III. 11}$$

shows how impurities and secondary electrons chang the current balance within the sheath and impact the sheath floating potential. Thus, the electron current to the target can increase both due to SEE and impurity ions:

$$\mathbf{j_e} = \frac{1+ZS_{eff}}{1-\gamma}\,\mathbf{j_i} \tag{III.12}$$

The second term in numerator corresponds to contribution of impurities and zero total current requirements at the target. On the other side, there is an increase of electron density upstream to the target due to the existence of impurities and quasi neutrality requirements. As it follows from the second equation that governs the sheath potential drop in the presence of SEE and impurities:

$$\phi = ln\left\{\sqrt{\frac{\mu_{ie}}{\pi\varepsilon}}\ \frac{(1-\gamma)}{\left(1+\gamma\frac{e^{-\phi}}{\sqrt{\pi\phi}}\right)}\frac{1+Z\frac{n_Z}{n_i}}{\left[1+\frac{\mathbf{j_Z}}{\mathbf{j_i}}\right]}\right\} \propto ln\,(1-\gamma)\frac{1+Z\frac{n_Z^{\infty}}{n_i^{\infty}}}{1+ZS_{eff}} \tag{III. 13}$$

the excess of electrons, coming to the surface (see the second term in numerator (III.11)) increases the floating potential. The competition between two these processes defines the real changes of the potential drop. Cold electron emission has been found to affect the potential drop in many previous papers [28]. Here we examine this effect in the presence of impurities, sputtered from the target.

III.4 Bohm stability condition at the sheath entrance

The third equation here describes the stability condition at the sheath entrance:

$$\varepsilon \geq \frac{\frac{1}{2} + Z^2 S_{eff}\sqrt{\varepsilon\eta_{iZ}})\frac{\mathbf{j_i}}{\mathbf{j_e}}\sqrt{\mu_{ie}\phi/\varepsilon}}{e^{\phi}\sqrt{\pi\phi}\,Erf(-\sqrt{\phi}) + 1 - \gamma/2\phi} \approx \approx \frac{1}{2} + \frac{\gamma}{1-\gamma}\sqrt{\frac{\mu_{ie}\varepsilon}{\phi}}(\phi + 1/2) + \ldots \quad \text{(III.14)}$$

This condition is generalization of the Bohm criteria for multi-component plasma. It is clear, that the kinetic energy at the entrance to the sheath is also affected by impurities and SEE. The generalised transmission coefficient $\delta_t = Q/T_e\mathbf{j_i}$ (for energy Q carried by all particles to the target) can be written as $\delta_t = \delta_e + \delta_i + \delta_Z$ where

$$\delta_e = \frac{2}{1-\gamma}(1 + ZS_{eff}), \quad \text{(III.15a)}$$

$$\delta_i = \varepsilon + \phi(T_e, \gamma), \quad \text{(III.15b)}$$

$$\delta_z = ZS_{eff}(\varepsilon + \phi) \quad \text{(III.15c)}$$

Calculations are performed for typical tokamak ranges of plasma parameters [27].
Two types of graphite with different SEE and tungsten with a high electron emissivity have chosen as a surface material. Fig. III.2 shows the potential drop and the SEE yield with and without

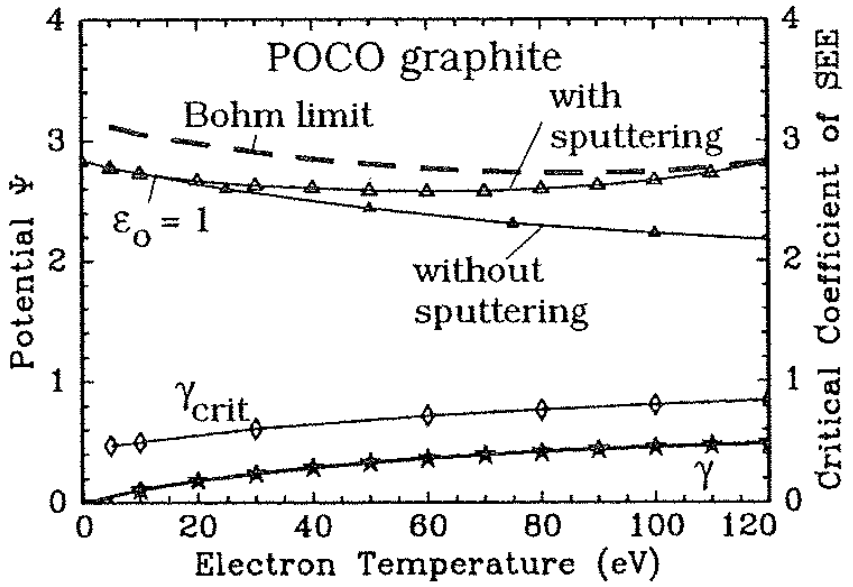

Fig. III.2: Potential drop and secondary

electron emission vs. T_e for POCO graphite impurities for POCO graphite (with low SEE) as a function of electron temperature. The case $\varepsilon = 1, \eta = 0.5$ is chosen. Saturation limit of SEE and the upper limit for the potential drop caused by Bohm limit $(\varepsilon = 0.5)$ are also shown in the plot. The same plot for carbon is shown in Fig III.3.

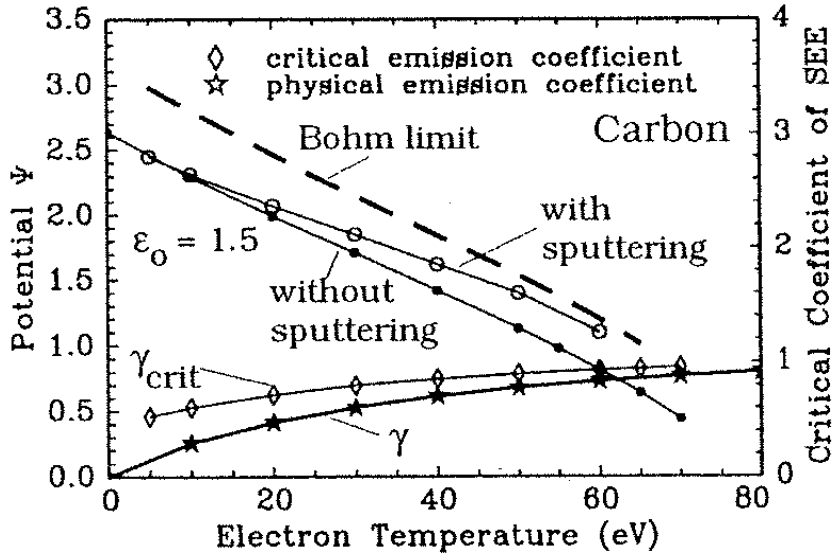

Fig. III.3: Potential drop and secondary electron emission vs. T_e for carbon

The difference in SEE yields causes a strong change in variation of the potential drop and other parameters. The same parameters for tungsten case are shown in Fig III.4. The temperature transmission coefficients as a function of electron temperature are plotted in Figs III.5 and III.6. It's

clear that the most of energy coming from plasma to the target carried by electrons because of both decrease of potential drop caused by SEE and enhancement of electron current to plate by sputtering.

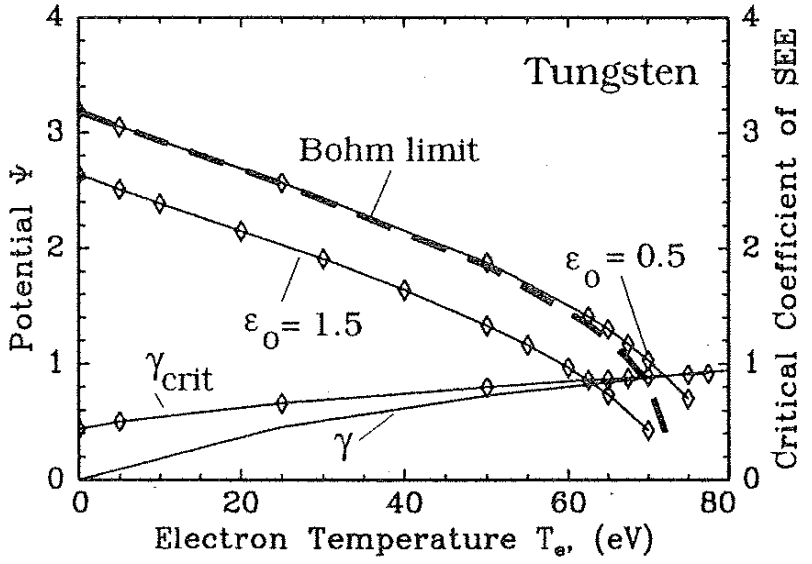

Fig. III.4: Potential drop and secondary electron emission vs. T_e for tungsten.

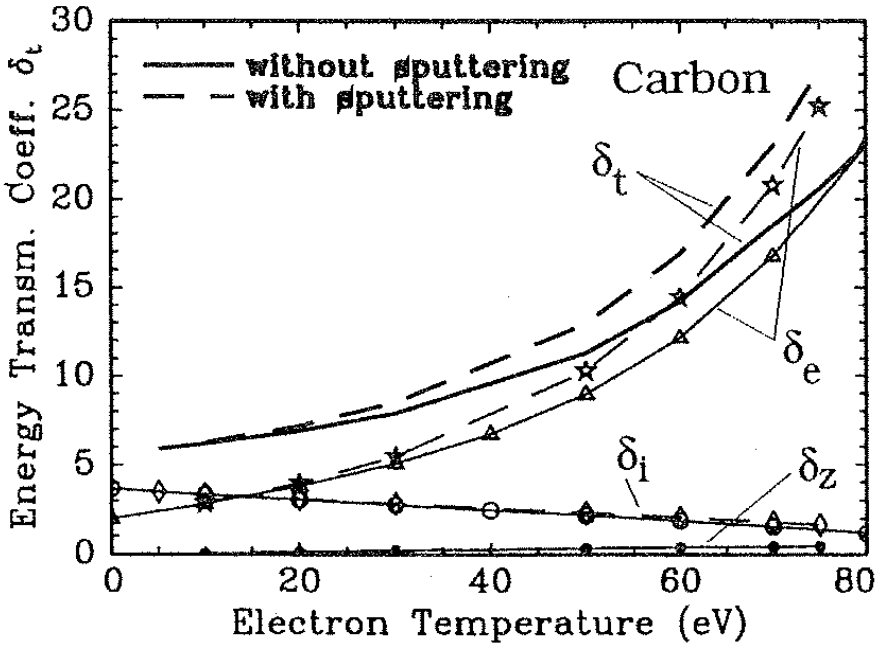

Fig. III. 5: Energy transmission coefficient. vs. T_e for carbon (sputtering is included).

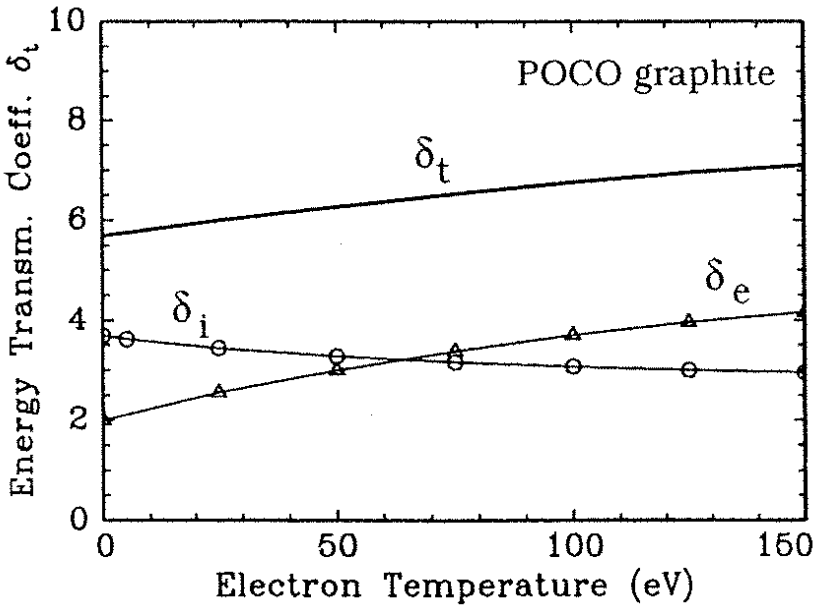

Fig. III.6: Energy transmission coefficient vs. T_e for POCO graphite.

In the case of tungsten the enhancement of the energy, exhaust due to the strong surface erosion, (see Fig. III.7) starts to be significant at some critical electron temperature (which depends on the level of impurity recycling at

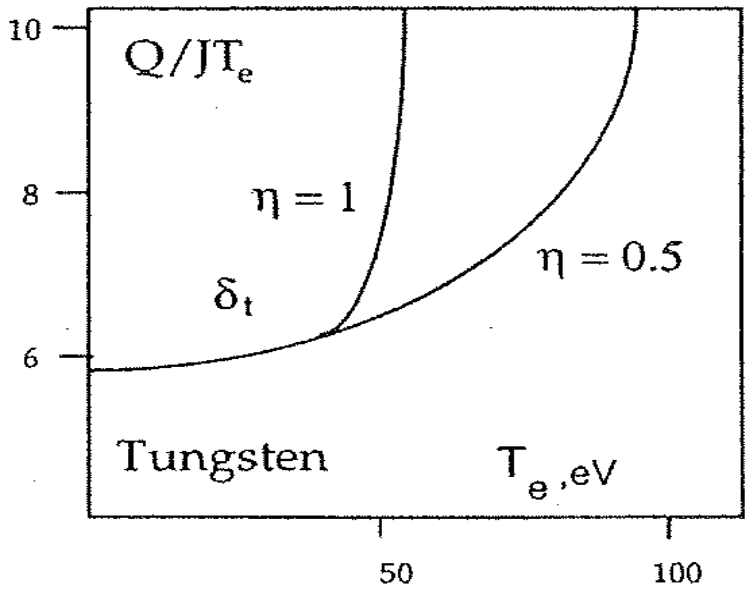

Fig. III.7 Energy transmission coefficient *vs.* T_e for tungsten; η is equal to the function of impurities returning to the surface the target). At a temperature higher than this critical temperature, self-sputtering yield above unity can occur.

Variation of potential drop by the secondary electron emission decreases potential drop, whereas the impurity sputtering of the target can increases or decrease drop, depending on variation of upstream electron density and impurity ion current at the target. The SEE yield saturates (space charge limitations) and does not offset acceleration due to the potential drop, and at the same time the dilution of negative charged layer by positive charged impurities seems to be not effective [29].

Two types of graphite (with different SEE) have different potential drop and therefore sputtering yields. For high electron emissivity (e.g. tungsten) impurity effect not pronounced since there is strong reduction of potential drop due to SEE. Most of energy coming from plasma to target carried by electrons because of both decrease of potential drop caused by SEE and enhancement of electron current to plate by sputtering. For conditions considered (perpendicular incidence, high impurity recycling) the total sheath transmission coefficient rises with Te and can reach 25 (without sputtering) or 28 (with sputtering) for graphite at $T_e > 50eV$, which means a little effect at divertor typical temperatures $(T_e < 10eV)$. These effects must be accounted for divertor plate erosion due to sputtering and the arcs formation.

IV. Simulation of drifts in transport equations

Classical particle drifts across the magnetic field can play an important role in tokamak edge-plasma transport. The relative influence of these terms is important for self-consistent simulations by including them, together with anomalous diffusion transport, in a 2-D fluid model of edge-plasma transport for the tokamak geometry. The drifts cause asymmetries in the plasma equilibrium, which depend on the direction of the magnetic field, B. The basic results can be understood by dividing the drifts into three categories: diamagnetic, E x B, and ∇B. The dominant effect near the divertor plates is from the E x B drifts, while the weaker ∇B drifts cause an increase in the magnitude of the radial electric field inside the magnetic separatrix. The diamagnetic terms, defined as divergence free, do not contribute to transport.

Classical particle drifts from E x B and ∇B (including curvature) drifts are believed important for understanding tokamak edge/scrape-off-layer (SOL) transport even in the presence of turbulent transport. For example, the asymmetry of the plasma density and temperature in front of the inner and outer divertor plates changes with the sign of the toroidal magnetic field, B_t [14] and the power threshold for the L-H confinement transition often depends on the direction of B_t [15]. There have been various analyses of the basic equations which describe these drift terms in toroidal geometry, e.g. [16]. However, careful assessment of their effects in 2-D transport codes has been lacking. Furthermore, it is important to have a valid model that calculates the electrostatic potential (and thus radial electric field, E_r) that extends across the magnetic separatrix into the core region. In this vicinity, shear in magnetic field is believed to play an important role in suppressing edge turbulence.

In this chapter, we focus on assessments of the different classical drifts, which can be implemented into TOKES code, including the calculation of radial electric field, on both sides of the separatrix [17-19]. The relative importance of the different drift terms, although not the details, can be predicted by simple arguments:

- First, the diamagnetic terms, defined here as being the divergence-free portion of the pressure-driven drift, give no transport as they cancel exactly in the transport equations; this is well-known result, which is sometimes overlooked.
- Second, the E x B drifts are larger than the ∇B drifts since the former scales as the inverse of the edge-plasma scale length while ∇B scales as the inverse major radius, L/R.
- Third, since the E x B drift is the same for ions and electrons, it generates no current; only the smaller ∇B drift enters the current continuity equation for the potential.

IV.1 Transport equations with drifts

In the TOKES code, all plasma equations can be written as:

$$\frac{\partial \psi_k}{\partial t} + \nabla \cdot \left(\alpha \psi_k \mathrm{V} - D \cdot \nabla \psi_k \right) = S_k + F_k \qquad \text{(IV. 1)}$$

where ψ_k represents variables of density, n_i ($k = 1$, $\alpha = 1$, $F_1 = 0$), parallel momentum density, $m_i n_i V_{//}$ ($k = 2$, $\alpha = 1$), and electron and ion temperature densities, $3 n_e T_e / 2$ and $3 n_i T_i / 2$ ($k = 3,4$, $\alpha = 5/3$). Here $\mathrm{V}(V_{//}, V_{drift})$ is the convection velocity $V_{//}$ from the parallel and cross-field drifts, V_{drift}, D_k is the diffusion tensor, F_k is a force term, and S_k is the source term.

Poloidal transport is a combination of the cross-field drifts described below and the geometrical projection of the parallel transport from Braginskii [10], except that thermal flux limits are used. Radial transport also includes the cross-field drift components together with anomalous diffusion coefficients for density ($D_{\perp a}$), momentum (η_a), electron energy (χ_e), ion energy (χ_i). The electrostatic potential is obtained from the current continuity equation described in more detail below. If cross-field drifts are neglected, the convective velocity in Eq. (IV. 1) is written as

$$\mathrm{V} = V_{//} \cdot \mathrm{b}_\theta - \frac{D_\perp}{n} \frac{\partial n}{\partial r} \mathrm{e}_r \qquad \text{(IV. 2)}$$

where $b_\theta = B_\theta / B$, B_θ is the poloidal magnetic field, and, b_θ, e_r are the unit vectors in the poloidal and radial directions, respectively. Note that in the continuity equation [$\psi_k = n_i$ in Eq. (IV. 1)], the diffusion term is actually represented through the diffusion term in V (IV. 2). Inclusion of the cross-field drifts can be accomplished by adding to V a second convective velocity such that $\mathrm{V} \rightarrow \mathrm{V} + \mathrm{V}_\perp$. To improve numerical accuracy, it is best to omit divergence-free convective fluxes from the outset as they should give zero contribution to the conservation equations [21-22]. The separation of particle fluxes into divergence-free terms and those from guiding-centre motion can be clearly done [23], and one can use those results for modelling. The guiding-centre convection velocity for each species is

$$\mathrm{V}_\perp = \mathrm{V}_E + \mathrm{V}_{\nabla B} = \frac{[\mathrm{Eb}]}{B} + \frac{T}{ZeB^2}[\mathrm{b} \nabla B] + \frac{\left(T + m V_{//}^2\right)}{ZeB^2}[\mathrm{b}\ (\mathrm{b} \nabla \mathrm{b})], \qquad \text{(IV. 3)}$$

where $\mathrm{b} = \mathrm{B}/|\mathrm{B}|$ the first term on the right-hand side represents electric drift and the remaining terms give the ∇B drift velocity. Here E is the electric field, T is the electron or ion temperature, Ze is the particle charge, m is the mass, and $V_{//}$ is the parallel drift velocity. It should be emphasized that

including $\mathrm{V}_\perp$ (IV.3) incorporates all cross-field drift terms in the conservation equations properly; one should not include any additional diamagnetic terms, i.e., neither the gyro-viscosity term in the momentum equation nor the energy diamagnetic terms [10].

IV.2. Electrostatic potential in presence of drifts

The potential is calculated from the current continuity equation obtained by subtracting the ion and electron continuity equations and assuming quasi-neutrality ($n_i = n_e = n$), yielding

$$\nabla \mathrm{j}(\varphi) = 0 \qquad \text{(IV.4)}$$

Here we follow the description given in [17] with the generalization of including the currents from the ∇B terms in Eq. (IV.3). (Note that V_E yields zero current.) Thus, in addition to the classical parallel current, $j_{//}$ [10], which dominates in the SOL, we have a radial current driven by anomalous ion transport, which in the thin SOL region can be approximated as [17]:

$$j_r(\varphi) = \frac{1}{ZeB^2}\frac{\partial}{\partial r}\left\{\eta_1 \frac{\partial}{\partial r}\left(\frac{1}{n}\frac{\partial P_i}{\partial r} + e\frac{\partial \varphi}{\partial r}\right)\right\} \qquad \text{(IV.5)}$$

where φ is the potential, $P_i = n_i T_i$, and $\eta_1 = m_i n_i D_\perp$ is an anomalous viscosity coefficient. In an the inhomogeneous magnetic field of a tokamak, currents from $\mathrm{V}_{\nabla B}$ become

$$\mathrm{J}_{\nabla B} = \frac{(P_e + P_i)}{B}\left[\mathrm{b}\frac{\nabla B}{B}\right] + \frac{\left(P_e + P_i + n_i m_i V_{//}^2\right)}{B}[\mathrm{b}(\mathrm{b}\nabla \mathrm{b})] \approx 2\left(P_e + P_i + n_i m_i V_{//}^2/2\right)[\mathrm{e}_r \mathrm{b}_\phi]/BR \qquad \text{(IV.7)}$$

where we assume singly charge ions; this is easily generalized to impurities. The unit vectors e_r, b_ϕ correspond to the direction of the major radius, R, and toroidal B-field, respectively. Equation (IV.7) is typically accurate for tokamaks, yielding a vertical current. The current continuity equation thus becomes fourth order in the radial direction (from j_r) and second order in the poloidal direction (from $j_{//}$). The sheath boundary conditions or the poloidal direction, including the cross-field drifts, is discussed in [23]. On the inner core boundary in the radial direction, we impose two boundary conditions: one is that the potential is constant on a flux surface, with the constant being supplied by requiring no radial current over the flux surface. The second condition is, that the shape of the potential on the second set of cells determined from parallel Ohm's law [10]. The remaining constant can be found by setting the flux-surface averaged toroidal momentum to some input value (zero for our cases). At the radial wall, simple boundary conditions making the first and second numerical derivatives of φ zero are used.

IV.3. Effect of E x B drift

As mentioned earlier, the magnitude of the **E x B** velocity is much larger than of the ∇B terms owing to the shorter scale-length of the potential compared to the magnetic field. Turning on the **E x B** velocity could give the dominant effect on plasma transport as shown in Fig. IV.2 from B2 calculation [16]. Here the standard direction of B_t is out of the plane, giving the ion $V_{\nabla B}$ velocity downward. Note from this figure that the profiles shift outward or inward in response to the radial drift caused by the poloidal electric field (always pointing toward the divertor plates). The most dramatic effect of **E x B** in the divertor region is the strong drop in the density on the inner plate for reversed B_t which results in loss of detachment on the inner divertor. The drop in ion density n_i can be understood by considering the vector plot of the ion flux shown in Fig. IV.3. Note the strong reversal of the flow under the X-point as B_t changes sign; here the flow is dominated by the **E x B** drift from the large radial electric field that arises from the drop of T , in moving across the separatrix into the private flux region. Two diagnostics confirm that the particle flow under the X-point is very important here. First, consider three net ion-plus-neutral currents: that passing the X-point in the SOL toward the outer plate, I_{out} , that likewise directed toward the inner plate, I_{inn} ;, and that passing under the X-point from inner plate to outer plate, I_{pf} .

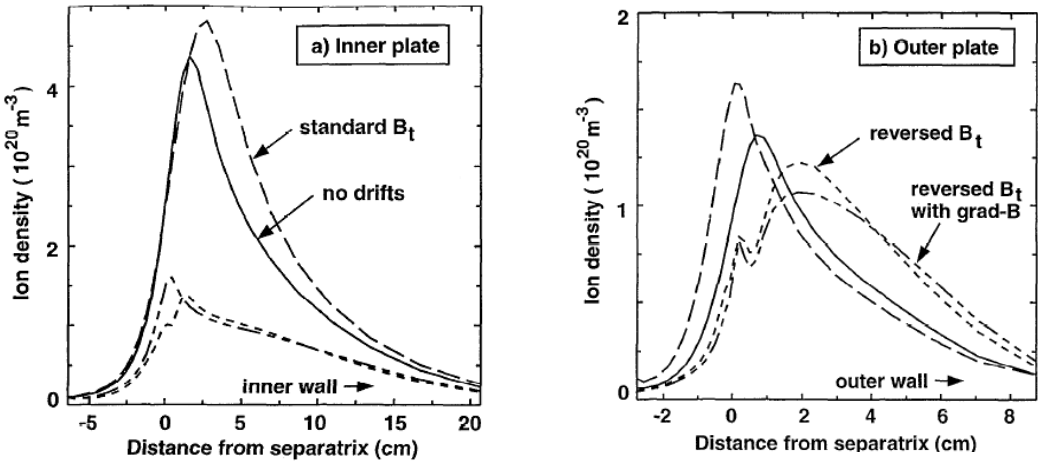

Fig IV.2 Ion density at the (a), inner divertor plate and (b), outer divertor plate for four cases; no cross-field drifts (solid line); ExB only for the standard toroidal B-field direction (long dashed line); ExB only for reversed toroidal field (dotted line), and ExB and grad-B drifts for reversed toloidal field (dot-dashed line)[16].

For the standard B_t , we find (I_{inn} , I_{pf} , I_{out} ,) = (0.13,-0.81, 1.6) kA, whereas for the reversed B_t , (I_{inn} , I_{pf} , I_{out} ,) = (1.6, 1.1, 0.05) kA. Clearly, I_{pf} is comparable to the particle currents in the SOL and changes the sign of B_t . Second, one can insert a baffle vertically through the private flux region to the X-point for the reversed B_t case; Note from Fig. IV.3 that the E x B induces rather complex

flow patterns with flow reversal regions. Indeed, the self-consistent solution of the SOL plasma has many facets. It was shown that even in a 1-D model including only poloidal drifts, but with temperature asymmetries, that solutions arise where the density asymmetry is enhance in the direction opposite to that found in 1-D models for uniform temperatures

IV.4. Effect of ∇B drift

The effect of the ∇B velocities on plasma transport has shown in Fig.IV.2 on the density at the plate where the dot-dashed line gives the result with the $V_{\nabla B}$ velocity. The weak effect reflects the fact, that these velocities are small. However, $V_{\nabla B}$ does have a significant effect on the potential though their contributions to the net current via $j_{\nabla B}$, especially in the core-edge region. Note from Eq. (IV. 6) that $j_{\nabla B}$ does not explicitly depend on φ, so it behaves like a source term in the equation used for the potential, $\nabla j(\varphi) = 0$ although the variables are coupled nonlinearly. The profiles of the radial electric field, E_r,are shown in Fig. IV. 4 at the outer mid-plane without and with $j_{\nabla B}$ added. The electric field is substantial changed near the separatrix and in the core region with $j_{\nabla B}$; well outside the separatrix, the parallel currents dominate the potential equation. The large radial shear in E_r is believed important for suppressing edge turbulence, although quantitative evaluation of this process requires coupling this model with a turbulence simulation. In addition, these simulations assuming no toroidal rotation at the core-edge boundary and thus are representative without strong neutral beam injection, which can cause toroidal rotation. Allowing finite toroidal velocity at the core-edge boundary changes E_r inside the separatrix.

Finally, the inclusion of $j_{\nabla B}$ changes the current structure on the divertor plates. The currents at the plate in both standard and reversed B_t cases are qualitatively similar to that measured on JET by Schaffer, et al. [24], who also gave an interpretation, which includes $j_{\nabla B}$. Even though the overall density profile on the plates are not very sensitive to ∇B effects (see Fig. IV. 2) very near the separatrix, strong currents do flow, especially for the reversed ∇B case. These plate currents are still dominated by the parallel current, but the self-consistent adjustment to $j_{\nabla B}$ have a strong effect on $j_{//}$.

In conclusion, one can expect that the classical cross-field drifts can have a substantial effect on plasma spatial distribution in the edge/SOL region of a tokamak. The drifts can be separated into three categories: diamagnetic, **E x B** and ∇B. The diamagnetic drift is defined as the (large) divergence-free portion of the pressure-driven drift and thus does not contribute in the net transport. The **E x B** drift can be substantial in the edge region giving important contributions to particle transport. A large radial electric field exists in moving into the private flux region because of the

rapid drop in the electron temperature there. The associated poloidal drift of private-flux region plasma is away from the outer plate and toward the inner plate for the ion gradient-B drift toward the X-point. This particle transport further enhances the tendency from toroidal asymmetries for the inner plate to have higher plasma density and thus detach before the outer plate. Upon reversal of the toroidal field, B_t, the drifts reverse, and the plasmas profiles at the inner and outer plates are much more similar. This behaviour is consistent with the experimental observations reported in [14]. Because the **E x B** drift is the same for ions and electrons, it generates no net current and does not contribute directly in the electrostatic potential. The ∇B drift is pressure-driven, but is typically smaller than the **E x B** drift by the ratio of Δ / R, where Δ is the scrape-off layer width and R is the major radius, but here ions and electrons drifting in opposite directions; this drift therefore first becomes important in the current continuity equation for determining the electrostatic potential. In the core region, the current contribution from the ∇B drift increases the magnitude of E_r and its shear. In the SOL, the ∇B drift has a small effect on E_r, because there the current is dominated by the parallel electron dynamics.

Classical particle drifts across the magnetic field can play an important role in tokamak edge-plasma transport. The relative influence of these terms is important for self-consistent simulations by including them, together with anomalous diffusion transport, in a 2-D fluid model of edge-plasma transport in TOKES code. The drifts cause asymmetries in the plasma equilibrium which depend on the direction of the magnetic field, B. The basic results can be understood by dividing the drifts into three categories: diamagnetic, E x B, and ∇B. The dominant effect near the divertor plates is from the E x B drifts, while the weaker ∇B drifts cause an increase in the magnitude of the radial electric field inside the magnetic separatrix. The diamagnetic terms, defined as divergence free, do not contribute to transport.

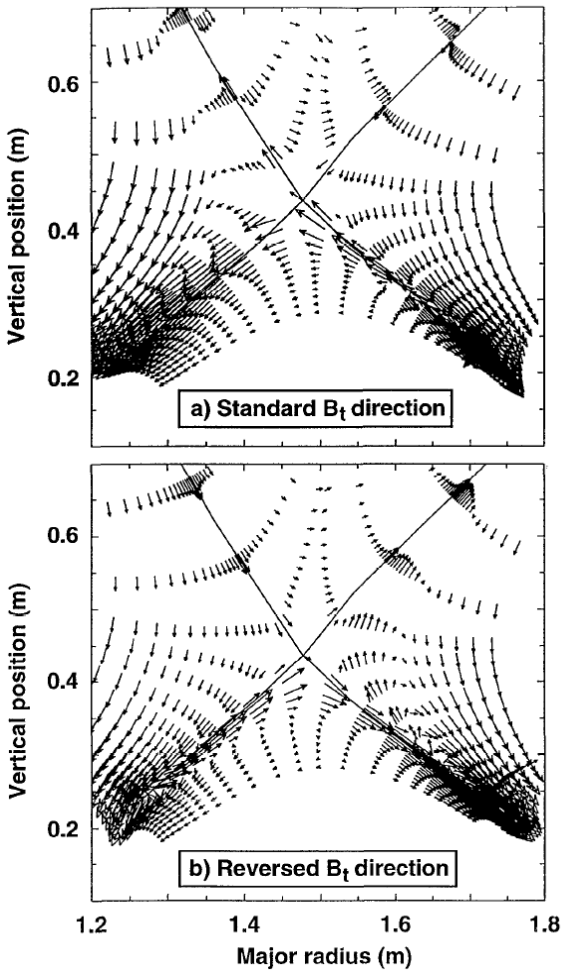

Fig IV.3 Vectors of ion particle flux for (a), the standard direction of the toroidal magnetic field corresponding to the ion grad-B drift toward the X-point, and (b), the opposite direction for the toroidal field [16].

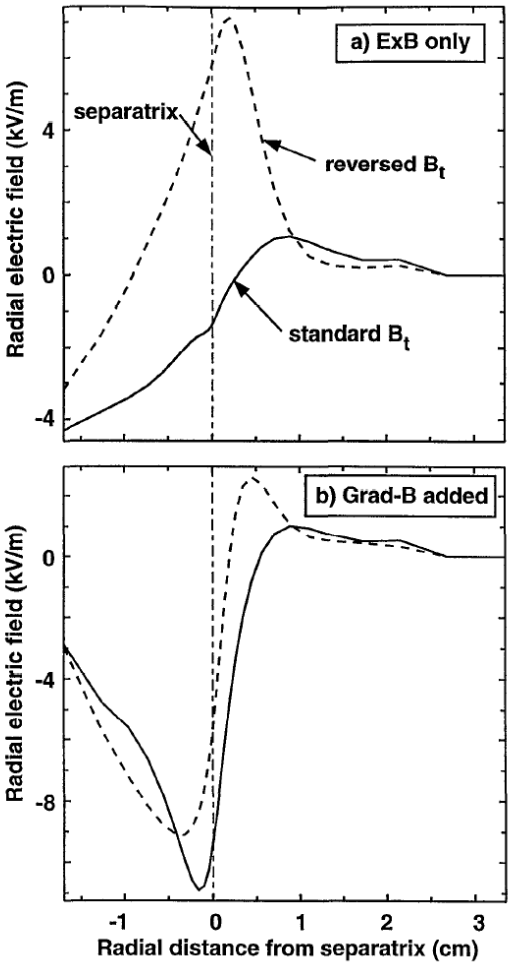

Fig. IV.4 Radial electric field at the outer midplane for (a), ExB drifts only, and (b), ExB and grad-B drifts together. The ion grad-B drifts are toward the X-point for the standard B case [16].

V.The modelling of neutral atoms in tokamak boundary plasma

The effect of neutral atoms is not included in standard tokamak transport treatments [37]. However, recent experiments [38-45] have shown that neutral atoms in the tokamak edge can influence global confinement by affecting the transition from low *L* to high *H* confinement. The physical mechanism by which this occurs is not yet clearly identified, but it is well known that neutrals influence ion dynamics through charge-exchange interactions. Furthermore, the radial neutral flux of toroidal angular momentum can modify or even determine the edge radial electric field and plasma rotation. The radial localization of the neutrals also introduces a shear in the flow that may affect edge turbulence [46]. Neutral atoms play an essential role in momentum transfer from the plasma to the wall, thereby facilitating the transition from attached to detach operation regime with increasing input power [47]. They could also play an important role in mitigation of ELMs and runaway electrons [48].

In this chapter, we consider first simple models of neutral atoms behaviour in the tokamak boundary plasmas and then will describe the neutral transport in the SOL and divertor plasma.

V.1 Kinetic description of neutral atoms near the first wall

The neutral atoms (e.g. of hydrogen isotopes) realised from the first wall of tokamak and penetrating in the boundary plasma undergo charge-exchange collisions and ionization. The neutral atoms before being ionised undergo many charge exchange collisions and experiencing a random motion. Therefore, the penetration length into plasma can be assessed as a diffusive length.

$$\lambda_D \approx \sqrt{D_{cx}\tau_{ion}} = \sqrt{\frac{v_{T0}^2}{n_i < \sigma v >_{cx}} \frac{1}{n_i < \sigma v >_{ion}}} = \frac{v_{T0}}{n_i} \frac{1}{\sqrt{< \sigma v >_{cx} < \sigma v >_{ion}}} \tag{V.1}$$

where the diffusion occurs due to multiple resonance charge exchange collusions. Here $\tau_{ion} = 1 / n_i < \sigma v >_{ion}$ is the ionization time and the mean free pass for atoms against ionisation and charge exchange, respectably:

$$\lambda_{cx} \approx \frac{v_{T0}}{n_i < \sigma v >_{cx}} \tag{V.2}$$

$$\lambda_{ion} \approx \frac{v_{T0}}{n_i < \sigma v >_{ion}} \tag{V.3}$$

Under reactor tokamak conditions at the edge neural atoms will normally penetrate rather shallow and neutral distribution can be considered in the slab geometry (see Fig. V.1)

It is useful to introduce the following definitions:

$$\beta(x) = < \sigma v >_{cx} / \left(< \sigma v >_{cx} + < \sigma v >_{ion} \right) \tag{V.4}$$

$$k(x) = \frac{< \sigma v >_{ion}}{\left(< \sigma v >_{ion} + < \sigma v >_{cx} \right)}; \tag{V.5}$$

and the reflective property of plasma, so called Albedo:

$$\mathrm{A(x)} \approx \frac{\beta / 2}{1 - \beta / 2} = \frac{1 - k}{1 + k} \tag{V.6}$$

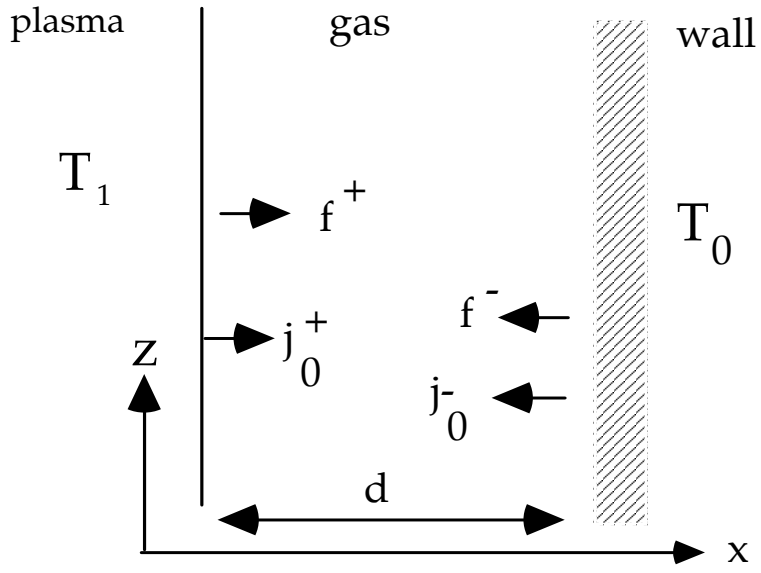

Fig. V.1

Here $\mathrm{f^-}$ and $\mathrm{j_0^-}$ are the distribution function and flux of atoms coming from the wall, $\mathrm{f^+}$ and $\mathrm{j_0^+}$ are the corresponding quantities for reflected back atoms. Assuming the complete absorption of atoms at the wall, the distribution functions for incident and reflected atoms can be taken as a one directed Maxwellian with the wall T_0 and plasma T_1 temperatures, respectably:

$$f_0^- \approx \frac{2 j_0^-}{\pi v_{T_0}^4} \exp - \frac{m}{2} \frac{v^2}{T_0} \qquad for \quad v_x < 0$$

$$f_0^- \approx \frac{2 j_0^-}{\pi v_T^4} \exp - \frac{m}{2} \frac{(v - V)^2}{T} \qquad for \quad v_x < 0 \tag{V.7}$$

Here velocity V describes the plasma flow in vertical direction $V(V_z, 0, 0)$. Using the definition given above and integrating over velocity space one can easily find the following moments for

- Particle flux of atoms:

$$j_0^+ \approx \frac{1-k}{1+k} j_0^-; \qquad J \equiv j_0^- - j_0^+ = \frac{2k}{1+k} j_0^-; \tag{V.8}$$

- Atoms density:

$$n \approx n_0^+ + n_0^- = 2\sqrt{\pi}\left(\frac{j_0^-}{v_{T0}} + \frac{j_0^+}{v_{T1}}\right) = \frac{\sqrt{\pi}(1+k)}{v_{T0}} \frac{J}{k}(1 + \frac{1-k}{1+k}\sqrt{\frac{T_0}{T_1}}); \tag{V.9}$$

$$n(x) = j_0^- \frac{2\sqrt{\pi}}{v_{T0}}(1 + \frac{1-k}{1+k}\sqrt{\frac{T_0}{T_1}}); \tag{V.10}$$

- Velocity of atoms:

$$V = \frac{J}{n} = \frac{k}{\sqrt{\pi}(1+k)(1+\beta\sqrt{\frac{T_0}{T_1}})} v_{T0}; \tag{V.11}$$

- Pressure of atoms:

$$p = n_0 T_0 + n_1 T_1 = \sqrt{2\pi m}\, \frac{J}{2k}(1+k)\left(\sqrt{T_0} + \sqrt{T_1}\right) \tag{V.12}$$

- and the friction force (or viscosity):

$$F_0 = -F_1 = \pi_{xy} \equiv m\int v_x v_y f_1^+ dv == mV\frac{1-k}{k} J = mV\frac{1}{4} n\sqrt{\frac{8T_*}{m\pi}}; \tag{V.13}$$

where T_*:

$$T_* \equiv \frac{2T_0 T_1}{\left(\sqrt{T_0} + \frac{1+k}{1-k}\sqrt{T_1}\right)^2} \tag{V.14}$$

V.2 Fluid description of neutral atoms in the SOL

In this chapter the fluid equation are derived for simulation of neutral atoms in the SOL and divertor region of tokamak. We will assume that in the toroidal direction the distribution of neutrals is homogeneous in that boundary region, therefore considering only the radial and poloidal directions. As far as radial direction concerns, we will integrate across the relatively thin layer in the SOL region.

- **Geometry chart & coordinate system**

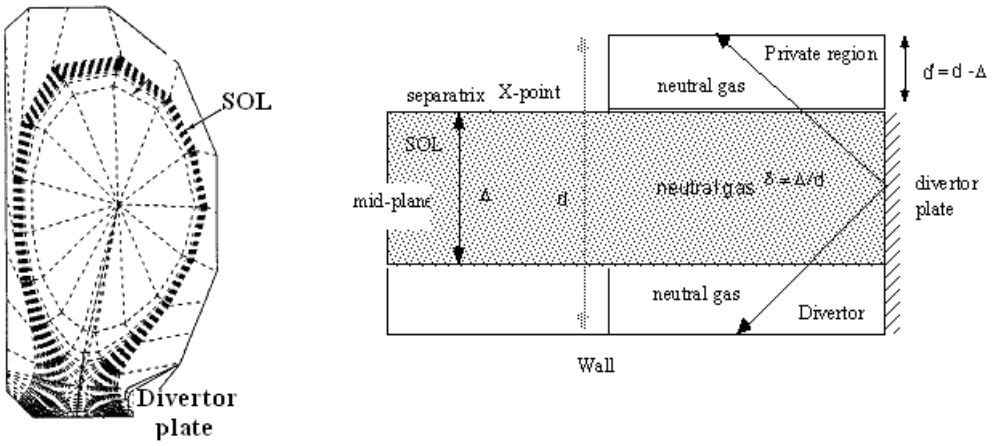

where δ is the thickness of the plasma column in the SOL and the divertor area, $\delta = \dfrac{\Delta}{d}$ and $\delta d = d - \Delta$ is the thickness of the private zone. We will choose the curvilinear orthogonal coordinate system $\psi(\rho), \theta, \varphi$ and will use hereafter the following definitions:

$U(U_\psi, U_\theta, U_\varphi)$ the fluid velocity of neutral atoms,

N is the neutral density,

m_0 is the mass of atom,

ρ is neutrals mass density, $Nm_0 \equiv \rho$

Metric coefficients (with co- and contra-variant components)

$$g^{\psi\psi} = \frac{1}{g_{\psi\psi}} = 4\pi^2 R^2 B_\theta^2 = const, \quad g^{\theta\theta} = \frac{1}{g_{\theta\theta}} = 4\pi^2 B_\theta^2 = \sqrt{g} = const$$

$$U_\psi = \sqrt{g_{\psi\psi}} U^\psi = U_\rho$$

$$U_\theta = \sqrt{g_{\theta\theta}} U^\theta = U_\theta$$

$$U_\varphi = \sqrt{g_{\varphi\varphi}} U^\varphi = U_\varphi$$

- **2-D Fluid equations for neutral atoms**

- *Continuity equation:*

$$\frac{\partial N}{\partial t}+\frac{\partial NU_\theta}{\partial \theta}+\frac{\partial}{\partial \psi}\left(NU_\psi\right)=-\delta nN(x)k_{ion}(T)+\delta\frac{n}{\tau_{rec}(n,T_e)}\quad ;\quad Nm_0\equiv\rho;\ \frac{\partial}{\partial\varphi}=0;\ \ \delta=\Delta/d \tag{V.15}$$

- *Momentum equations along toroidal direction:*

$$\frac{\partial \rho U_\varphi}{\partial t}+\frac{\partial}{\partial\theta}\left(\rho U_\theta U_\varphi-\eta_0\frac{\partial U_\varphi}{\partial\theta}\right)=$$

$$=-\frac{\partial}{\partial\psi}\left(-\eta_0\frac{\partial U_\varphi}{\partial\psi}\right)-\delta\rho nU_\varphi k_{ion}(T,n)+\delta\rho nk_{cx}(T)(V_{//}h_\varphi-U_\varphi)+\delta m_0nU_\varphi k_{rec}(n,T); \tag{V.16}$$

- *Energy equation:*

$$\frac{\partial\varepsilon_0}{\partial t}+\frac{\partial}{\partial\theta}\left((\varepsilon_0+NT_0)U_\theta-\chi_0\frac{\partial T_0}{\partial\theta}-\eta_0\left(\frac{4}{3}U_\theta\frac{\partial U_\theta}{\partial\theta}-\frac{2}{3}U_\theta\frac{\partial U_\psi}{\partial\psi}+U_\psi\frac{\partial U_\theta}{\partial\psi}+U_\psi\frac{\partial U_\psi}{\partial\theta}+U_\varphi\frac{\partial U_\varphi}{\partial\theta}\right)\right)$$
$$+\frac{\partial}{\partial\psi}\left((\varepsilon_0+NT_0)U_\psi-\chi_0\frac{\partial T}{\partial\psi}-\eta_0\left(\frac{4}{3}U_\psi\frac{\partial U_\psi}{\partial\psi}-\frac{2}{3}U_\psi\frac{\partial U_\theta}{\partial\theta}+U_\theta\frac{\partial U_\psi}{\partial\theta}+U_\theta\frac{\partial U_\theta}{\partial\psi}+U_\varphi\frac{\partial U_\varphi}{\partial\psi}\right)\right)$$

$$=-\delta\varepsilon_0Nn\,k_{ion}(T)+\delta nN\left(\varepsilon_i-\varepsilon_N\right)k_{cx}(T)+\delta nN\varepsilon_Nk_{ion}(T)+\delta Q_{rec,i} \tag{V.17}$$

$$\varepsilon_i\equiv\frac{m_inV^2}{2}+\frac{3}{2}nT\ ;\qquad \varepsilon_N\equiv\frac{m_NNV_0{}^2}{2}+\frac{3}{2}NT_0;\qquad Q_{rec,i}=n\left(\frac{m_iV_{//}{}^2}{2}+\frac{3}{2}T_i\right) \tag{V.18}$$

New variables and ordering:

$$U_\theta=U_{//}h_\theta+U_\perp h_\varphi;\qquad U_\varphi=U_{//}h_\varphi-U_\perp h_\theta;\qquad h_\theta\equiv B_\theta/B$$
$$U_{//}=U_\varphi h_\varphi+U_\theta h_\theta;\qquad U_\perp=U_\theta h_\varphi-U_\varphi h_\theta;\qquad h_\varphi=\sqrt{1-h_\theta{}^2} \tag{V.19}$$

$$U_\theta\propto\ \varepsilon;\quad U_\varphi\propto\ 1;\quad U_\psi\propto\ \varepsilon^2;$$
$$\lambda_\theta\propto\ 1;\quad \lambda_\varphi\propto\ \infty;\quad \lambda_\psi\propto\ 1/\varepsilon; \tag{V.20}$$

Then, the equation can be written as:

$$\frac{\partial N}{\partial t}+\frac{\partial NU_\theta}{\partial\theta}=-\delta Nnk_{ion}(n,T_e)+\delta nk_{rec}(n,T_e)+\frac{N}{\tau_{\perp w}}; \tag{V.19}$$

$$\frac{\partial \rho U_\theta}{\partial t} + \frac{\partial}{\partial \theta}\left(\rho U_\theta{}^2 + p_0 - \frac{4}{3}\eta_0 \frac{\partial U_\theta}{\partial \theta}\right) =$$

$$\overline{-\frac{\partial}{\partial \psi}\left(-\eta_0 \frac{\partial U_\theta}{\partial \psi}\right)} - \delta\rho n U_\theta k_{ion}(T,n) + \delta\rho n k_{cx}(T)(h_\theta V_{//} - U_\theta) + \delta m_0 n U_\theta k_{rec}(n,T); \qquad \text{(V.20)}$$

$$\frac{\partial \rho U_\varphi}{\partial t} + \frac{\partial}{\partial \theta}\left(\rho U_\theta U_\varphi - \eta_0 \frac{\partial U_\varphi}{\partial \theta}\right) =$$

$$= \overline{-\frac{\partial}{\partial \psi}\left(-\eta_0 \frac{\partial U_\varphi}{\partial \psi}\right)} - \delta\rho n U_\varphi k_{ion}(T,n) + \delta\rho n k_{cx}(T)(V_{//} h_\varphi - U_\varphi) + \delta m_0 n U_\varphi k_{rec}(n,T); \qquad \text{(V.21)}$$

- Since the SOL region is relative thin, $\Delta << 2\pi qR$ we averaged over the radial direction and simulate the radial distribution via a source of neural atoms coming through wall or separatrix Therefore, the radial term in continuity equation can be replaced as

$$\overline{\frac{\partial N U_\psi}{\partial \psi}} \approx \frac{N}{\tau_{\perp w}};$$

For the parallel momentum $\Pi_{//}$ we will take into account that due to the charge –exchange collisions with the plasma ions, neutrals surrounding the plasma flow will hamper the flow and therefore acquire the parallel momentum.

$$\Pi_{//} = \overline{\frac{\partial}{\partial \psi}\left(-\eta_0 \frac{\partial U_{//}}{\partial \psi}\right)} \approx \eta_0 \frac{3V_{//}}{(\delta d)^2} f_m(Kn); \qquad f_m(Kn) = 1 - e^{-L/\lambda_*(Kn)},$$
$$\Pi_\perp \approx 0 \qquad \text{(V.22)}$$

where Kn is the Knudsen number of neutrals, δ and Δ are shown on the sketch (see Fig.1), σ_{n-n} is the neutral-neutral elastic collision cross-section.

$$\lambda_*(Kn) = 2.4(\delta d)_{(m)}(11.5(\delta d)_{(m)} N \sigma_{n-n} + 1); \qquad d - \Delta \equiv d'; \quad \delta = \Delta / d;$$
$$\sigma_{n-n} \approx 2\,10^{-19}\, m^{-3} \qquad \text{(V.23)}$$

Instead of U_θ, U_φ we will introduce the velocity projections along and across B: $U_{//}, U_\perp$,

$$\frac{\partial}{\partial t} N + \frac{\partial}{\partial \theta}\left(N\left(U_{//} h_\theta + U_\perp h_\varphi\right)\right) = -\delta N n k_{ion}(n, T_e) + \delta n k_{rec}(n, T_e) + \frac{N}{\tau_{\perp w}}; \qquad \text{(V.24)}$$

$$\frac{\partial \rho U_{//}}{\partial t} + \frac{\partial}{\partial \theta}\left((\rho U_{//}^{2} + p_0) h_\theta + U_{//} U_\perp h_\varphi \right) - \eta_0 \left(\left(1 + \frac{h_\theta^2}{3}\right) \frac{\partial U_{//}}{\partial \theta} + \frac{h_\theta h_\varphi}{3} \frac{\partial U_\perp}{\partial \theta} \right) \right) =$$

$$= -\Pi_{//} - \delta \rho n U_{//} k_{ion}(T, n) + \delta \rho n k_{cx}(T)(V_{//} - U_{//}) + \delta m_0 n U_{//} k_{rec}(n, T); \qquad \text{(V.25)}$$

$$\frac{\partial \rho U_\perp}{\partial t} + \frac{\partial}{\partial \theta}\left(h_\varphi (\rho U_\perp^2 + p_0) + h_\theta U_{//} U_\perp - \eta_0 \left(\left(1 + \frac{h_\varphi^2}{3}\right) \frac{\partial U_\perp}{\partial \theta} + \frac{1}{3} h_\varphi h_\theta \frac{\partial U_{//}}{\partial \theta} \right) \right) =$$

$$= -\Pi_\perp - \delta \rho n U_\perp k_{ion}(T, n) - \delta \rho n k_{cx}(T) U_\perp + \delta m_0 n U_\perp k_{rec}(n, T); \qquad \text{(V.26)}$$

•

$$\frac{\partial \varepsilon_0}{\partial t} + \frac{\partial}{\partial \theta}\left((\varepsilon_0 + N T_0) U_\theta - \chi_0 \frac{\partial T_0}{\partial \theta} - \eta_0 \left(\frac{4}{3} U_\theta \frac{\partial U_\theta}{\partial \theta} + U_\varphi \frac{\partial U_\varphi}{\partial \theta} \right) \right) =$$

$$= -\delta \varepsilon_0 N n\, k_{ion}(T) + \delta n N (\varepsilon_i - \varepsilon_N) k_{cx}(T) + \delta n N \varepsilon_N k_{ion}(T) + \delta Q_{rec,i}$$

$$\varepsilon_i \equiv \frac{m_i n V^2}{2} + \frac{3}{2} n T \; ; \qquad \varepsilon_N \equiv \frac{m_N N V_0^{\,2}}{2} + \frac{3}{2} N T_0; \qquad Q_{rec,i} = n \left(\frac{m_i V_{//}^{\,2}}{2} + \frac{3}{2} T_i \right) \nu_{rec} \qquad \text{(V.27)}$$

•

$$U_\theta = U_{//} h_\theta + U_\perp h_\varphi; \qquad U_\varphi = U_{//} h_\varphi - U_\perp h_\theta; \qquad h_\theta \equiv B_\theta / B \; ; \quad h_\varphi = \sqrt{1 - h_\theta^{\,2}}$$

(V.28)

Projection of poloidal velocities along B $h_\theta \frac{\partial}{\partial \theta} \equiv \frac{\partial}{\partial x}$

$$\frac{\partial N}{\partial t} + \frac{\partial}{\partial x}\left(N \left(U_{//} + U_\perp h_\varphi / h_\theta \right) \right) = -\delta N n k_{ion}(n, T_e) + \delta n k_{rec}(n, T_e) + \frac{N}{\tau_{\perp w}}; \qquad \text{(V.29)}$$

$$\frac{\partial \rho U_{//}}{\partial t} + \frac{\partial}{\partial x}\left[(\rho U_{//}^{\,2} + p_0) + U_{//} U_\perp h_\varphi / h_\theta) - \eta_0 \left(\left(1 + \frac{h_\varphi^2}{3}\right) \frac{\partial U_{//}}{h_\theta \partial x} + \frac{1}{3} h_\varphi \frac{\partial U_\perp}{\partial x} \right) \right]$$

$$= -\Pi_{//} - \delta \rho n U_{//} k_{ion}(T, n) + \delta \rho n k_{cx}(T)(V_{//} - U_{//}) + \delta m_0 n U_{//} k_{rec}(n, T); \qquad \text{(V.30)}$$

$$\frac{\partial \rho \mathrm{U}_{\perp}}{\partial \mathrm{t}} + \frac{\partial}{\partial x}\left(\mathrm{h}_{\varphi}(\rho \mathrm{U}_{\perp}^{2} + \mathrm{p}_{0}) / \mathrm{h}_{\theta} + \mathrm{U}_{//}\mathrm{U}_{\perp} - \eta_{0}\left(\left(1 + \frac{\mathrm{h}_{\varphi}^{2}}{3}\right) \frac{\partial \mathrm{U}_{\perp}}{\mathrm{h}_{\theta}\partial x} + \frac{1}{3}\mathrm{h}_{\varphi}\frac{\partial \mathrm{U}_{//}}{\partial x} \right) \right) =$$

$$= -\Pi_{\perp} - \delta\rho \mathrm{n}\mathrm{U}_{\perp} k_{ion}(\mathrm{T}, \mathrm{n}) - \delta\rho \mathrm{n} k_{cx}(\mathrm{T})\mathrm{U}_{\perp} + \delta m_{0} \mathrm{n}\mathrm{U}_{\perp} k_{rec}(\mathrm{n}, \mathrm{T}); \qquad \text{(V.31)}$$

$$\frac{\partial \varepsilon_{0}}{\partial t} + \frac{\partial}{\partial x}\left(\left(\varepsilon_{0} + NT_{0}\right)\frac{U_{\theta}}{h_{\theta}} - \frac{\chi_{0}}{h_{\theta}^{2}}\frac{\partial T_{0}}{\partial x} - \frac{\eta_{0}}{h_{\theta}^{2}}\left(\frac{4}{3}U_{\theta}\frac{\partial U_{\theta}}{\partial x} + U_{\varphi}\frac{\partial U_{\varphi}}{\partial x} \right) \right) =$$

$$= -\ \delta\varepsilon_{0}\, Nn\ k_{ion}(T) + \delta n N\left(\varepsilon_{i} - \varepsilon_{N}\right)\ k_{cx}(T) + \delta n N \varepsilon_{N} k_{ion}(T) + \delta Q_{rec,i}$$

$$\varepsilon_{i} \equiv \frac{m_{i} n V^{2}}{2} + \frac{3}{2} nT \ ; \qquad \varepsilon_{N} \equiv \frac{m_{N} N V_{0}^{2}}{2} + \frac{3}{2} NT_{0}; \qquad Q_{rec,i} = n\left(\frac{m_{i} V_{//}^{2}}{2} + \frac{3}{2} T_{i} \right) \nu_{rec}$$

(V.32)

$$\frac{4}{3}U_{\theta}\frac{\partial U_{\theta}}{\partial x} + U_{\varphi}\frac{\partial U_{\varphi}}{\partial x} = \frac{2}{3}\frac{\partial}{\partial \theta}\left(U_{\theta}^{2} + \frac{3}{4}U_{\varphi}^{2} \right) = \frac{2}{3h_{\theta}}\frac{\partial}{\partial x}\left(U_{//}^{2}\left(h_{\theta}^{2} + \frac{3}{4}h_{\varphi}^{2} \right) + U_{\perp}^{2}\left(h_{\varphi}^{2} + \frac{3}{4}h_{\theta}^{2} \right) + \frac{1}{2}U_{//}U_{\perp}h_{\theta}h_{\varphi} \right)$$

$$U_{\theta} = U_{//}h_{\theta} + U_{\perp}h_{\varphi}; \qquad U_{\varphi} = U_{//}h_{\varphi} - U_{\perp}h_{\theta}; \qquad h_{\theta} \equiv B_{\theta} / B$$

$$U_{//} = U_{\varphi}h_{\varphi} + U_{\theta}h_{\theta}; \qquad U_{\perp} = U_{\theta}h_{\varphi} - U_{\varphi}h_{\theta}; \qquad h_{\varphi} = \sqrt{1 - h_{\theta}^{2}}$$

- **Dimensionless form of equations:**

We will introduce the following dimensional units

N_g, T_{gg}, L, $\tau_g = L/v_g$, $v_g = \sqrt{T_{gg}/m_g}$,

and dimensionless variables

$t = t/\tau_g$, $U = U/v_g$, $\tau_g = x/L$, $N = N/N_g$, $T_g = T_g/T_{gg}$,

then the equations read:

$$\frac{\partial N}{\partial t} + \frac{\partial}{\partial \xi}\left(N\left(U_{//} + U_{\perp}\frac{h_\varphi}{h_\theta}\right)\right) = -\delta\frac{N}{\tau^*_{ion}} + \delta\left(\frac{n_s}{N_g}\right)\frac{n}{\tau^*_{rec}} + \frac{N}{\tau^*_{\perp w}};$$

$$\frac{\partial N U_{//}}{\partial t} + \frac{\partial}{\partial \xi}\left(N(U_{//}^2 + T_g + U_{//}U_{\perp}h_\varphi / h_\theta) - \eta_{g0}\left(\left(1+\frac{h_\varphi^2}{3}\right)\frac{1}{h_\theta}\frac{\partial U_{//}}{\partial \xi} + \frac{h_\varphi}{3}\frac{\partial U_{\perp}}{\partial \xi}\right)\right) =$$

$$= -\Pi_{0//} - \delta N U_{//}\left(\frac{1}{\tau^*_{ion}} + \frac{1}{\tau^*_{cx}}\right) + \delta n\left(\frac{n_s}{N_g}\right)\frac{U_{//}}{\tau^*_{rec}} + \delta\frac{N}{\tau^*_{cx}}\left(\frac{V_s}{V_g}V_{//}\right);$$

$$\frac{\partial N U_{\perp}}{\partial t} + \frac{\partial}{\partial \xi}\left((U_{\perp}^2 + T_g)N\frac{h_\varphi}{h_\theta} + N U_{//}U_{\perp} - \eta_{g0}\left(\left(1+\frac{h_\varphi^2}{3}\right)\frac{1}{h_\theta}\frac{\partial U_{\perp}}{\partial \xi} + \frac{1}{3}h_\varphi\frac{\partial U_{//}}{\partial \xi}\right)\right) =$$

$$= -\Pi_{0\perp} - \delta N U_{\perp}\left(\frac{1}{\tau^*_{ion}} + \frac{1}{\tau^*_{cx}}\right) + \delta n\left(\frac{n_s}{N_g}\right)\frac{U_{\perp}}{\tau^*_{rec}}$$

$$\frac{\partial \varepsilon_{g0}}{\partial t} + \frac{\partial}{\partial \xi}\left(\left(\varepsilon_{g0} + N T_g\right)\frac{U_\theta}{h_\theta} - \frac{\chi_{g0}}{h_\theta^2}\frac{\partial T_g}{\partial \xi} - \frac{\eta_{g0}}{h_\theta^2}\left(\frac{4}{3}U_\theta\frac{\partial U_\theta}{\partial \xi} + U_\varphi\frac{\partial U_\varphi}{\partial \xi}\right)\right) =$$

$$= -\delta\frac{\varepsilon_{g0}}{\tau^*_{ion}} + \delta\frac{\left(\frac{N}{n}\varepsilon_{i0} - \varepsilon_{g0}\right)}{\tau^*_{cx}} - \frac{\varepsilon_{g0} - N T_w}{\tau^*_{\perp w}} + \frac{\varepsilon_{i0}}{\tau^*_{rec}};$$

where:

$$\varepsilon_{g0} \equiv \frac{\mathrm{NU}^2}{2} + \frac{3}{2}\mathrm{NT_g}; \quad \varepsilon_{i0} \equiv \frac{\left(\frac{m_i}{m_g}\frac{n_s}{N_g}\frac{V_s^2}{U_g^2}\right)\mathrm{nV}_{//}^2}{2} + \frac{3}{2}\left(\frac{n_s}{N_g}\frac{T_s}{T_{gg}}\right)\mathrm{nT_i};$$

$$\mathrm{U}_\theta = \mathrm{U}_{//}h_\theta + \mathrm{U}_\perp h_\varphi; \qquad \mathrm{U}_\varphi = \mathrm{U}_{//}h_\varphi - \mathrm{U}_\perp h_\theta; \qquad h_\theta \equiv B_\theta / B = 0.02$$

$$\mathrm{U}_{//} = U_\varphi h_\varphi + \mathrm{U}_\theta h_\theta; \qquad \mathrm{U}_\perp = \mathrm{U}_\theta h_\varphi - \mathrm{U}_\varphi h_\theta; \qquad h_\varphi = \sqrt{1 - h_\theta^{\,2}}$$

$$\frac{4}{3}\mathrm{U}_\theta \frac{\partial \mathrm{U}_\theta}{\partial \xi} + \mathrm{U}_\varphi \frac{\partial \mathrm{U}_\varphi}{\partial \xi} = \frac{2}{3}\frac{\partial}{\partial \xi}\left(\mathrm{U}_\theta^2 + \frac{3}{4}\mathrm{U}_\varphi^2\right) =$$

$$= \frac{2}{3h_\theta}\frac{\partial}{\partial \xi}\left(\mathrm{U}_{//}^2\left(h_\theta^2 + \frac{3}{4}h_\varphi^2\right) + \mathrm{U}_\perp^2\left(h_\varphi^2 + \frac{3}{4}h_\theta^2\right) + \frac{1}{2}\mathrm{U}_{//}\mathrm{U}_\perp h_\theta h_\varphi\right)$$

$$\eta_{g0} = \frac{\eta_0(T_g)}{m_g V_g^2 N_g L / V_g}, \quad \eta_0(T_g) = \eta_0\sqrt{T_g};$$

$$\eta_0 = \frac{0.998 \cdot 2.5 m_{p,gramm}}{\pi\zeta^2\sqrt{5\pi}} 1.38 \cdot 10^6 = 0.00065;$$

$$\zeta \equiv 2.68 \cdot 10^{-8}$$

$$\chi_{g0} = \frac{\chi_0(T_g)}{V_g N_g L}; \qquad \chi_0(T_g) = \chi_0\sqrt{T_g}; \quad \chi_0 = \eta_0 \frac{15}{4 \cdot 2.5 m_{p,gramm}};$$

$$m_{p,gramm} = 1.6726 \cdot 10^{-24}$$

$$\Pi_{0//,0\perp} = \frac{\Pi_{//,\perp}\tau_g}{m_g N_g V_g}; \qquad \Pi_{//} \equiv 3\eta_0(T_g) \cdot \frac{\delta^2 V_{//}}{(1-\delta)^2}\frac{(1 - e^{-L/\lambda_*})}{\Delta^2}; \qquad \Pi_\perp = 0$$

$$\lambda_* \equiv 5.52 \cdot Kn + 0.48; \quad Kn \equiv \Delta\frac{(1-\delta)}{\delta} N\sigma_{n-n};$$

$$\sigma_{n-n} = 2 \cdot 10^{-15} cm^2; \quad \delta \equiv \frac{\Delta}{d}$$

$$\tau^*_{rec/ion/cx} = \tau_{rec/ion/cx}\frac{\tau_s}{\tau_g}, \quad \tau_s \equiv tau0; \quad \tau_{rec}(\mathrm{n}, \mathrm{T_e}) \equiv taurec(dd, te);$$

$$\tau_{ion}(\mathrm{n}, \mathrm{T_e}) \equiv tauion(den, te);$$

$$\tau_{cx}(\mathrm{T_e}) \equiv taucx(x, te);$$

$$\tau^*_{w\perp} = \tau_w \frac{\Delta^2}{D_{\perp 0}}\frac{1}{\tau_g}, \quad \tau_w = const.$$

- **Numerical procedure (discretesation of equations):**

$$\left.\frac{\partial\left[N\left(U_{//}+U_{\perp}h_{\varphi}/h_{\theta}\right)\right]}{\partial x}\right|_i = \frac{\left[N\left(U_{//}+U_{\perp}h_{\varphi}/h_{\theta}\right)\right]_{i+} - \left[N\left(U_{//}+U_{\perp}h_{\varphi}/h_{\theta}\right)\right]_{i-}}{h} = \tag{V.33}$$

$$= \frac{1}{h}\left[\left[N\left(U_{//}+U_{\perp}h_{\varphi}/h_{\theta}\right)\right]\right]_i = \frac{1}{h}\left\{\left[N\left(U_{//}+U_{\perp}h_{\varphi}/h_{\theta}\right)\right]_{i+} - \left[N\left(U_{//}+U_{\perp}h_{\varphi}/h_{\theta}\right)\right]_{i-}\right\}$$

$$\frac{N_{new}(i)-N_{old}(i)}{\tau_g} + \frac{\left[N\left(U_{//}+U_{\perp}h_{\varphi}/h_{\theta}\right)\right]_i}{h} = N_{new}(i)\nu_w - \delta N_{new}(i)\nu_{ion} + \delta n_{new}\nu_{rec};$$

$$\nu_{rec} \equiv \frac{\tau_s}{\tau_{rec}};\quad \nu_w \equiv \frac{\tau_s}{\tau_{\perp w}}$$

$$N_{new}(i) = \frac{N_{old}(i) + \left\{\frac{\tau_g}{\tau_{rec}}\delta n_{new} - \frac{\tau_g}{h}\left[N\left(U_{//}+U_{\perp}h_{\varphi}/h_{\theta}\right]_i\right\}\right.}{\left[1-\tau_g/\tau_w + \delta\tau_g/\tau_{ion}(n_{old}(i),T_{old}(i))\right]}$$

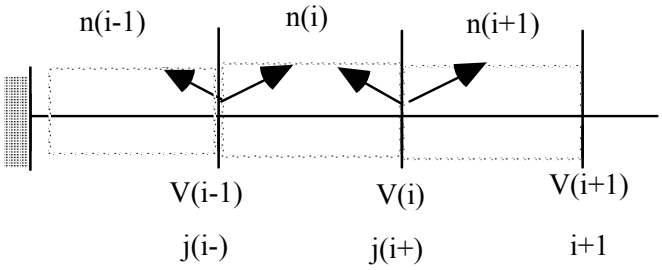

j(i+) = n(i)max(V(i),0)-n(i+1)max(-V(i),0)

j(i-) = n(i-1)max(V(i-1),0)-n(i)max(-V(i-1),0)

○ *first volume* :

$$N_{new}(1)=\frac{N_{old}(1)+\left\{\frac{\tau_g}{\tau_{rec}}\delta n_{new}(1)-\frac{\tau_g}{h}\left(N_{old}(1)d\max 1\left[(U_{//}(1))_{old}+(U_{\perp}(1))_{old}h_{\varphi}/h_{\theta}\right]-N_{old}(2)d\max 1\left[-(U_{//}(1))-(U_{\perp}(1)h_{\varphi}/h_{\theta})\right]\right)\right\}}{\left[1-\frac{\tau_g}{\tau_s}+\delta\frac{\tau_g}{\tau_{rec}(n_{old}(1),T_{old}(1))}\right]}$$

○ $i=2,na$

$$N_{new}(i)=\frac{N_{old}(i)+\left\{\frac{\tau_g}{\tau_{rec}}\delta n_{new}(i)-\frac{\tau_g}{h}\left(\left[N_{old}(i)d\max 1(W_{old}(i))-N_{old}(i+1)d\max 1(-W_{old}(i))\right]-\left[N_{old}(i-1)d\max 1(W_{old}(i-1))-N_{old}(i)d\max 1(-W_{old}(i-1))\right]\right)\right\}}{\left[1-\frac{\tau_g}{\tau_w}+\delta\frac{\tau_g}{\tau_{rec}(n_{old}(i),T_{old}(i))}\right]}$$

$$W(i)=U_{//}(i)+\frac{h_{\varphi}}{h_{\theta}}U_{\perp}(i)$$

○ $i=na+1,nxi\ 2$

$$n_{new}(i)=\frac{\left\{-\frac{\tau}{h}\left(\left[n_{old}(i)\max(V_{old}(i),0)-n_{old}(i+1)\max(-V_{old}(i),0)\right]-\left[n_{old}(i-1)\max(V_{old}(i-1),0)-n_{old}(i)\max(-V_{old}(i-1),0)\right]\right)\right\}}{\left[1-\frac{\tau}{\tau_s}+\frac{\tau}{\tau_{rec}(n_{old}(i),T_{old}(i))}\right]}$$

○ *last volume*

$$N_{new}(\xi 1)=\frac{A}{\left[1+\frac{\tau}{\tau_s}+\frac{\tau}{\tau_{rec}(n_{old}(\xi 1),T_{old}(\xi 1))}\right]}$$

$$A\equiv\left\{-\frac{\tau}{h}\left(n_{old}(\xi 1)\max(V_{old}(\xi 1),0)-n_{old}(\xi 2)\max(V_{old}(\xi 2),0)+n_{old}(\xi 1)\max(-V_{old}(\xi 2),0)\right)+n_{old}(\xi 1)+\frac{\tau N_0(\frac{h}{2})}{\tau_{ion}(n_{old}(\xi 1)T_{old}(\xi 1))}\right\}$$

○ $i=2,na$

$$N_{new}(i)=\frac{N_{old}(i)+B}{\left[1-\frac{\tau_g}{\tau_w}+\delta\frac{\tau_g}{\tau_{rec}(n_{old}(i),T_{old}(i))}\right]}$$

$$B\equiv\left\{\frac{\tau_g}{\tau_{rec}}\delta n_{new}(i)-\frac{\tau_g}{h}\left(\left[N_{old}(i)d\max 1(W_{old}(i))-N_{old}(i+1)d\max 1(-W_{old}(i))\right]-C\right)\right\}$$

$$C\equiv\left[N_{old}(i-1)d\max 1(W_{old}(i-1))-N_{old}(i)d\max 1(-W_{old}(i-1))\right]$$

$$W(i)=U_{//}(i)+\frac{h_{\varphi}}{h_{\theta}}U_{\perp}(i)$$

V.3 Boundary conditions for neutrals

The distribution function of the incident atoms at the Plate

$$F_0^+(N,T_0) = \beta \frac{N}{n_i} f_M{}^+(n_i,T_i) \approx \beta \frac{N}{n_i} \frac{e^{-\frac{m_i \vec{v}^2}{2T_i}}}{\left(\sqrt{\pi} v_{T_i}\right)^3} \quad \text{(V.34)}$$

reflected particles:

$$F_0^-(N,T_0) = f_0^-(N_0,T_0) + + R_0 \beta \frac{N}{n_i} f_M{}^+(n_i,T_i)$$

$$f_0^-(N_0,T_0) \equiv R \frac{2\Gamma_w}{\pi v_{T_0}^4} e^{-\frac{m_i \vec{v}^2}{2T_0}} \quad \text{(V.35)}$$

; $\quad q_w^i = q_{//}^i + e\varphi; \quad e\varphi \approx 3T_e$

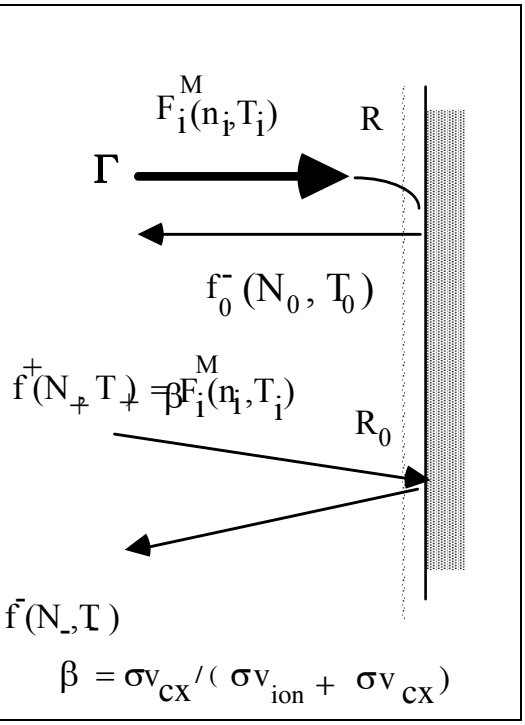

Here

$$N = N_{0i} + N_+ + N_-;$$

$$N_{0i} = \Gamma R_N \sqrt{\frac{2\pi m_i}{T_{i-}}}; \qquad N_+ = \beta n_i; \qquad N_- = \frac{\beta n_i}{R_N} \sqrt{\frac{T_i}{T_-}}$$

where

$T_+ \cong T_i$

$T_{i-} = \frac{q_w^i}{2\Gamma_w} R_E\left(\frac{q_w^i}{\Gamma_w}\right)$

$T_- = \frac{f_i T_i}{2} R_E(f_i T_i); \qquad where$

$f_i = \left[\left(2 + M_0^2\right)e^{-M_0^2} + M_0\sqrt{\pi}(2.5 + M_0^2) Erf(-M_0)\right] / G(M_0)$

(see for details concerning function last function in [21])

- **Heat and viscose fluxes**

$$q_N = 3T_e R_N \Gamma R_E(3T_e) + \left(\frac{q_i}{\Gamma}\right)\left(1 - R_N R_E\left(\frac{q_i}{\Gamma}\right)\right) \cdot \frac{N_+}{4}\sqrt{\frac{8T_i}{\pi m_i}}$$

$$\hat{\pi}_{//} = N_{0i}T_{i-} + N_+\left(T_i + mV_i^2\right) + N_-T_-,$$
$$\hat{\pi}_{\perp} = N_{0i}T_{i-} + N_+T_i + N_-T_-,$$

- **Boundary conditions for neutrals in dimensionless form**

$$\mathrm{N} = \mathrm{N}_{0\,\mathrm{i}} + \mathrm{N}_+ + \mathrm{N}_-;$$

$$\mathrm{N}_{0\mathrm{i}} = \Gamma R_N \sqrt{\frac{2\pi}{\mathrm{T}_{i-}\left(\frac{m_i T_g}{m_g T_s}\right)}}; \qquad \mathrm{N}_+ = \beta \mathrm{n}_i \left(\frac{n_s}{N_g}\right); \qquad \mathrm{N}_- = \frac{\beta \mathrm{n}_i}{R_N}\left(\frac{n_s}{N_g}\right)\sqrt{\frac{\mathrm{T}_i}{\mathrm{T}_-}}$$

$$\Gamma \equiv \mathrm{N}(\mathrm{U}_{//} + \mathrm{U}_{\perp}\frac{\mathrm{h}_\varphi}{\mathrm{h}_\theta})$$

$$\mathrm{T}_{i-} = \varepsilon_i R_E\left(\varepsilon_i \cdot T_s\right) \qquad\qquad \varepsilon_i \equiv \left(\mathrm{T}_i + V_{//}^2/4\right)$$

$$\mathrm{T}_- = \frac{f_i \mathrm{T}_i}{2} R_E\left(f_i \mathrm{T}_i \cdot T_s\right);$$

$$f_i = \left[\left(2 + M_0^2\right)e^{-M_0^2} + M_0\sqrt{\pi}(2.5 + M_0^2)Erf(-M_0)\right]/G(M_0)$$

$$\mathrm{q}_N = 3\mathrm{T}_e\left(\frac{T_s}{T_g}\right)R_N \cdot R_E(3\mathrm{T}_e \cdot T_s)\cdot\Gamma + \varepsilon_i(1 - R_N R_E(\varepsilon_i \cdot T_s))\left(\frac{T_s}{T_g}\right)\frac{\mathrm{N}_+}{4}\sqrt{\frac{8\mathrm{T}_i}{\pi}\frac{m_g}{m_i}\left(\frac{T_s}{T_g}\right)}$$

$$\mathrm{q}_N \equiv \left(\varepsilon_{g0} + \mathrm{NT}\right)\frac{\mathrm{U}_\theta}{\mathrm{h}_\theta} - \frac{\chi_{g0}}{\mathrm{h}_\theta^2}\frac{\partial \mathrm{T}_g}{\partial \xi} - \frac{\eta_{g0}}{\mathrm{h}_\theta^2}\left(\frac{4}{3}\mathrm{U}_\theta\frac{\partial \mathrm{U}_\theta}{\partial \xi} + \mathrm{U}_\varphi\frac{\partial \mathrm{U}_\varphi}{\partial \xi}\right)$$

$$\hat{\pi}_{//} = \mathrm{N}_{0i}\mathrm{T}_{i-}\cdot\left(\frac{T_s}{T_g}\right)+\mathrm{N}_{+}\left(\mathrm{T}_i+V^2\right)\left(\frac{m_i V_s^2}{m_g U_g^2}\right)+\mathrm{N}_{-}\mathrm{T}_{-}\cdot\left(\frac{T_s}{T_g}\right),$$

$$\hat{\pi}_{\perp} = \mathrm{N}_{0\mathrm{i}}\mathrm{T}_{\mathrm{i}-}\cdot\left(\frac{T_s}{T_g}\right)+\mathrm{N}_{+}\mathrm{T}_{\mathrm{i}}\left(\frac{T_s}{T_g}\right)+\mathrm{N}_{-}\mathrm{T}_{-}\left(\frac{T_s}{T_g}\right),$$

$$\hat{\pi}_{//} \equiv \mathrm{N}(\mathrm{U}_{//}{}^2+\mathrm{T}_g+\mathrm{U}_{//}\mathrm{U}_{\perp}\mathrm{h}_{\varphi}/\mathrm{h}_{\theta})-\eta_{g0}\left(\left(1+\frac{\mathrm{h}_{\varphi}^2}{3}\right)\frac{1}{\mathrm{h}_{\theta}}\frac{\partial \mathrm{U}_{//}}{\partial\xi}+\frac{\mathrm{h}_{\varphi}}{3}\frac{\partial \mathrm{U}_{\perp}}{\partial\xi}\right)$$

$$\hat{\pi}_{\perp} \equiv (\mathrm{U}_{\perp}^2+\mathrm{T}_{\mathrm{g}})\mathrm{N}\frac{\mathrm{h}_{\varphi}}{\mathrm{h}_{\theta}}+\mathrm{N}\mathrm{U}_{//}\mathrm{U}_{\perp}-\eta_{g0}\left(\left(1+\frac{\mathrm{h}_{\varphi}^2}{3}\right)\frac{1}{\mathrm{h}_{\theta}}\frac{\partial \mathrm{U}_{\perp}}{\partial\xi}+\frac{1}{3}\mathrm{h}_{\varphi}\frac{\partial \mathrm{U}_{//}}{\partial\xi}\right)$$

The numerical program, solving these equations is presented in **Appendix VIII**

VI. Sputtering of the first wall and divertor plates.

It is now recognized that the lifetime of a tokamak reactor is determined by damage of structural elements facing the plasma (e.g. the first wall and divertor plates). For this reason, it is important to obtain the most accurate estimates of erosion rates for these elements. Available experimental data applied to steady state or long pulse operation indicate that the first wall erosion rate is due mainly to charge exchange neutral sputtering, and that the erosion rate of divertor plates is determined by fuel and impurity ion sputtering (particularly self-sputtering).

VI.1 Objectives

Here the calculations are presented for the sputtering yields averaged over energy and angular distributions of incident deuterium and tritium ions on various materials proposed for the divertor plates and first wall of a tokamak reactor (C, Al, Ti, Fe, MO, W). Modifications to the particle distribution function due to acceleration in the sheath electric field are included and the calculations are performed over the energy range characteristic of the particles in the plasma boundary. The results are restricted to the case of magnetic field lines normal to the divertor plate surface.

Calculations of the sputtering yield for first wall materials have been performed in several papers (see, e.g. ref. [30]), Assuming normal incidence, the different expressions are extrapolated to the low energy range characteristic of the plasma edge and used to calculate the divertor plate erosion rate. In general, the sputtering yields so obtained correspond to those which would be produced by particles whose are consistent with acceleration through the Debye sheath. It is easy to show that the thickness, A of structural elements sputtered during one year of continuous operation, by particle fluxes of different species j, can be expressed as

$$\Delta = \frac{5.27 \cdot 10^{-16}}{\rho} A \sum_j \left\langle S_j q_j \right\rangle \qquad \text{(VI. 1)}$$

Here Δ is in mm/year, A is the target atom mass (in amu), ρ is the target material density (g/cm3), $S_j(E,\theta)$ is the sputtering yield of particle j with energy E and angle of incidence θ and q_j, is the flux of particles j (particles cm^{-2} s^{-1}). The brackets $\langle\ \rangle$ represent an average over the angular and energy distribution of incident particles. Thus, the precise determination of the erosion rate needs the correct form of the energy distribution function of the incident particles and the sputtering yield $S_j(E,\theta)$. Although a Maxwellian distribution is commonly chosen, the distribution function of charged particles near the divertor plates may be strongly distorted. This paper presents the results of erosion rate calculations taking into account modifications of the distribution function and the angular dependence of the sputtering yield.

VI. 2 **Distribution functions**

Let us consider the distribution function for particles arriving at a material surface. It is clear that many effects can influence the energy distribution function near the divertor plates. In practise, it is impossible to take into account all of these effects by an exact method. For this reason we consider only the main effects which determine the difference between the near and far distribution functions in the edge plasma flow.

Far from the divertor plates, the ion distribution function can be considered a Maxwellian shifted by some velocity V_0. The longitudinal gradients in the boundary plasma, particle sources and acceleration in the presheath field determine the value of V_0, [31]. For typical boundary plasma parameters the inequality $\rho_e \le \lambda_D < \rho_i < \lambda_p$ is satisfied ($\rho_{e,i}$ is the electron (ion) Larmor radius, λ_D is the Debye length and λ_p - the mean free path of a charged particle). If λ_p, exceeds the characteristic length of the neutral atom distribution near the plate, then this neutral gas will not influence the charged particle distribution function. This condition is satisfied if the plasma density, which determines the width of the neutral atom spatial distribution exceeds or is comparable with the atom density. The effect on the distribution function of a magnetic field and of ionization of atoms may be neglected for the conditions considered here.

The ion velocity distribution at the plasma sheath interface (i.e. at a distance λ_D, from the plate) can be expressed as

$$f_0(M_0) = \frac{2j_0}{V_T^2}\frac{1}{\pi V_T^2}\exp\left[-u_{\perp 0}^2 - (u_{//0} - M_0)^2\right] \qquad \text{(VI. 2)}$$

where $j_0 = n\sqrt{T/2\pi m_i}$ is the ion flux to the plate, $u_{\perp 0} = V_\perp / V_T$, $u_{//0} = V_{//} / V_T$ are the transverse and longitudinal components of the velocity along the magnetic field normalized to the thermal velocity $V_T = \sqrt{2T_i / m_i}$ and $M_0 = V_{//} / V_{T0}$. Expression (VI.2) represents the distribution function for collisionless ions accelerated by the presheath field so that at the entrance to the sheath their mean velocity satisfies the Bohm sheath criterion. According to this condition, the value of M_0 at the plasma-sheath interface is given by $M_0 = \sqrt{Z_j e\varphi_0 / T_i} \approx \sqrt{Z_j / 2}$ where Z_j is the charge of an ion accelerated in the presheath field, $e\varphi_0 \sim T_e / 2$.

In so far as that in this regime the distribution function is determined only by the constants of motion, near the plate the distribution function is

$$f = \iint f_0(u_{//0}, u_{\perp 0})\delta\left(u_\perp^2 - u_{\perp 0}^2\right)\delta\left(u_{//}^2 + \frac{Z_j e(\varphi - \varphi_0)}{T_i} - u_{//0}^2\right) du_{//0}^2 du_{\perp 0}^2 \qquad \text{(VI. 3)}$$

Here φ is the plasma potential far from the plate, and δ is the Dirac delta function. Taking the plate potential to be zero, the distribution function for the ions at the plate may be written as:

$$f_d = \begin{cases} \dfrac{2j_0}{V_T^4 F(M_0)}\exp\left(-u_\perp^2 - \left(\sqrt{u_{//}^2} - \dfrac{Z_j e\varphi_0}{T_i} - M_0\right)^2\right) & u_{//} > \sqrt{\dfrac{Z_j e\varphi_0}{T_i}} \\ f_d = 0 & u_{//} < \sqrt{\dfrac{Z_j e\varphi_0}{T_i}} \end{cases} \quad \text{,(VI. 4)}$$

and $F(M_0) \equiv 2\pi\int_0^\infty f(V)dV_\perp \int_0^\infty V_{//}dV_{//} = e^{-M_0^2} + \sqrt{\pi}M_0 Erf(-M_0)$ (VI. 5)

It should be noted that in obtaining eq. (VI. 4) the ions are assumed to completely recombine on the plate and the lines of force are assumed to be oriented normally to the divertor plates. Clearly, if the angle, θ, between the normal to the plate and the line of force increases, then the value of M_0, which is proportional to $\cos\theta$ tends to zero. In the limiting case of grazing incidence ($\theta \to \pi/2$) the distribution function (4) transforms into an unshifted Maxwellian. The effect of the magnetic field can be neglected in this case since $\rho_i > \lambda_D$. The dependence of the shift in the distribution function on the inclination angle of the line of force is connected with the fact the sheath electric

field is oriented normal to the surface. The value of the component of this field along the direction of the lines of force decreases when the inclination angle increases. In reality, they are normal and tangential intersections of the lines of force with the surface because of surface roughness. The most unfavourable case, corresponding to normal incidence (θ = 0), has been taken into account in the calculations of sputtering yields which follow. The usual expression for the potential drop in the sheath is used: $e\varphi_0 \approx T_e \ln\sqrt{m_i / 2\pi m_e}$ .This expression is valid in the absence of secondary electron emission and if the inequality $\sum_k n_{Z_k} Z_k << n_i$ is satisfied, (n_i is the plasma ion density and n_z, is the density of impurity ions in ionization state Z_k ,). From eq. (VI. 4) we note that in general there is a large difference between the distribution of ions arriving at the plate and a simple Maxwellian. For the distribution function of neutrals near the plate, we assume the ion distribution function of eq. (VI. 2). This assumption is based on the fast relaxation (over a time of order the collision time) of the distribution function of cold atoms leaving the plate surface to the ion distribution function near the plate. We assume further that the distribution function of the atoms arriving at the first wall is also Maxwellian.

VI.3 Energy dependence of the sputtering yield

We now turn to the energy dependence of the sputtering yield for the case of normal incidence. The exact solution of the sputtering yield problem for the low energy range $E < 1keV$ has not obtained yet. For this reason, we must use empirical relations that agree well with the available (scarce) experimental data. The following expression for the sputtering yield is proposed in [32-34]:

$$S_1(E,0) = \frac{C}{U_0} Z_1^{3/4} (Z_2 - 1.8)^2 \left(\frac{M_1 - 0.8}{M_2} \right)^{3/2} \cdot \frac{(E - E_{TH})}{\left(E - E_{TH} + 50 Z_1^{3/4} Z_2^{3/4}\right)^2} \qquad \text{(VI. 6)}$$

where $C = 2 \cdot 10^3$ for hydrogen atoms (ions) and C = 400 for other projectiles. U , is the binding energy of the surface atoms (sublimation energy) in eV , Z_1, Z_2, M_1, M_2 are the atomic numbers and masses (in amu) of the target and projectile respectively, ***E*** is the projectile energy (eV) and E_{TH} **,** is the threshold energy given by the expression (VI. 7):

$$E_{TH} = \frac{(4M_1 + M_2)^2}{4M_1 M_2} \qquad \text{(VI. 7)}$$

From equation (VI. 6) we see that $S_1 \sim 1/E_1$ for large E but the experimental data agree fairly well with the law $S \sim \ln E / E$ [33]. The expression proposed in [34], based on the results of both theoretical and experimental investigations, and predicts just such energy dependence.

According to [34] the sputtering yield is

$$S_2(E,0) = Q\left\{3.441\sqrt{\frac{E}{E_{TF}}}\ln\left(\frac{E}{E_{TF}}+2.718\right)\cdot\left[1-\left(\frac{E}{E_{TF}}\right)^{-2/3}\right]\cdot\left(1-\frac{E_{TH}}{E}\right)^2\right\}\cdot F(E,E_{TH}) \qquad \text{(VI. 8)}$$

where

$$F(E,E_{TH}) = \left\{1+6.355\sqrt{\frac{E}{E_{TF}}}+\frac{E}{E_{TF}}\left(6.882\sqrt{\frac{E}{E_{TF}}}-1.708\right)\right\}^{-1} \qquad \text{(VI. 9)}$$

Here, E_{TF}, is the energy in the centre-of-mass system for a head-on collision with the screening radius for a Thomas-Fermi potential as the closest approach and E_{TH}, is the threshold energy. The parameters Q, E_{TF}, E_{TH} are given in [34] for some representative cases. Calculations show that the predictions of equation (VI. 8) are somewhat closer to the experimental data than those from equation (VI. 6). We therefore choose the former for use in our estimation of the sputtering yields at low energy.

VI. 4 Angular dependence of the sputtering yield

Several authors (see, e.g. [32]) have considered the sputtering yield dependence on the projectile angle of incidence.

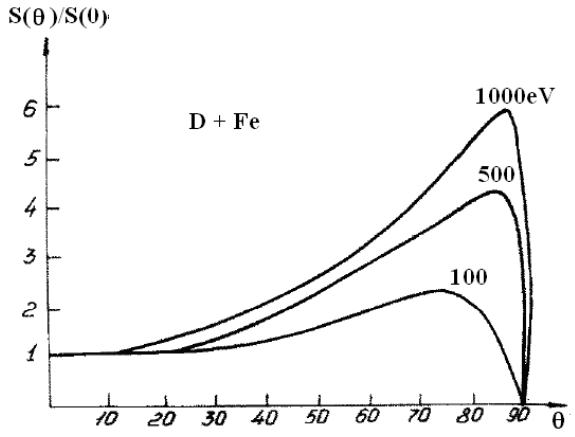

Fig. VI.1. The angular dependence of the sputtering yield $S(\theta)$ for varying projectile energy.

The most complete treatment is given in [34], according to which the following approximation may be used:

$$S(\theta) = \frac{1}{\cos^f\theta}\exp\left\{-f\cos\theta_{opt}\cdot\left(\frac{1}{\cos\theta}-1\right)\right\} \qquad \text{(VI. 9)}$$

The parameters f and θ_{opt}, have been determined both from available experimental data and numerical calculations. f is independent of projectile energy for the case of sputtering by light ions, and θ_{opt} (in degrees) is given by the expression

$$\theta_{opt} = 90^\circ - 57.3\frac{\eta}{E^{1/4}} \qquad \text{(VI. 10)}$$

f and η (for $E = 1$ keV) are given in ref. [35] for H, D, T, He and various target materials. Fig. 1 shows the function $S(\theta)$ for the combination (D +Fe). It should be noted that equation (VI. 9) and (VI. 10) predict the angular dependence of the sputtering yield well only for light ion sputtering. Their validity to the case of heavy ion sputtering is doubtful, especially if calculations of the sputtering yield averaged over an energy spectrum are required. In addition, it can be shown that the sputtering yield averaged over the energy and angular distributions of the incident particles is very sensitive to the behaviour of its components in the near threshold energy range and near $\theta = 90^\circ$. There is evidence that equations (VI. 9) and (VI. 10) are not valid in this case.

VI. 5. The average sputtering yield

The twice-averaged sputtering yield, which we define as the yield averaged over the distributions of energy and angle of incidence of the projectiles, is given by

$$\overline{S_j} = \frac{\int f_d S(E,\theta) V_{//} dV}{\int f_d V_{//} dV} =$$

$$= \frac{\int f_d(E,\theta)) S(E,\theta)\sqrt{E} dE \cos\theta \cdot d(\cos\theta)}{\int f_d(E,\theta))\sqrt{E} dE \cos\theta \cdot d(\cos\theta)} \qquad \text{(VI. 11)}$$

This expression may be transformed to the following

$$\overline{S_j}\left(\frac{atom}{ion}\right) = S_{T_0}\int_0^1 tS(t)\int_{\varepsilon^*}^{\infty}\exp\left(-\frac{\varepsilon}{\beta}(1-t^2)\right)S(\varepsilon)\exp\left[-\left(\sqrt{\frac{\varepsilon}{\beta}t^2 - \delta} - M_0\right)^2\right]\varepsilon d\varepsilon \qquad \text{(VI. 12)}$$

where

$$S_{T_0} = \frac{2E_T^2}{T_i^2 F(M_0)}, \qquad t = \cos\theta$$

$$\varepsilon^* = \max(1, \delta); \qquad \varepsilon = E / E_{TH}$$

$$\beta = T_i / E_{TH} \qquad \delta = Z_j e\varphi_0 / T_i$$

In equation (VI. 12) $S(t)$ represents, the angular dependence of the sputtering yield [see eq. (VI. 9)] and $S(\varepsilon)$ the energy dependence [see eq. (VI. 9)]. We note that the dependence of $\overline{S}$ on δ (i.e. on Z_j and φ_0) is rather complex. On the one hand $\overline{S}$ evidently increases when δ increases due to an increase in the population of fast particles, but on the other hand, $\overline{S}$ must decrease if the minimum energy gained in the sheath exceeds the threshold energy so long as the integration region over ε decreases when δ increases.

VI. 6 Results and conclusions

In accordance with the above, we have calculated the twice-averaged sputtering yields for a number of target/projectile combinations. Table 1 shows the results for deuterium ion sputtering. Table 2 shows the results for the same target materials but for the case of incident tritium ions. It is interesting to note that in both cases the sputtering yield decreases as the target mass increases in this low energy range; this is valid even for mono-energetic ions.

Table VI. **I**

Variation of the twice averaged sputtering yield, $\overline{S}$ for various target materials as a function of the temperature of incident deuterium ions

T (eV)	Target					
	C	Al	Ti	Fe	Mo	W
5	3.23(−3) [a]	2.2(−4)	1.75(−5)	6.8(−5)	2.8(−12)	2.63(−14)
10	1.97(−2)	5.8(−3)	1.08(−3)	2.94(−3)	3.9(−7)	3.62(−8)
50	5.85(−2)	5.1(−2)	1.8(−2)	3.95(−2)	2.6(−3)	1.53(−3)
100	5.63(−2)	6.06(−2)	2.44(−2)	5.36(−2)	6.3(−3)	4.57(−3)
500	2.9(−2)	4.45(−2)	2.32(−2)	5.4(−2)	1.1(−2)	1.07(−2)
1000	1.9(−2)	3.18(−2)	1.8(−2)	4.29(−2)	1.01(−2)	1.11(−2)

[a] Note: 3.23(−3) means 3.23×10^{-3}.

Table VI. **2**

Variation of the twice averaged sputtering yield, 9, for various target materials as a function of the temperature of incident tritium ions T (ev)

T (eV)	Target					
	C	Al	Ti	Fe	Mo	W
5	1.82(−3) [a]	7.99(−4)	1.6(−4)	3.12(−4)	4.15(−7)	1.62(−12)
10	2.94(−2)	1.24(−2)	3.97(−3)	7.81(−3)	1.6(−4)	3.59(−7)
50	1.94(−1)	7.72(−2)	3.63(−2)	7.37(−2)	1.08(−2)	3.57(−3)
100	2.12(−2)	8.99(−2)	4.68(−2)	9.7(−2)	1.75(−2)	9.29(−3)
500	1.3(−1)	6.52(−2)	4.31(−2)	9.57(−2)	2.36(−2)	2.00(−2)
1000	8.9(−2)	4.66(−2)	3.32(−2)	7.60(−2)	2.08(−2)	2.05(−2)

[a] Note: 1.82(−3) means 1.82×10^{-3}.

These calculations enable us to estimate the relative importance of the effects of acceleration in the sheath potential, modifications of the distribution function and the angular dependence of the sputtering yield. Analysis of the results shows that variations in the sputtering yield are mainly due to the accelerating potential. So, if for example, we take into account only the angular dependence for deuterium atoms at $T = 100eV$ incident on tungsten, then the sputtering yield is increased by about a factor 3 over that for the case of normal incidence. Taking into account the sheath acceleration the yield is enhanced by a factor 35. Fig. VI. 2 show the effect of the angular dependence on the sputtering yield. One can see that the ratio of the twice averaged yield to the energy averaged yield (for the case $\delta = 0,\ M_0 = 0$) increases as the temperature increases. This result is expected so long as the fast particle population increases as the temperature increases since, from equation (VI. 9) the yield is enhanced as grazing incidence is approached. The above leads us to the following conclusion: despite the weak dependence of the sputtering yield on the angle of incidence in the energy range below 200 eV, it is essential to account for the angular dependence in this range if the energy averaged sputtering yield is to be accurately predicted. For example, even at $T = 10eV$, the enhancement factor is 2.5 for D-W sputtering. The calculated data also show that the distribution function distortion introduced by the sheath acceleration effect leads to sputtering yield increases of 1.5-2. This enhancement is comparable with that due to the angular effect. As an illustration, it is interesting to compare the calculated values of the yield with those obtained from equation (VI. 8) for $E = 5.5Z_jT_e$ the energy gain because of acceleration in the sheath and pre-sheath electric fields. It is easy to show that for all projectile/target combinations the values of s given in tables 1 and 2 exceed those of $S_2(3.5ZT)$ the actual enhancement factor depends on the type of projectiles' result also valid if we use expression (VI. 8) to estimate the sputtering yield for $E = 5.5.Z_jT_e$.

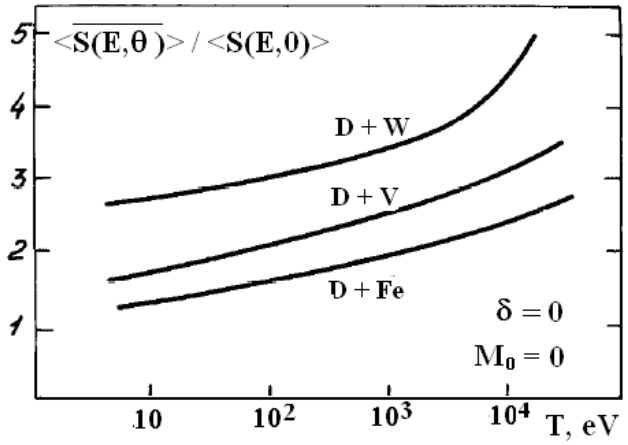

Fig. VI. 2. Ratio of the sputtering yield averaged over energy and angle of incidence to the yield averaged over energy only (i.e. for $\theta = 0$).

The sputtering yields averaged over the distribution function and over the projectile incident angle have been obtained for some candidate target materials (C, Al, Ti, Fe, MO, W) and incident deuterium and tritium ions.

We have shown that the sputtering yield increases if the sheath potential is taken into account and that the usual estimation of the sputtering yield at energy $E = 3.5 Z_j T_e$ is too low

It is found that it is essential to account for the angular distribution of incident light ions at low and high temperatures in order to calculate correctly the sputtering yield averaged over the distribution function of the incident particles [36].

Conclusive remarks

The main objectives of the project have been fulfield. The review of transport models, suitable for simulation of stationary and transient processes in multi-species plasma (ELMs, Massive Gas Injection etc.) are presented and the following tasks are completed:

- An analytical model of impurity distribution in the SOL region, based on the force balance equations along the magnetic field lines.
- The fluid transport equations for impurity ions of arbitrary concentration and in arbitrary charge states in the SOL and divertor plasma (the 21-Gread moment equations) are derived.
- The Braginskii version of the 2-D equations for mulri-component plasma (in the frame of the Chapmen-Enscog procedure) is prepared for implementation.
- The fluid and kinetic models of neutrals (atoms of the hydrogen isotopes and impurity atoms) are prepared for implementation. The proper boundary conditions are derived.

These preparations are foreseen for simulation of the following main tasks:

a) to evaluate ITER core plasma pollution with tungsten impurities sputtered from the divertor plates by small (mitigated) ELMs during the discharge time. This gives the answer to which extent ELMs have to be suppressed to be tolerable for ITER operation in the sense of PSC life-time and dilution. The model will include a sputtering of divertor plates by incident ELMy hot particles as a source of impurity ions, dynamics of impurity ions in the SOL region and “entraining” effect of ELMs in the pedestal area.

b) to simulate the radiation energy distribution on the first wall during TQ and CQ stage in ITER caused by Massive Gas Injection (MGI). Impurities of Ne and Ar will be introduced in H-mode ITER discharge by MGI and their poloidal and radial distribution will be calculated by 2D TOKES Code. To estimate the injected particles stopping radius and required amount of injected gas for ITER by taking into account results and arguments from JET experiments. Such calculations are 2D and address the poloidal asymmetry in the first instance.

It is worth wile to make some remarks, concerning the issues, which are not mentioned above, however remain very important for tokamak-reactor plasmas. In this report the analytical and numerical transport models are presented for multi-component complex plasma, when impurity ions are in arbitrary concentration and in various charge states dominate in plasma and mainly determined transport properties. Description of impurity transport, presented here is done in classical terms. However, in many experimental situations, neoclassical (i.e. collisional) effects alone cannot explain impurity transport [50] Turbulence should be taken into account to explain the observed anomalous transport. Theoretical models predict that turbulence is highly sensitive to the electron temperature gradient [51]. The turbulent transport theoretical predictions show that

decreasing the temperature gradient leads to reduced transport coefficient down to neoclassical level [52]

Also, the effect of neutral atoms is not included in standard tokamak transport treatments. However, it is well known, that neutral atoms in the tokamak edge can influence global confinement by affecting the transition to H-mode. The physical mechanism by which this occurs is not yet clearly identified, but it is well known that neutrals influence ion dynamics through charge-exchange interactions. Furthermore, the radial neutral flux of toroidal angular momentum can modify or even determine the edge radial electric field and plasma rotation. The radial localization of the neutrals also introduces a shear in the flow that may affect edge turbulence [53]. Earlier theoretical work [54] explored the effect of neutrals on collisional ion flow and radial electric field within the framework of neoclassical theory. The neutrals provide a drag on the ions that leads to an effective no slip boundary condition for the toroidal ion rotation within an ion temperature gradient modification. The effect of the neutrals is typically significant if the fraction of atoms in the plasma exceeds about 10^{-4}, which is usually the case in the tokamak edge region just inside the separatrix. The effect of the poloidal variation of the neutral source is imoportent and will be reported next time. Particularly is important to investigate the effect of a poloidally varying source of atoms on the electric field and flow velocity of collisional edge plasma. This effect can be substatianal in the case of massive gas injection or strong repetitive pellet injection. An asymmetry in impurity radiation can be strongly dependent on electric field, therefore dpendent on neutral distribution in edge plasma. All these issues will be addressed in the next contract.

Acknowlegement

This work supported by the European Communities under the contract EFDA/05-1305 between EURATOM and Forschungzentrum Karlsruhe, was carried out within the framework of the European Fusion Development Agreement. The views and opüinions expressed herein not necessarly reflect those of the European Commission.

References

[1] Igitkhanov Yu, Pestchanyi S and Landman I, Modelling of Boundary Plasma in TOKES Preprint FZK, 2009

[2] Landman,I, Janeschitz,G, 17th PSI, Hefei Anhui, China, May 22-26, 2006;

[3] Landman,I, Janeschitz,G, J. Nucl. Mater. 363-365, (2007) 1061;

[4] Landman,I, Janeschitz,G " Plasma Convection in ITER Integrated Modelling with the Code TOKES", paper in 34thEPS Conference on Plasma Physics, 2 - 6 July 2007.

[5] Landman,I, Janeschitz,G., in Proc. 33rd EPS Conf., 2006, ECA Vol. 301, P5.165;

[6] Zhdanov B. and Yushmanov P., (1977) Sov. Plasma Physics, v3,1193

[7] Grad H., (1949) Comment Pure and Applied Mathematic 2, 331,

[8] Igitkhanov Yu., (1988) Contribution to Plasma Physics, 28, 477

[9] Igitkhanov Yu. et. al., (1987) Controlled Fusion and Plasma Physics, (Proc. 14th Eur. Conf. Madrid, 1987) EPS, Pt II.760

[10] Braginskii S., "Transport phenomena in a plasma", in Problems of Plasma Theory, Vol. 1, Ed. M.A. Leontovich (Consultants Bureau, New York, 1965), p. 205.

[11] Herdan R. and Liley B., Rev. Mod. Physics, 32, 731 (1960

[12] Chapmen S. and Cowling T., (1960) The mathematical theory of non-uniform gases, (Cambridge University London).

[13] Zhdanov B.Transport phenomena in multi-component plasma, Moscow, 1982

[14] Hutchinson I.H., et al. Plasma Phys. Contr. Fusion 37 (1995) 1389.

[15] Burrell K.H., Ejima S., Schissel D.P., et al., Phys. Rev. Lett. 59 (1987) 1432.

[16] Chankin A., J. Nucl. Mat. 241-243 (1997) 199.

[17] Rognlien T.D. and Ryutov D.D., Contrib. Plasma Phys. 38 (1998) 152.

[18] Hinton F.L. Kim Y.-B., Nucl. Fusion 34 (1994) 899.

[19] Rognlien T.D., Brown P.N., et al., Contr. Plasma Phys. 34 (1994) 362.

[20] Smith G.R., Brown P.N., et al., J. Nucl. Mat. 220-222 (1995) 1024.

[21] Игитханов Ю. Л., Крашенинников С. И., Кукушкин А. С., Юшманов П. Н.. Особенности процессов переноса в пристеночной плазме токамака // Итоги науки и техники. Сер. Физика плазмы. Т. П. М.: ВИНИТИ, 1989. С. 6-149

[22] G.J. Radford, A.V. Chankin, G. Corrigan, et al., Contrib. Plasma Phys. 36 (1996) 187.

[23] Cohen R.H. and Ryutov D.D., Phys. Plasmas 2 (1995) 2001.

[24] Schaffer M.J.,Chankin A.V, Guo H.Y., et al., Nucl. Fusion 37 (1997) 83.

[25] Post, D., et al. Atomic Data and Nuclear Data Tables, 20 (1987)

[26] Pletnev, V. et al., Sov. J. Plasma Physics, 11 (1980) 338

[27] Igitkhanov, Yu. et.a1., J. Nucl. Mater., (1989) 162

[28] Hobbs, G., Wesson, J., Plasma Phys., 9 (1967) 85

[29] Igitkhanov Yu. and Naujoks D., in Contribution of. Plasma Phys. 36 (1996) S, 67-72, Igitkhanov, Yu. et.a1., J. Nucl. Mater., (1989) 162

[30] Guseva M.,. Ionova E and Martynenko Yu., IAE preprint IAE- 3225 (1979).

[31] Igitkhanov Yu., Pistunovich V.and Pozharov V., IAE preprint IAE-4217/8 (1985).

[32] Smith D.et al. in Proc. 9th Symp. on Engineering Problems in Fusion Research, Chicago, IL, USA, 1981.

[33] Martynenko Yu., Itogi nauki i tekniki [Science and Technology Results] 3 (1982) 119.

[34] Bohdansky J. et al. Nucl. Fusion Special issue (1984) 61.

[35] Yamamura Y., Itikawa Y. and Itoh N. Institute of Plasma Physics, Nagoya University, Report IPPJ-AM-26 (1983).

[36] Igitkhanov J., Journal of Nuclear Materials 162-164 (1989) 462-466

[37] Hinton F. and Hazeltine R., Rev. Mod. Phys. **48**, 239 (1976); S. P. Hirshman and D. J. Sigmar, Nucl. Fusion **21**,1079 (1981).

[38] Carreras B., Owen L., Maingi R., Mioduszewski P., Carlstrom T., and Groebner R., Phys. Plasmas **5**, 2623 (1998); L.Owen,*et. al.,* Plasma Phys. Controlled Fusion **40**, 717 (1998).

[39] Gohil P., Bayrol L. R., Jernigan T. C., *et. al*., Phys. Rev. Lett., **86**, 644 (2001).

[40] R.Boivin et al., Phys. Plasmas **7**, 1919 (2000).

[41] A.Field et al., Plasma Phys. Controlled Fusion **44**, A113 (2002).

[42] A.Field et al., in Proceedings of the 29th EPS Conference on Plasma Physics and Controlled Fusion in Montreux, 2002.

[43] M. Valovic et al., Plasma Phys. Controlled Fusion **44**, A175 (2002).

[44] M. A. Mahdavi et al., Nucl. Fusion **42**, 52 (2002).

[45] T. Fukuda, T. Takizuka, et.al., Plasma Phys. Controlled Fusion **42**, A289,(2000).

[46] R. E.Waltz et.al.,, Phys. Plasmas **1**, 2229 (1994);

[47] Y. Igitkhanov et.al*.,* in Proceedings of the 22thEPS Conference, Bounemouth, 1995

[48] S. Putvinski, *private communication*

[49] Belotserkovski O., Davidov Yu., Large Particle Method in Gas Dynamics, Nauka, Moscow (1982), (in Russian)

[50] Guirlet R. et al. Plasma Physics and Controlled Fusion 48 B63 (2006)

[51] Bourdelle C. et al. Physics of Plasmas 14, 112501 (2007)

[52] Parisot Th. et al. Plasma Physics and Controlled Fusion 50, 055010 (2008)

[53] Guirlet R. et al. Nuclear Fusion 49, 055007 (2009)

[54] Catto P., Helander P., Connor J, and Hazeltine R., Phys. Plasmas **5**, 3961 (1998). T. Fuolop, P. J. Catto, and P. Helander, Phys. Plasmas **5**, 3398 (1998); **5**, 3969 (1998

Appendix I The friction and thermal force in complex plasma

- **For impurity ions**. The general expression for drag (friction) force acting on the impurity ion α in z charge state due to collisions with other impurity species β in ξ charge state , including the mutual collisions with α species in different charge states, ($\beta = \alpha$) reads as:

$$R^u_{\alpha z} = -m_\alpha n_{\alpha z_j} \left\{ \sum_{\beta,\xi} c^{(1)}_{\alpha z,\beta\xi} \cdot \nu_{\alpha z,\beta\xi} \cdot \left(V_{\alpha z} - \overline{V}_\beta \right) \right\} \tag{AI.1}$$

$n_{\alpha z}$ – *is partial impurity concentration in* z_j *charge state,*

$V_{\alpha z}$ – *velocity of impurity ion in z charge state*

β, ξ – *sum over different species and charge states*

(including α *species and their charge states)*

$\overline{V}_\beta = \dfrac{\sum_{\xi_k} n_{\beta\xi} Z_k^2 V_k}{\sum_{z_k} n_{z_k} Z_k^2}$ is the average velocity of β specie over its charge states (AI.2)

Neglecting the mutual collisions of impurities and assuming that they collide mainly with background ions (protons), the drag force reads as:

$$R^u_{\alpha z} \cong -c^{(1)}_{\alpha z,i} m_\alpha n_{\alpha z} \nu_{\alpha z,i} \cdot \left(V_{\alpha z} - V_i \right) \tag{AI.3}$$

when $m_{\alpha z} >> m_i$,

$$c^{(1)}_{\alpha z,i} = \frac{\left(1 + 0.24 Z_0\right) \cdot \left(1 + 0.93 Z_0\right)}{\left(1 + 2.65 Z_0\right) \cdot \left(1 + 0.285 Z_0\right)}, \tag{AI.4}$$

where $Z_0 = \dfrac{\sum_z n_{\alpha z_j} z^2}{n_i} = \dfrac{n_\alpha \sum_z n_{\alpha z_j} z^2 / n_\alpha}{n_i} = \dfrac{n_\alpha}{n_i} \cdot \overline{Z}^2$ and (AI.5)

$$\overline{Z}^2 = \sum_z n_{\alpha z} z^2 / n_\alpha \tag{AI.6}$$

$c^{(1)}_{\alpha z,\beta\xi}$ in the case of arbitrary mass of species, can be evaluate numerically.

For arbitrary heavy masses (not too different) coefficients can be found by using the following expression:

$$C = P_1 + \frac{P_2}{P_3 + Z_{ih}} \tag{AI.7}$$

where $Z_{ih} = \dfrac{\sum_h n_{hz} z^2}{\sum_i n_{i\xi} \xi^2}$. Index h corresponds to the heaviest impurity in the charge state z and i - to the lighter species in the charge state ξ.
The P_n values in equation (AI.6) in plasma with two different species are listed in the Table I. for different pares from the set of impurities. Here

$$Z_{eff} = \frac{n_i + \sum_j n_{z_j} z_j^2}{n_e} \quad \text{and} \tag{AI.8}$$

$$n_e = n_i + \sum_{\alpha z} n_{\alpha z} z \tag{AI.9}$$

In practical units:

$$\nu_{z_j,i}[\text{sec}] = 4.79 \cdot 10^{-8} \cdot c_{z,i}^{(1)} \frac{n_i[cm^{-3}]}{T_i^{3/2}[eV]} \cdot \Lambda Z_j^2 \left(\frac{2 m_i m_p}{(m_z + m_i) m_z} \right)^{1/2} \tag{AI.10}$$

$$R_{\alpha z}^u [g/cm^2 \sec^2] \cong$$
$$\cong 8.012 \cdot 10^{-32} \cdot c_{\alpha z,i}^{(1)} \cdot \frac{n_{\alpha z}[cm^{-3}]}{T_i^{3/2}[eV]} \cdot \Lambda Z^2 \left(\frac{2 m_i m_\alpha}{(m_\alpha + m_i) m_p} \right)^{1/2} n_i[cm^{-3}] \cdot V_i[cm/\sec] \tag{AI.11}$$

The drag force for light impurities (hydrogen isotopes).

$$R_i^u = -m_i n_i \left\{ \sum_{\beta,\xi} c_{i,\beta\xi}^{(1)} \cdot \nu_{i,\beta\xi} \cdot \left(V_i - \overline{V}_\beta \right) \right\} \tag{AI.12}$$

$c_{i,\beta\xi}^{(1)} = c_{\beta\xi,i}^{(1)}$ (see (AI.4))

$\nu_{i,\beta\xi} = \dfrac{m_\beta}{m_i} \dfrac{n_{\beta\xi}}{n_i} \nu_{\beta\xi,i}$ (see(AI.10))

$$\overline{V}_\beta = \frac{\sum_{\xi_k} n_{\beta\xi} Z_k^2 V_k}{n_i}$$

- **The drag force for electrons** in multi-component plasma:

$$R_e^u = -m_e n_e \left\{ \sum_{\beta,\xi} c_{e,\beta\xi}^{(1)} \cdot \nu_{e,\beta\xi} \cdot \left(V_i - \overline{V}_\beta \right) \right\} \tag{AI.13}$$

$$\nu_{e,\beta\xi} = \nu_0 \cdot \xi^2 \frac{n_{\beta\xi}}{T_e^{3/2}} \frac{1}{\sqrt{m_e}} \qquad c_{e,\beta\xi}^{(1)} = c_{e,\alpha}^{(1)} \qquad \text{(see (II.1.33))}$$

$$\overline{V}_\beta = \sum_{\xi_k} n_{\beta\xi} Z_k^2 V_k / n_e = n_i V_i / n_e + \sum_{\xi_k \neq i} n_{\beta\xi} Z_k^2 V_k / n_e \tag{AI.14}$$

- **The general expression for thermal force** acting on specie α in z charge state consist of three terms, associated with temperature gradients of electron, ion and impurity ions:

$$R_{\alpha z}^T = m_\alpha n_{\alpha z} \left\{ \sum_{\beta\xi} \left[c_{\alpha z,\beta\xi}^{(2)} \frac{\nu_{\alpha z,\beta\xi}}{\nu_\beta} \frac{1}{m_\beta} \frac{\partial T_\beta}{\partial y} - c_{\beta\xi}^{(5)} \frac{1}{m_\beta} \frac{\partial T_\alpha}{\partial y} \right] \right\} \tag{AI.15}$$

$$\nu_k = \sum_{\text{over all species } Z} \nu_{k,z} \tag{AI.16}$$

$$R_{Z_J}^t \equiv \alpha_i \frac{\partial T_i}{\partial y} + \alpha_z \frac{\partial T_z}{\partial y} + \alpha_e \frac{z_j^2}{z_{eff}} n_{z_j} \frac{\partial T_e}{\partial y} \tag{AI.17}$$

$$\alpha_i = n_{z_j} \frac{m_z}{m_i} \frac{\nu_{z_j,i}}{\nu_i} c_{z,j}^{(2)} \approx n_{z_j} \frac{m_z}{m_i} c_{z,j}^{(2)} \frac{\nu_{z_j,i}}{\nu_{ii} \left(1 + \dfrac{\sum_j \nu_{i,z_j}}{\nu_{ii}} \right)} = n_{z_j} \frac{m_z}{m_i} c_{z,j}^{(2)} \frac{\alpha_e}{1 + \alpha_e Z_0} \tag{AI.18}$$

In equation (AI.15) , since $n_{z_j} m_z \nu_{z_j,i} = n_i m_i \nu_{i,z_j}$, and (AI.19)

$$\frac{\nu_{i,z_j}}{\nu_{ii}} = z_j^2 \frac{m_i}{m_z} \sqrt{\frac{\mu_{z,i}}{\mu_{i,i}}} = \alpha_e \frac{m_i}{m_z} z_j^2 \tag{AI.20}$$

$$\alpha_z = n_{z_j} \left(\frac{z_j^2 \sum_j n_{z_j}}{\sum_j n_{z_j} z_j^2} - 1 \right) c_z^{(5)} \tag{AI.21}$$

The last term corresponds to the mutual impurity interaction. It is clear that

$$\sum_j \alpha_{z_j} = 0 \ . \tag{AI.22}$$

$$\alpha_e = 2.2 Z_{eff} \frac{\left(1 + 0.52 Z_{eff}\right)}{\left(1 + 2.65 Z_{eff}\right)\left(1 + 0.285 Z_{eff}\right)} \tag{AI.23}$$

$$c_{z,i}^{(2)} = \frac{1.56 \cdot \left(1 + \sqrt{2} Z_0\right) \cdot \left(1 + 0.52 Z_0\right)}{\left(1 + 2.65 Z_0\right) \cdot \left(1 + 0.285 Z_0\right)} \tag{AI.24}$$

$$c_{z,i}^{(5)} = \frac{3}{5} \tag{AI.25}$$

- **Electron thermal force** in multi-component plasma

$$R_e^T = -\alpha_e n_e \nabla T_e \qquad \text{(for } \alpha_e \text{ see (AI.23))} \tag{AI.26}$$

Appendix II Coulomb collision frequencies & equipartition time

- **Coulomb collision frequencies between two species α and β:** (sec, eV, cm^{-3})

$$\nu_{\alpha Z,\beta\xi} = \nu_0 \cdot Z^2 \xi^2 \frac{n_{\beta\xi}}{T_{\alpha\beta}^{3/2}} \frac{\sqrt{\mu_{\alpha\beta}}}{m_\alpha} \qquad \nu_0 \equiv \frac{4\sqrt{2\pi}}{3k^{3/2}} \Lambda e^4 = 0.9 \cdot 10^{-18} \left(\frac{\Lambda}{10}\right) \tag{AII.1}$$

$$T_{\alpha\beta} = \frac{T_\alpha m_\beta + T_\beta m_\alpha}{m_\alpha + m_\beta} \qquad \mu_{\alpha\beta} = \frac{m_\alpha m_\beta}{m_\alpha + m_\beta} \tag{AII.2}$$

$$\nu_{\alpha Z,\beta\xi} = \frac{m_\beta n_\beta}{m_\alpha n_\alpha} \cdot \nu_{\beta\xi,\alpha Z} \qquad \nu^{\varepsilon}_{\alpha\varepsilon,\beta\xi} = \frac{2\mu_{\alpha\beta}}{m_\alpha + m_\beta} \nu_{\alpha Z,\beta\xi} \qquad \tau^{\varepsilon}_{\alpha\varepsilon,\beta\xi} = \frac{\left(m_\alpha + m_\beta\right)^2}{m_\alpha m_\beta} \tau_{\alpha Z,\beta\xi} \tag{AII.3}$$

Elektrons	*Ions*	*Impurity ions equal nucleus* ($\alpha = \beta$)
$\nu_e = \nu_{ee} + \nu_{ei} + \sum \nu_{e,\beta\xi}$	$\nu_i = \nu_{ii} + \nu_{ie} + \sum \nu_{i\beta\xi}$	$\nu_\alpha = \nu_{\alpha\varepsilon,e} + \nu_{\alpha\varepsilon,i} + \sum \nu_{\alpha\varepsilon,\beta\xi}$
$\nu_{ee} = \frac{\nu_0}{\sqrt{2}} \cdot \frac{n_e}{T_e^{3/2}} \frac{1}{\sqrt{m_e}}$	$\nu_{ii} = \frac{\nu_0}{\sqrt{2}} \cdot \frac{n_i}{T_i^{3/2}} \frac{1}{\sqrt{m_i}}$	$\nu_{\alpha\varepsilon,\alpha\xi} = \frac{\nu_0}{\sqrt{2}} \cdot \frac{n_\alpha}{T_\alpha^{3/2}} \frac{Z^2\xi^2}{\sqrt{m_\alpha}}$
$\nu_{ei} = \nu_0 \cdot \frac{n_i}{T_e^{3/2}} \frac{1}{\sqrt{m_e}}$	$\nu_{ie} = \nu_0 \cdot \frac{n_e}{T_e^{3/2}} \frac{\sqrt{m_e}}{m_i}$	$\nu_{\alpha\varepsilon,i} = \nu_0 \cdot Z^2 \frac{n_i}{T_i^{3/2}} \frac{\sqrt{m_i}}{m_\alpha}$
$\nu_{e,\beta\xi} = \nu_0 \cdot \xi^2 \frac{n_{\beta\xi}}{T_e^{3/2}} \frac{1}{\sqrt{m_e}}$	$\nu_{i,\beta\xi} = \nu_0 \cdot \xi^2 \frac{n_{\beta\xi}}{T_i^{3/2}} \frac{1}{\sqrt{m_i}}$	$\nu_{\alpha\varepsilon,e} = \nu_0 \cdot Z^2 \frac{n_e}{T_e^{3/2}} \frac{\sqrt{m_e}}{m_\alpha}$

$$\frac{\partial}{\partial t}\left(m_\alpha n_\alpha \vec{V}_\alpha\right) = \ldots - n_\alpha \sum_\beta \mu_{\alpha\beta} \nu_{\alpha\varepsilon,\beta\xi} \left(\vec{V}_\alpha - \vec{V}_\beta\right); \tag{AII.4}$$

$$\frac{\partial}{\partial t} \varepsilon_\alpha = \ldots - \frac{3}{2} n_\alpha \sum_\beta \nu^{\varepsilon}_{\alpha\varepsilon,\beta\xi} \left(T_\alpha - T_\beta\right) = -3 n_\alpha \sum_\beta \frac{\mu_{\alpha\beta}}{m_\alpha + m_\beta} \nu_{\alpha Z,\beta\xi} \left(T_\alpha - T_\beta\right); \qquad \varepsilon_\alpha = \frac{3}{2} n_\alpha T_\alpha \tag{AII.5}$$

- The equipartition time $\tau^{\varepsilon}_{\alpha Z,\beta\xi}$

$$\frac{3}{2}\frac{\partial}{\partial t}n_\alpha T_\alpha = \ldots + Q_\alpha \qquad Q_\alpha = 3n_\alpha k\sum_\beta \frac{\mu_{\alpha\beta}}{m_\alpha + m_\beta}\nu_{\alpha Z,\beta\xi}\left(T_\beta - T_\alpha\right) \tag{AII.6}$$

$$\frac{\partial}{\partial t}T_\alpha = \ldots + \sum_\beta \frac{2\mu_{\alpha\beta}}{\left(m_\alpha + m_\beta\right)}\nu_{\alpha Z,\beta\xi}\left(T_\beta - T_\alpha\right) = \sum_\beta \nu^{\varepsilon}_{\alpha z,\beta\xi}\left(T_\beta - T_\alpha\right) \approx -\frac{\left(T_\alpha - T_\beta\right)}{\tau^{\varepsilon}_{\alpha Z,\beta\xi}} \tag{AII.7}$$

$$\nu^{\varepsilon}_{\alpha Z,\beta\xi} = \frac{2\mu_{\alpha\beta}}{\left(m_\alpha + m_\beta\right)}\nu_{\alpha z,\beta\xi} \qquad \tau^{\varepsilon}_{\alpha Z,\beta\xi} = \frac{\left(m_\alpha + m_\beta\right)}{2\mu_{\alpha\beta}}\tau^{\varepsilon}_{\alpha z,\beta\xi} \tag{AII.8}$$

In the case $(\alpha = e\ ,\ \beta = i)$ $$\tau^{\varepsilon}_{e,i} \approx \frac{m_i}{2m_e}\tau_{ei} = \frac{m_i}{2\nu_0\sqrt{m_e}}\cdot\frac{T_e^{3/2}}{n_i} \tag{AII.9}$$

In the case $(\alpha = i\ ,\ \beta = Z)$ $$\tau^{\varepsilon}_{i,z} = \frac{m_z}{2m_i}\tau_{iz} = \frac{m_z}{2\nu_0\sqrt{m_i}}\cdot\frac{T_i^{3/2}}{n_z} \tag{AII.10}$$

$$\boxed{T_\alpha - T_\beta = \left(T_\alpha - T_\beta\right)_0 e^{-\frac{t}{\tau^{\varepsilon}_{\alpha Z,\beta\xi}}}} \tag{AII.11}$$

- **The equipartition between protons and impurity ions**

$$\nu_{z,i} = \nu_0 \cdot Z^2 \frac{n_i}{T_i^{3/2}}\frac{\sqrt{m_i}}{m_z} \tag{AII.12}$$

$$T_z = T_i\left(1 - \exp(-\frac{t}{\tau^{\varepsilon}_{z,i}})\right) \tag{AII.13}$$

for $(\alpha = z\ ,\ \beta = i)$ $$\tau^{\varepsilon}_{z,i} = \frac{m_z}{2m_i}\tau_{z,i} = \frac{\sqrt{m_i}}{2\nu_0}\left(\frac{m_z}{m_i}\right)^2 \cdot \frac{T_i^{3/2}}{n_i Z^2} \tag{AII.14}$$

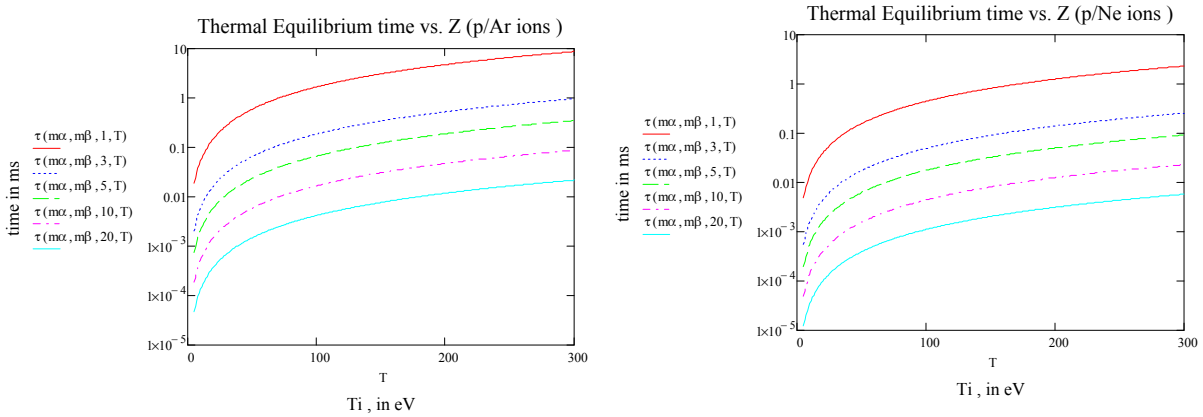

Thermal equilibrium time for Ar and Ne in different Z and protons.

$$\Delta T \equiv (T_\alpha - T_\beta)/(T_\alpha - T_\beta)_0 = \exp(-\nu^{\varepsilon}_{\alpha z,\beta\xi} \cdot t) \qquad \text{(AII.15)}$$

$$\Delta T(t, Z, T_p) \equiv \left(T_p - T_\alpha\right)/T_p = \exp(-\nu^{\varepsilon}_{\alpha z,\beta\xi} \cdot t) \qquad \text{(AII.16)}$$

$T_i = 5eV$

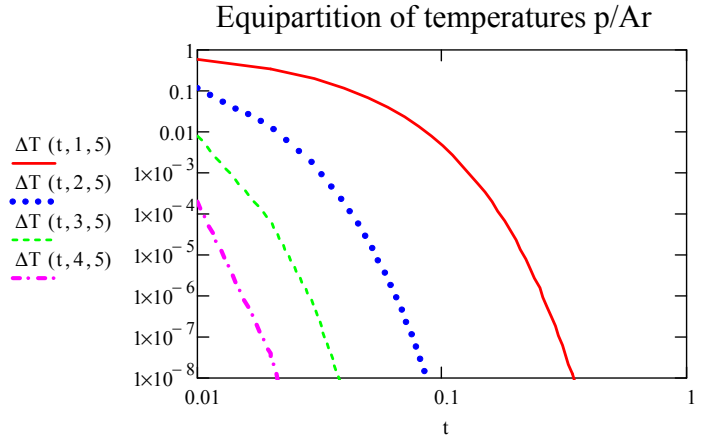

time in ms

$$\Delta T \equiv (T_\alpha - T_\beta)/(T_\alpha - T_\beta)_0 = \exp(-\nu^{\varepsilon}_{\alpha z,\beta\xi} \cdot t)$$

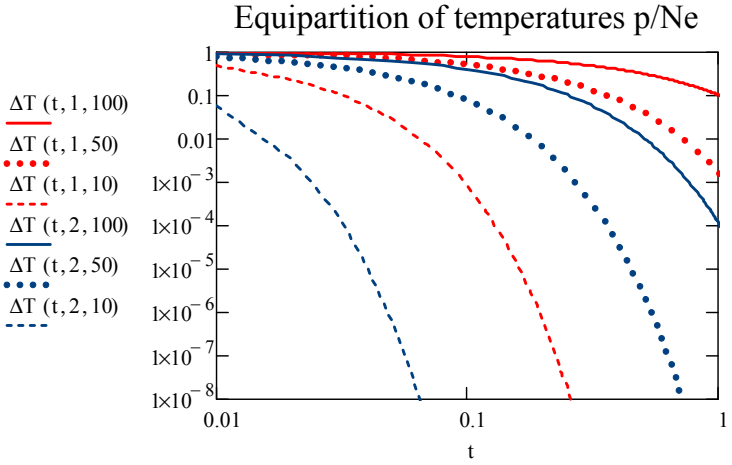

time in ms

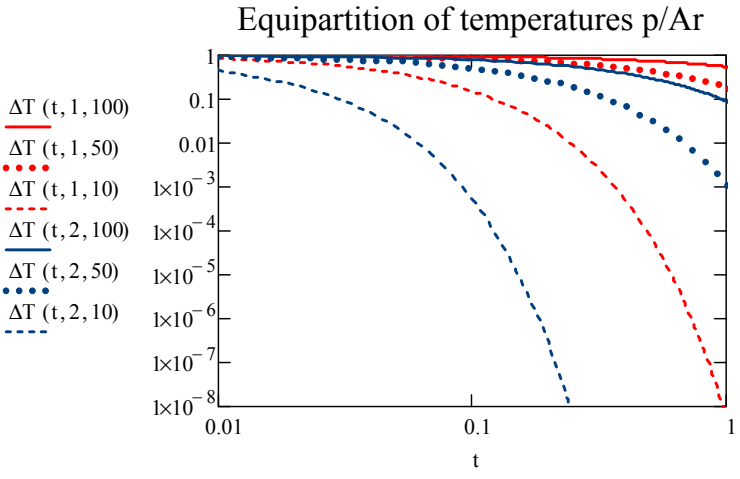

time in ms

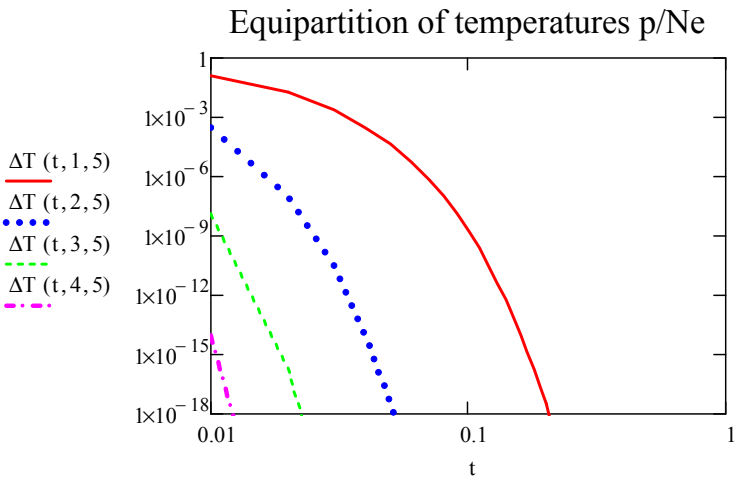

$$T_z = T_i\left(1-\exp(-\nu^{\varepsilon}_{\alpha z,\beta\xi}\cdot t)\right) \qquad T_{z0}\approx 0 \tag{AII.17}$$

- **Equipartition between impurity ions of neighbouring charge states**

$$\nu^{\varepsilon}_{\alpha Z,\alpha Z'} = \frac{\nu_0}{2\sqrt{2}} Z^2 Z'^2 \frac{n_{\alpha Z}}{T_\alpha^{3/2}} \frac{1}{\sqrt{m_\alpha}} \qquad \nu^{\varepsilon}_{\alpha Z,p} = 2\nu_0 Z^2 \frac{n_p}{T_p^{3/2}} \frac{\sqrt{m_p}}{m_\alpha} \tag{AII.18}$$

$$\frac{\nu^{\varepsilon}_{\alpha Z,\alpha Z'}}{\nu^{\varepsilon}_{\alpha Z,p}} = \frac{Z'^2}{4\sqrt{2}}\left(\frac{T_p}{T_\alpha}\right)^{3/2} \frac{n_{\alpha Z}}{n_p}\sqrt{\frac{m_\alpha}{m_p}} \tag{AII.16}$$

$$Z=1,\quad Z'=Z+1=2 \qquad n_{\alpha Z}\approx n_p,\quad T_\alpha \approx T_p$$

for Ar: $\dfrac{\nu^{\varepsilon}_{Ar^+,Ar^{++}}}{\nu^{\varepsilon}_{Ar^+,p}} \approx \dfrac{2^2}{4\sqrt{2}}\sqrt{40} \approx 4.5$ for Ne: $\dfrac{\nu^{\varepsilon}_{Ar^+,Ar^{++}}}{\nu^{\varepsilon}_{Ar^+,p}} \approx \dfrac{2^2}{4\sqrt{2}}\sqrt{20} \approx 3.16$

Resume:

- The energy exchange time between protons and impurity ions in the first charge state strongly depends on proton temperature. At high temperatures $T_p \geq 100eV$ equipartition for the first state of ionization is week. However, for the higher states of ionizations (starting from $Z \geq 2$) the energy exchange time is short enough to assume that $T_{Ar^+} \approx T_p$.

- At low temperatures, $T_p \le 5eV$ the assumption that $T_{Ar^+} \approx T_p$ is correct (with the accuracy of about 1%) in time duration $\ge 0.1ms$. For Ne $T_{Ne^+} \approx T_p$ it is correct even for shorter times.
- The energy exchange time between protons and next charge states is short enough to assume that their temperatures become equal in time duration $\le 1ms$.
- The energy exchange time between impurity ions of neighbouring charge states $Z \ge 2$ is short enough to assume their temperature equal to proton temperature.

The justification for a common ion temperature is that the ion-impurity energy exchange time is assumed to significantly shorter than the ion-electron energy exchange time. The ratio of the relaxation times for $T_i - T_{\alpha z}$ and $T_i - T_e$ is:

$$\frac{\tau^{\varepsilon}_{p,\beta z}}{\tau^{\varepsilon}_{p,e}} \approx \frac{m_\beta}{m_i}\left(\frac{m_e}{m_p}\right)^{3/2}\frac{1}{Z^2}\frac{n_e}{n_\beta}\left(\frac{T_i}{T_e}\right)^{3/2} \approx A\left(\frac{m_e}{m_p}\right)^{3/2}\frac{1}{Z^2},$$

here we assume that in the plasma edge $\left(\frac{T_i}{T_e}\right)^{3/2} \propto O(1)$, then

- for a hydrogen/Ar plasma: $\frac{\tau^{\varepsilon}_{p,\beta\xi}}{\tau^{\varepsilon}_{p,e}} \approx \frac{5.084\cdot 10^{-4}}{Z^2}\frac{n_e}{n_{Ar,z}}$
- for a hydrogen/Ne plasma: $\frac{\tau^{\varepsilon}_{p,\beta\xi}}{\tau^{\varepsilon}_{p,e}} \approx \frac{2.542\cdot 10^{-4}}{Z^2}\frac{n_e}{n_{Ar,z}}$

Whence, even for low charge state Z of impurity ions, the proton-impurity temperature relaxation time is shorter than the energy exchange time of protons with electrons. Therefore, one can assume that $T_\beta \approx T_i$

Appendix III The origin of 5/2 term in the energy balance equation.

We will show here that 5/2 term in the energy flux appears without taking into account the joule dissipation term. It arise due to contribution to heat flux the work done by pressure gradient in the convective plasma and occurs also in non-dissipative plasmas without current.

Lets start with kinetic equation without collision term, $St = 0$ and the external force, $F_\beta = 0,$ thus excluding any dissipation

$$\frac{\partial f}{\partial t} + \frac{\partial}{\partial x_\beta}\left(v_\beta f\right) + \frac{\partial}{\partial v_\beta}\left(\frac{F_\beta}{m} f\right) = St \qquad \frac{\partial f}{\partial t} + \frac{\partial}{\partial x_\beta}\left(v_\beta f\right) = 0 \qquad \text{(AIII.1)}$$

Multiplying last Eq. (AIII.1) by $\frac{m\vec{v}^2}{2}$ and integrating over velocity v, we have:

$$\frac{\partial}{\partial t}\left(\int \frac{m}{2}\vec{v}^2 f d\vec{v}\right) + \frac{\partial}{\partial x_\beta}\left(\int \frac{m}{2}\vec{v}^2 v_\beta f d\vec{v}\right) = 0 \qquad \text{(AIII.2)}$$

Then, one can introduce as usual the moments of distribution functions and the mean and random velocities:

$$n \equiv \int f d\vec{v}\,,\ V \equiv \int \vec{v} f d\vec{v} / n\,,\quad \vec{V} \equiv \vec{v} - \vec{v}'\,,\ T = \frac{m}{3n}\int v'^2 f dv = \frac{m}{3}\left\langle v'^2 \right\rangle = \frac{m}{3}\left\langle \left(\vec{v} - \vec{V}\right)^2 \right\rangle \qquad \text{(AIII.3)}$$

The integration of the first term in (AIII.2) gives:

$$\int \frac{m}{2}\vec{v}^2 f d\vec{v} = \int \frac{m}{2}\left(\vec{v}' + \vec{V}\right)^2 f d\vec{v} \equiv \frac{mn}{2}\left\langle \left(\vec{v}' + \vec{V}\right)^2 \right\rangle = n\left(\frac{3T}{2} + \frac{m\vec{V}^2}{2}\right) \qquad \text{(AIII.4)}$$

$$\text{because} \left\langle \left(\vec{v}' + \vec{V}\right)^2 \right\rangle = \left\langle v'^2 \right\rangle + \left\langle 2\left(\vec{v}'\vec{V}\right) \right\rangle + \vec{V}^2 = \left\langle v'^2 \right\rangle + \vec{V}^2\,,\quad \left\langle 2\left(\vec{v}'\vec{V}\right) \right\rangle = 0\,! \qquad \text{(AIII.5)}$$

$$\text{Therefore} \quad \left\langle \left(\vec{v}' + \vec{V}\right)^2 \right\rangle = \frac{3T}{m} + \vec{V}^2 \qquad \text{(AIII.6)}$$

Integration of the second terms gives:

$$\int \frac{m}{2}\vec{v}^2 v_\beta f d\vec{v} \equiv mn\left\langle \frac{\vec{v}^2}{2} v_\beta \right\rangle = n\left(\frac{3T}{2} + \frac{mV^2}{2}\right)V_\beta + q_\beta + V_\alpha P_{\alpha\beta} = \qquad \text{(AIII.7)}$$

because

$$\left\langle \frac{\vec{v}^2}{2} v_\beta \right\rangle = \left\langle \frac{\left(\vec{v}' + \vec{V}\right)^2}{2}\left(V_\beta + v'_\beta\right) \right\rangle = \left\langle \frac{\left(\vec{v}'^2 + 2\vec{v}'\vec{V} + \vec{V}^2\right)}{2}\left(V_\beta + v'_\beta\right) \right\rangle =$$

$$= \frac{V_\beta}{2}\left\langle \vec{v}'^2 \right\rangle + \frac{\left\langle \vec{v}'^2 v'_\beta \right\rangle}{2} + V_\alpha\left\langle v'_\alpha v'_\beta \right\rangle + \frac{V_\beta V^2}{2} = \frac{3T}{2m}V_\beta + \frac{q_\beta}{mn} + V_\alpha\frac{P_{\alpha\beta}}{mn} + \frac{V_\beta V^2}{2} \qquad \text{(AIII.8)}$$

Using definition of energy $\varepsilon \equiv \frac{3T}{2} + \frac{m\vec{V}^2}{2}$ and momentum tensor $P_{\alpha\beta} = mn\left\langle v'_\alpha v'_\beta \right\rangle = p\delta_{\alpha\beta} + \pi_{\alpha\beta}$

the energy equation reads can be written for non-dissipative case as usual:

$$\frac{\partial}{\partial t}(n\varepsilon) + \frac{\partial}{\partial x_\beta}\left(n\varepsilon V_\beta + q_\beta + V_\alpha P_{\alpha\beta}\right) = 0 \qquad \text{(AIII.9)}$$

or, substituting $P_{\alpha\beta} = mn\left\langle v'_\alpha v'_\beta \right\rangle = p\delta_{\alpha\beta} + \pi_{\alpha\beta}$

$$\frac{\partial}{\partial t}(n\varepsilon) + \frac{\partial}{\partial x_\beta}\left((n\varepsilon + p)V_\beta + q_\beta + \pi_{\alpha\beta}V_\beta\right) = 0 \quad \text{where} \qquad \text{(AIII.10)}$$

$$(n\varepsilon + p) \equiv \frac{3p}{2} + \frac{m\vec{V}^2}{2} + p = \frac{5p}{2} + \frac{m\vec{V}^2}{2} \qquad \text{(AIII.11)}$$

Therefore $\frac{\partial}{\partial t} n\varepsilon + \frac{\partial}{\partial x_\beta}\left(\left(\frac{m\vec{V}^2}{2} + \frac{3}{2}nT\right)V_\beta + q_\beta\right) + \frac{\partial}{\partial x_\beta}\left(\vec{P}V_\alpha\right) = 0$ (AIII.12)

or

$$\frac{\partial}{\partial t}\left(\frac{3}{2}nT + \frac{mn\vec{V}^2}{2}\right) + \frac{\partial}{\partial x_\beta}\left(Q_\beta\right) = 0 \quad where \quad Q_\beta \equiv \left(\frac{m\vec{V}^2}{2} + \frac{3}{2}nT + p\right)V_\beta + \pi_{\alpha\beta}V_\alpha + q_\beta \qquad \text{(AIII.13)}$$

Therefore, the total energy flax Q_β consist of

1) macroscopic (kinetic+ internal) flux of energy $\left(m\vec{V}^2/2\right)\cdot V_\beta$

2) the energy flux done by the total pressure forces $pV_\beta + \pi_{\alpha\beta}V_\alpha$

3) and the thermo-conductivity flux q_β

Therefore even in the case of non-collision current-less plasma the energy flux contains the 5/2 term

$$Q_\beta \equiv \left(\frac{m\vec{V}^2}{2} + \frac{5}{2}nT\right)V_\beta + \pi_{\alpha\beta}V_\alpha + q_\beta \qquad \text{(AIII.14)}$$

In some cases it is convenient to eliminate the kinetic energy from Eq. (AIII.13) by means of the equation of continuity and the equation of motion. One can then obtain an equation for the transport of internal energy or the heat- balance equation. It is easy to show that

$$\begin{aligned} &\frac{\partial}{\partial t}\left(\frac{3}{2}nT + \frac{mn\vec{V}^2}{2}\right) + \frac{\partial}{\partial x_\beta}\left(\left(\frac{mn\vec{V}^2}{2} + \frac{5}{2}nT\right)V_\beta + \pi_{\alpha\beta}V_\alpha + q_\beta\right) = \\ &= \frac{\partial}{\partial t}\left(\frac{3}{2}nT\right) + \frac{\partial}{\partial x_\beta}\left(\left(\frac{3}{2}nT\right)V_\beta + q_\beta\right) + p\frac{\partial}{\partial x_\beta}V_\beta + \pi_{\alpha\beta}\frac{\partial V_\alpha}{\partial x_\beta} - \Delta \end{aligned} \qquad \text{(AIII.15)}$$

where $$\Delta \equiv \frac{\partial}{\partial t}\left(\frac{mn\vec{V}^2}{2}\right)+\frac{\partial}{\partial x_\beta}\left(\frac{mn\vec{V}^2}{2}\right)V_\beta + V_\beta\ \frac{\partial}{\partial x_\beta}(nT)+V_\alpha\frac{\partial}{\partial x_\beta}(\pi_{\alpha\beta})=0 \qquad \text{(AIII.16)}$$

Indeed,

$$\frac{\partial}{\partial t}\left(\frac{mn\vec{V}^2}{2}\right)=\frac{m\vec{V}^2}{2}\frac{\partial n}{\partial t}+n\frac{\partial}{\partial t}\left(\frac{m\vec{V}^2}{2}\right) \qquad \text{(AIII.17)}$$

$$\frac{\partial}{\partial x_\beta}\left(\frac{mn\vec{V}^2}{2}\right)V_\beta=\frac{m\vec{V}^2}{2}\frac{\partial}{\partial x_\beta}nV_\beta+nV_\beta\frac{\partial}{\partial x_\beta}\left(\frac{m\vec{V}^2}{2}\right) \qquad \text{(AIII.18)}$$

$$\frac{m\vec{V}^2}{2}\left(\frac{\partial n}{\partial t}+\frac{\partial}{\partial x_\beta}nV_\beta\right)+n\frac{\partial}{\partial t}\left(\frac{m\vec{V}^2}{2}\right)+nV_\beta\frac{\partial}{\partial x_\beta}\left(\frac{m\vec{V}^2}{2}\right)+V_\beta\ \frac{\partial}{\partial x_\beta}(nT)+V_\alpha\frac{\partial}{\partial x_\beta}(\pi_{\alpha\beta}) \qquad \text{(AIII.19)}$$

$$nV_\alpha\frac{\partial}{\partial t}(mV_\alpha)+nV_\beta V_\alpha\frac{\partial}{\partial x_\beta}(mV_\alpha)+V_\alpha\ \delta_{\alpha\beta}\frac{\partial}{\partial x_\beta}(nT)+V_\alpha\frac{\partial}{\partial x_\beta}(\pi_{\alpha\beta}) \qquad \text{(AIII.20)}$$

$$\begin{aligned} &n\frac{\partial}{\partial t}(mV_\alpha)+nV_\beta\frac{\partial}{\partial x_\beta}(mV_\alpha)+\frac{\partial P_{\alpha\beta}}{\partial x_\beta}= \\ &=\left[\frac{\partial}{\partial t}(nmV_\alpha)+\frac{\partial}{\partial x_\beta}(mnV_\beta V_\alpha)+\frac{\partial P_{\alpha\beta}}{\partial x_\beta}\right]-mV_\alpha\left(\frac{\partial}{\partial t}n+\frac{\partial}{\partial x_\beta}(nV_\beta)\right)\equiv 0 \end{aligned} \qquad \text{(AIII.21)}$$

Therefore

$$\begin{aligned} &\frac{\partial}{\partial t}\left(\frac{3}{2}nT\right)+\frac{\partial}{\partial x_\beta}\left(\left(\frac{3}{2}nT\right)V_\beta+q_\beta\right)+p\frac{\partial}{\partial x_\beta}V_\beta+\pi_{\alpha\beta}\frac{\partial V_\alpha}{\partial x_\beta}= \\ &=\frac{\partial}{\partial t}\left(\frac{3}{2}nT+\frac{mn\vec{V}^2}{2}\right)+\frac{\partial}{\partial x_\beta}\left(\left(\frac{5}{2}nT+\frac{mn\vec{V}^2}{2}\right)V_\beta+q_\beta+\pi_{\alpha\beta}V_\alpha\right)-\Sigma \end{aligned} \qquad \text{(AIII.22)}$$

and

$\Sigma \equiv \frac{\partial}{\partial t}\left(\frac{mn\vec{V}^2}{2}\right)+\frac{\partial}{\partial x_\beta}\left(\left(\frac{m\vec{V}^2}{2}\right)nV_\beta\right)+V_\alpha\frac{\partial P_{\alpha\beta}}{\partial x_\beta}$ equals to zero, because

$\frac{\partial}{\partial t}\left(\frac{mn\vec{V}^2}{2}\right)\equiv V_\alpha\frac{\partial}{\partial t}(mnV_\alpha)$ $\frac{\partial}{\partial x_\beta}\left(\left(\frac{m\vec{V}^2}{2}\right)nV_\beta\right)\equiv V_\alpha\frac{\partial}{\partial x_\beta}(mnV_\alpha V_\beta)$ and

$$\Sigma=V_\alpha\left[\frac{\partial}{\partial t}(mnV_\alpha)+\frac{\partial}{\partial x_\beta}(mnV_\alpha V_\beta+P_{\alpha\beta})\right]\equiv 0 \qquad \text{(AIII.23)}$$

Coming now back to collisional plasma ($St \neq 0$ and the external force, $F_\beta = e_\beta E$) for the electron and one hydrogen ion $n \equiv n_e = Zn_i$ the transport equations can be writer as:

The hydrogen ion energy:

$$\frac{\partial}{\partial t}\left(\frac{3}{2}nT_i + \frac{m_i n\vec{V}_i^{\,2}}{2}\right) + \frac{\partial}{\partial x_\beta}\left(\left(\frac{m_i n\,\vec{V}_i^{\,2}}{2} + \frac{5}{2}nT_i\right)V_{i\beta} + \pi^{i}{}_{\alpha\beta}V_{i\alpha} + q_{i\beta}\right) =$$

$$= ZenE\vec{V}_i + \vec{R}_i\vec{V}_i + Q_i \qquad \text{(AIII.24)}$$

The electron energy:

$$\frac{\partial}{\partial t}\left(\frac{3}{2}nT_e\right) + \frac{\partial}{\partial x_\beta}\left(\frac{5}{2}nT_eV_{e\beta} + \pi^{e}{}_{\alpha\beta}V_{e\alpha} + q_{e\beta}\right) = -enE\vec{V}_e + \vec{R}_e\vec{V}_e + Q_e \qquad \text{(AIII.25)}$$

The total energy:

$$\frac{\partial}{\partial t}\left(\frac{3}{2}n(T_e+T_i) + \frac{m_i n\vec{V}_i^{\,2}}{2}\right) + \frac{\partial}{\partial x_\beta}\left(\left(\frac{m_i n\vec{V}_i^{\,2}}{2} + \frac{5}{2}n(T_e+T_i)\right)V_{i\beta} - \frac{5}{2}nT_e(\vec{V}_i - \vec{V}_e) + \pi^{i}{}_{\alpha\beta}V_{i\alpha} + q_{i\beta} + q_{e\beta}\right) =$$

$$= e\vec{E}\left(Zn_i\vec{V}_i - n_e\vec{V}_e\right) + \vec{R}_i\vec{V}_i + R_e\vec{V}_e + Q_i + Q_e = -enE\vec{u} - \vec{R}_e\vec{u} \qquad \text{(AIII.26)}$$

One can denote the mass average velocity $\vec{V}$ and introduce a relative velocity : $\vec{u}$

$$\vec{V} = \frac{1}{\rho}(m_i n\vec{V}_i + m_e n\vec{V}_e) \approx \vec{V}_i \qquad \text{(AIII.27)}$$

$$\vec{u} \equiv \vec{V}_e - \vec{V}_i \qquad \text{(AIII.28)}$$

If $T_e = T_i \quad \rho = m_i n_i + m_e n_e \approx m_i n_i \quad p = p_e + p_i \quad \vec{j} = -en\vec{u}$ then

$$\frac{\partial}{\partial t}\left(\frac{\rho\vec{V}_i^{\,2}}{2} + \frac{3}{2}p\right) + \frac{\partial}{\partial x_\beta}\left(\left(\frac{\rho\vec{V}_i^{\,2}}{2} + \frac{5}{2}p\right)V_{i\beta} + \pi^{i}{}_{\alpha\beta}V_{i\alpha} + q_{i\beta} + q_{e\beta} + \frac{5}{2}p_e\vec{u}\right) =$$

$$= e\vec{E}\left(Zn_i\vec{V}_i - n_e\vec{V}_e\right) + \vec{R}_i\vec{V}_i + R_e\vec{V}_e + Q_i + Q_e = \vec{j}\vec{E} \qquad \text{(AIII.29)}$$

and since $\vec{R}_i\vec{V}_i + R_e\vec{V}_e + Q_i + Q_e = 0$ (AIII.28)

$$\frac{\partial}{\partial t}\left(\frac{\rho\vec{V}_i^{\,2}}{2}+\frac{3}{2}p\right)+\frac{\partial}{\partial x_\beta}\left(\left(\frac{\rho\vec{V}_i^{\,2}}{2}+\frac{5}{2}p\right)V_{i\beta}+\pi^i{}_{\alpha\beta}V_{i\alpha}+q_{i\beta}+q_{e\beta}+\frac{5}{2}p_e\vec{u}\right)=\vec{j}\vec{E} \qquad \text{(AIII.30)}$$

The total energy conservation including plasma and energy stored in magnetic field reads:

$\frac{\partial}{\partial t}\left(\frac{B^2}{8\pi}\right)+div\,\vec{S}=-\vec{j}\vec{E}$ where $\vec{S}=\frac{c}{4\pi}\left[\vec{E}\vec{B}\right]$ is the Pointing vector or in another form

$$\frac{\partial\varepsilon}{\partial t}+\frac{\partial}{\partial x_\beta}\vec{q}_\beta=0 \qquad \text{(AIII.31)}$$

where $\varepsilon=\frac{\rho\vec{V}_i^{\,2}}{2}+\frac{3}{2}p+\frac{B^2}{8\pi}$ and the most general expression for energy flux is

$$q_\beta\equiv\left(\frac{\rho\vec{V}_i^{\,2}}{2}+\frac{5}{2}p\right)V_\beta+\pi^i{}_{\alpha\beta}V_\alpha+q_{i\beta}+q_{e\beta}+\frac{5}{2}p_e\vec{u}_\beta+\vec{S}_\beta \qquad \text{(AIII.32)}$$

Finally, we will note another form of energy equation. Since

$$\frac{3}{2}\frac{\partial}{\partial t}(nT)+\frac{\partial}{\partial x_\beta}\left(\frac{3}{2}nTV_\beta\right)=\frac{3}{2}T\left(\frac{\partial n}{\partial t}+\frac{\partial}{\partial x_\beta}(nV_\beta)\right)+\frac{3}{2}n\left(\frac{\partial T}{\partial t}+V_\beta\frac{\partial T}{\partial x_\beta}\right)=\frac{3}{2}n\frac{dT}{dt} \qquad \text{(AIII.33)}$$

then the energy equation

$$\frac{3}{2}\frac{\partial}{\partial t}(nT_e)+\frac{\partial}{\partial x_\beta}\left(\frac{3}{2}nT_eV_{e\beta}\right)+p_e\frac{\partial}{\partial x_\beta}V_{e\beta}+\pi^e{}_{\alpha\beta}\frac{\partial V_{e\alpha}}{\partial x_\beta}+\frac{\partial q^e{}_\beta}{\partial x_\beta}=Q_e \qquad \text{(AIII.34)}$$

where $Q_i=Q_\Delta\equiv\frac{3m_e}{m_i}\frac{n}{\tau_e}(T_e-T_i)$ $\qquad Q_e=-Ru-Q_\Delta=\frac{j_{//}^2}{\sigma_{//}}+\frac{j_\perp^2}{\sigma_\perp}-Q_\Delta+\frac{\vec{j}\vec{R}_T}{en}$ $\qquad$ (AIII.35)

can be presented as

$$\frac{3}{2}\frac{\partial p}{\partial t}+\frac{\partial}{\partial x_\beta}\left(\frac{3}{2}pV_{i\beta}\right)+p_e\frac{\partial}{\partial x_\beta}V_{e\beta}+\pi^e{}_{\alpha\beta}\frac{\partial V_{e\alpha}}{\partial x_\beta}+\frac{\partial}{\partial x_\beta}\left(q^e{}_\beta+\frac{3}{2}p_eu_\beta\right)=\frac{j_{//}^2}{\sigma_{//}}+\frac{j_\perp^2}{\sigma_\perp}-Q_\Delta+\frac{\vec{j}\vec{R}_T}{en} \qquad \text{(AIII.36)}$$

where $p=p_e+p_i$

It is easy to prove, that

$$\frac{3}{2}\frac{\partial}{\partial t}(nT_e)+\frac{\partial}{\partial x_\beta}\left(\frac{3}{2}nT_eV_{e\beta}\right)+p_e\frac{\partial}{\partial x_\beta}V_{e\beta}+\pi^e{}_{\alpha\beta}\frac{\partial V_{e\alpha}}{\partial x_\beta}+\frac{\partial q^e{}_\beta}{\partial x_\beta}=\frac{j_{//}^2}{\sigma_{//}}+\frac{j_\perp^2}{\sigma_\perp}-Q_\Delta+\frac{\vec{j}\vec{R}_T}{en} \qquad \text{(AIII.37)}$$

$$\frac{3}{2}\frac{\partial}{\partial t}(nT_i)+\frac{\partial}{\partial x_\beta}\left(\frac{3}{2}nT_iV_{i\beta}\right)+p_i\frac{\partial}{\partial x_\beta}V_{i\beta}+\pi^i{}_{\alpha\beta}\frac{\partial V_{i\alpha}}{\partial x_\beta}+\frac{\partial q^i{}_\beta}{\partial x_\beta}=Q_\Delta \qquad \text{(AIII.38)}$$

Appendix IV. Plasma rotation in poloidal direction

Based on drift approximation the plasma rotation in poloidal direction can be written as

$$V_\theta = V_{E\theta} + V_{D\theta} + V_{\nabla B} + b_\theta V_{//} \approx$$

$$\approx \frac{c[E\mathrm{b}]_\theta}{B} + \frac{c}{Z_a eBn_a}[\mathrm{b}\nabla p_a]_\theta + \frac{cT_a}{Z_a eB}[\mathrm{b}, \nabla\mathrm{b} + (\mathrm{b}\nabla\mathrm{b})]_\theta + \frac{cT_a}{Z_a eB} b_\theta(\mathrm{b}\cdot\mathrm{rotb}) + b_\theta V_{//} \quad \text{(AIV.1)}$$

where the firs term is due to the radial electric field, $\mathrm{b} \equiv \mathrm{B}/|\mathrm{B}|$

$$E_r = \frac{T_i}{e}\left[\frac{1}{n_i}\frac{\partial n_i}{\partial r} + (1-k)\frac{1}{T_i}\frac{\partial T_i}{\partial r}\right] \quad \text{(AIV.2)}$$

The second term is a diamagnetic velocity:

$$V_{D\theta} = \frac{c}{ZeBn_a}[\mathrm{b}\nabla p_a]_\theta \approx -\frac{c}{ZeBn_a}\frac{\partial n_a T_a}{\partial r} \quad \text{(AIV.3)}$$

The third one is the magnetic drift

$$V_{\nabla B} = \frac{cT_a}{Z_a eB}\left([\mathrm{b}, \nabla\mathrm{b} + (\mathrm{b}\nabla\mathrm{b})]_\theta + b_\theta(\mathrm{b}\cdot\mathrm{rotb})\right) = \frac{cT_a}{Z_a eB}\left(\frac{\partial b}{\partial r}\right)(1 - b_\theta^2) \quad \text{(AIV.4)}$$

In the case of tokamak geometry

$$B_\phi = \frac{B_0}{1+\varepsilon\cos\theta}, \qquad B_\theta = \frac{b_\theta \cdot B_0}{1+\varepsilon\cos\theta} \quad \text{(AIV.5)}$$

$$b_\theta = B_\theta / B_\phi, \qquad \varepsilon = r/R, \qquad b_\theta = B_\theta / B_\phi$$

and the poloidal velocity can be written as

$$V_\theta = \frac{c}{eB}\cdot\left(\frac{\partial n_i T_i}{n_i \partial r} + k\cdot\frac{\partial T_i}{\partial r}\right) \quad \text{(AIV.6)}$$

$$k = \frac{1.17 - 0.35\cdot\nu_{i*}^{1/2} - 2.1\cdot\nu_{i*}^2\cdot\varepsilon^2}{1 + 0.7\cdot\nu_{i*}^{1/2} + \nu_{i*}^2\varepsilon^3} \quad \text{(AIV.7)}$$

$$\nu_{i*} = \nu_i \cdot qR\varepsilon^{-3/2} / \sqrt{2T_i / m_i} \quad \text{(AIV.8)}$$

$$V_\theta = \rho_i\sqrt{2T_i / m_i}\cdot\left(\frac{\partial n_i T_i}{n_i T_i \partial r} + k\cdot\frac{\partial T_i}{T_i \partial r}\right) \quad \text{(AIV.9)}$$

Appendix V Atomic data of Ar and Ne atoms

- **Electron Ionization cross-section of Ar and Ne**: (sec, eV, cm^{-3})

$$S_{ion}(T_e, I) \equiv 10^{-5} \frac{\sqrt{T_e / I}}{I^{3/2}(6 + T_e / I)} \exp(-\frac{I}{T_e}) \qquad \nu_{ion} = n_0 \cdot S_{ion} \tag{AV.1}$$

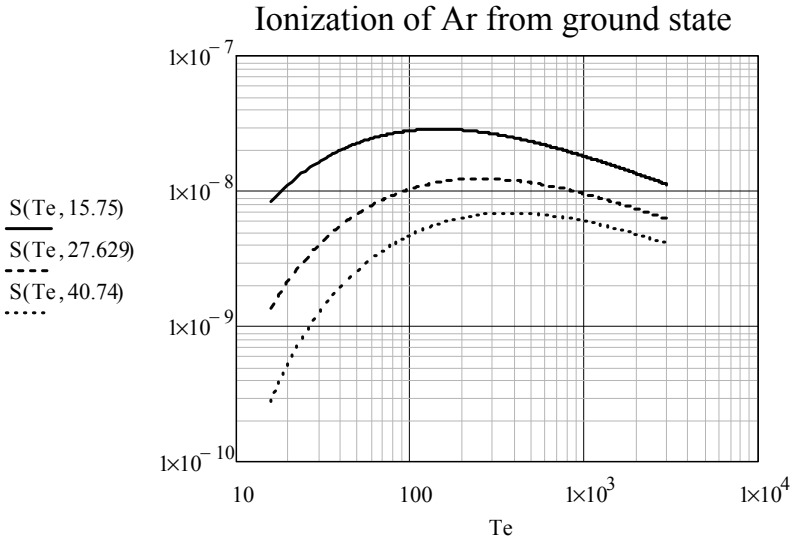

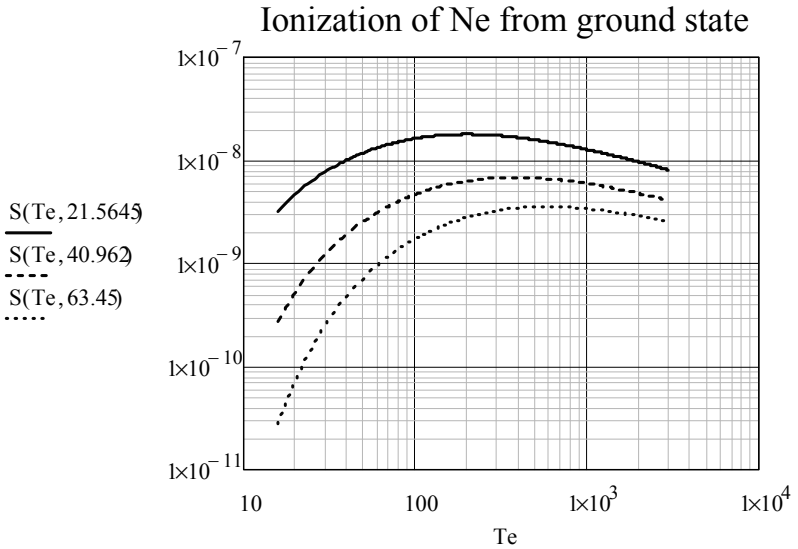

- **Ionization cross-section due to electron collisions (D. Post,1996)**

(sec, keV, cm^{-3})

Argon

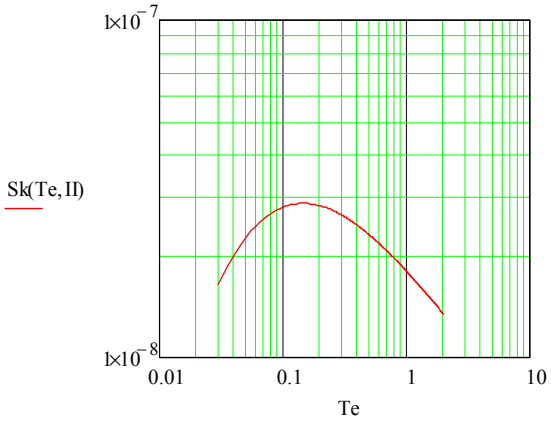

Neon

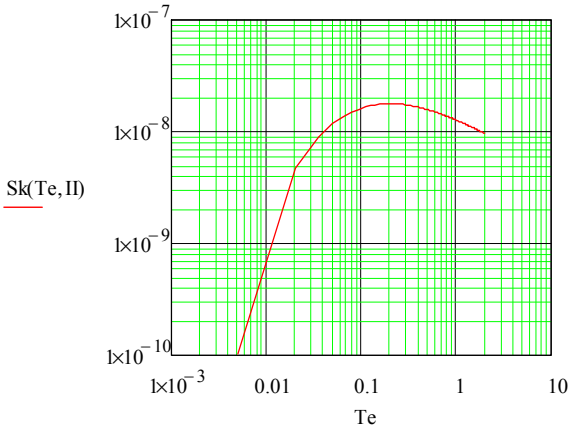

- **Ionization time of Ar and Ne atoms , electron mean-free pass before ionization**

$$\tau_{ion}(n_0, T_e, I) \equiv 1/n_0\, S_{ion} \qquad \text{(AV.2)}$$

($m$sec, eV, cm^{-3})

Electron ionization time of Ar atoms, msec

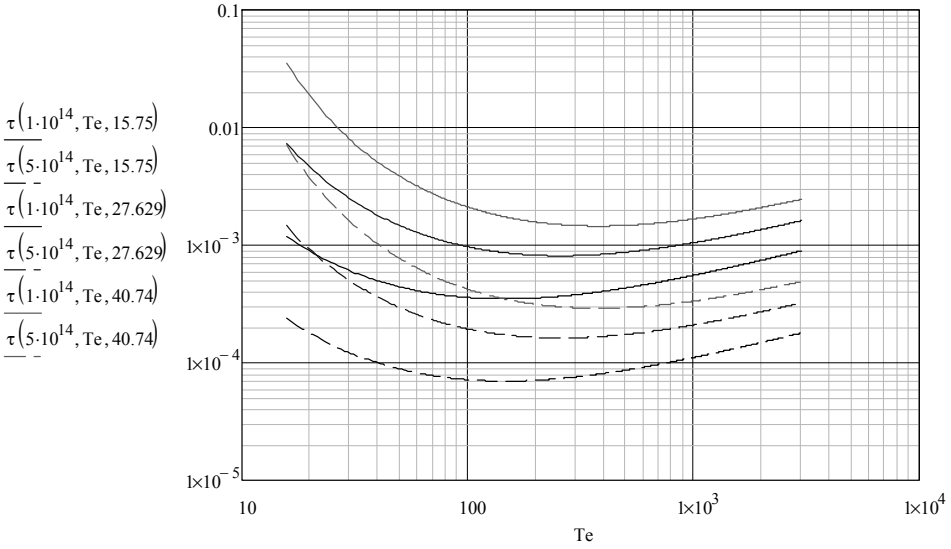

$(m\,\mathrm{sec},\ eV,\ cm^{-3})$

Ionization time of Ar for different ne

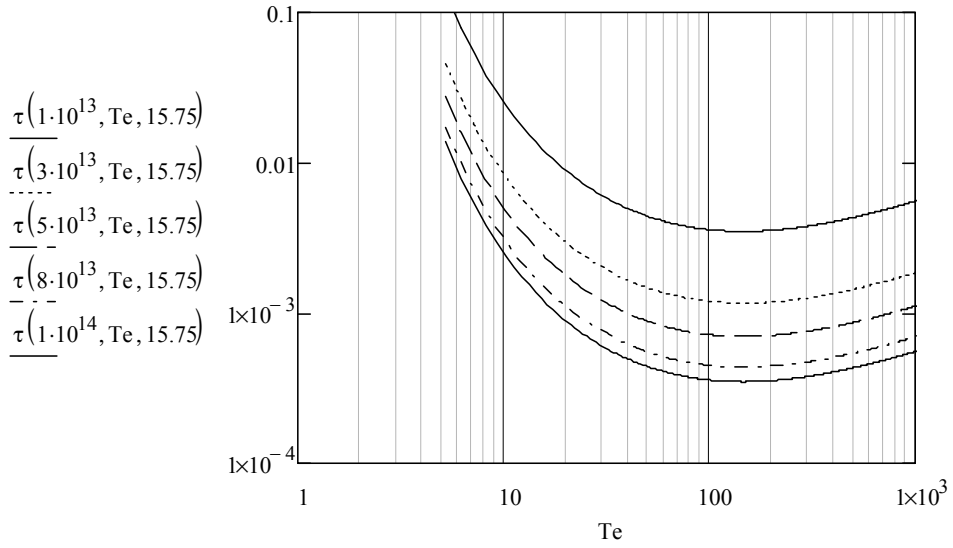

$(m\,\mathrm{sec},\ eV,\ cm^{-3})$

Ionization time of Ne for different ne

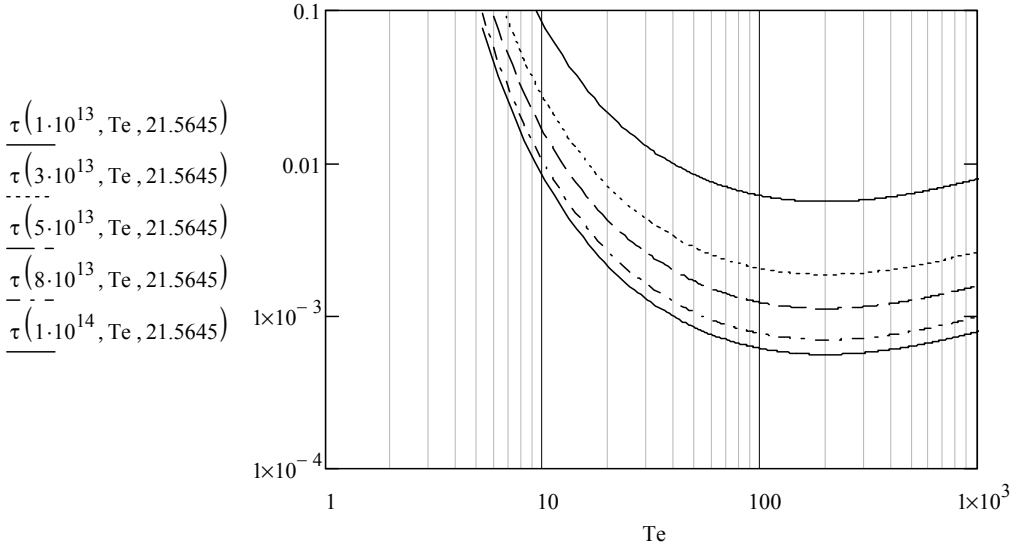

Neon Ionization Potentials

Ionization Stage	Charge	Isoelectronic State	Ionization Potential (eV)
I	0	Ne	21.564
II	1	F	40.962
III	2	O	63.45
IV	3	Ne	97.11
V	4	C	126.21
VI	5	B	157.93
VII	6	Be	207.26
VIII	7	Li	239.09
IX	8	He	1195.8
X	9	H	1362.2

- **Electron mean-free pass before ionization, cm**

$$\lambda e(n0, Te, I) := 4.19 \cdot 10^{7} \cdot \sqrt{Te} \cdot \tau(n0, Te, I) \qquad \text{(AV.3)}$$

Mfp of electrons for ionization vs Ar density, cm

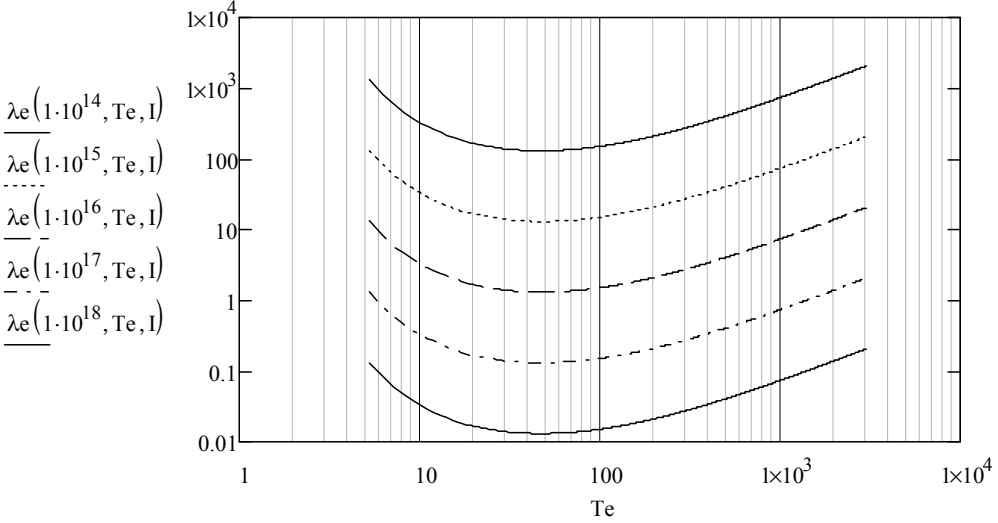

Mfp of electrons for ionization vs Ne density, cm

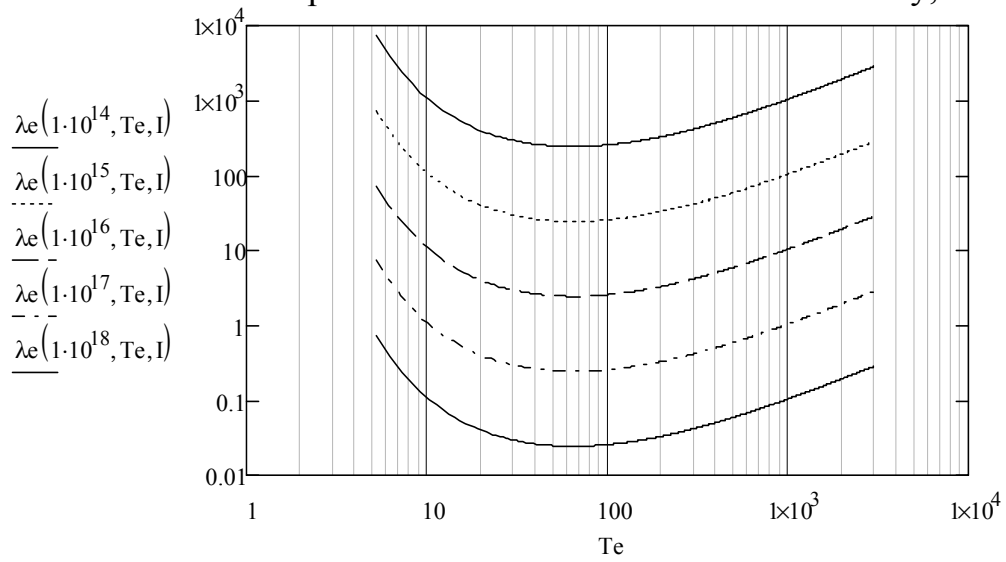

K-Shell Neon Ionization Potentials

Ionization Stage	Charge	Isoelectronic State	Ionization Potential (eV)
I	0	Ne	871.34
II	1	F	895.75
III	2	O	926.86
IV	3	Ne	961.21
V	4	C	1002.79
VI	5	B	1048.79
VII	6	Be	1095.27
VIII	7	Li	1144.17
IX	8	He	1195.8
X	9	H	1362.2

- **Mean free pass of Ar and Ne atoms before ionization (cm, eV)**

$$\Delta(ne, Te, I, A) := 9.79 \cdot 10^{5} \cdot \sqrt{\frac{Te}{A}} \cdot \frac{1}{ne \cdot S(Te, I)} \qquad \text{(AV.3)}$$

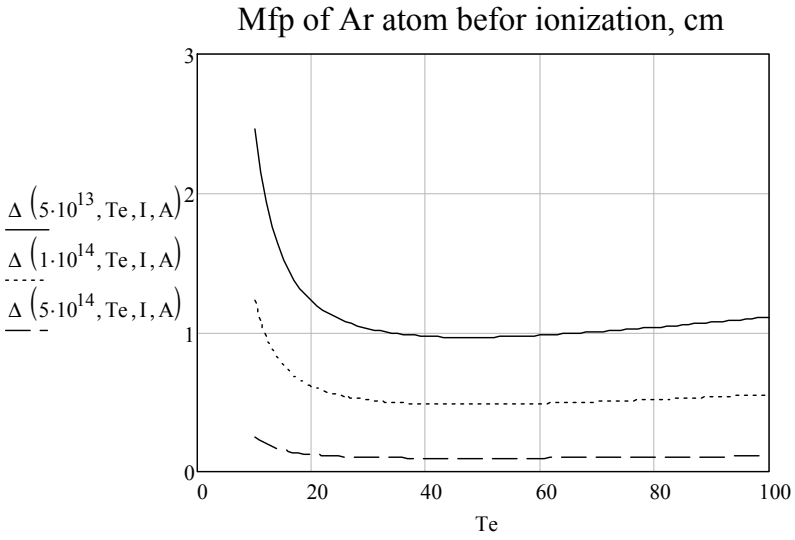

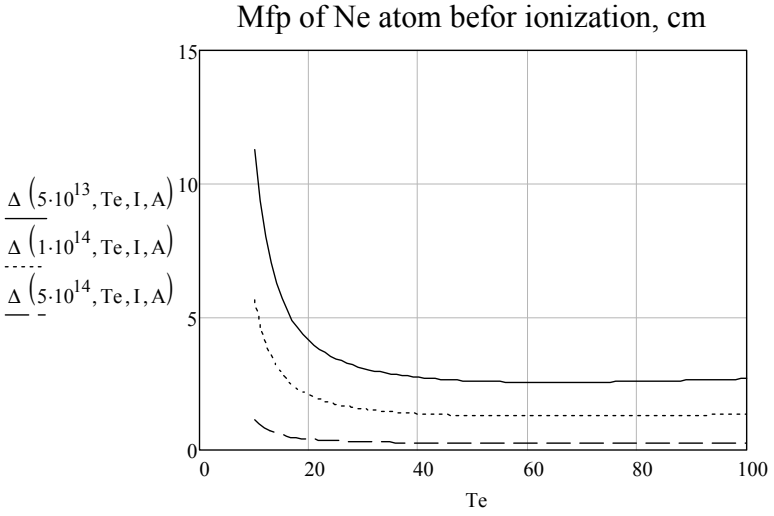

- **Recombination rates for Ar and Ne**

$$\alpha Ne(Te,Z,II) := \frac{\left(5.2\cdot 10^{-14}\right)}{\sqrt{1000}}\cdot Z\cdot\left(\frac{II}{Te}\right)^{\frac{1}{2}}\cdot\left[0.43 + 0.5\cdot\ln\left(\frac{II}{Te}\right) + 0.469\cdot\left(\frac{II}{Te}\right)^{\frac{-1}{3}}\right] \qquad \text{(AV.4)}$$

$\nu rec(Te,ne,Z,II) := ne\cdot\alpha Ne(Te,Z,II)$ $\quad \nu Neion(Te,ne,II) := ne\cdot Sk(Te,II)$ $\quad ne := 10^{14}$

Ne $\qquad n_e = 10^{14}\,cm^{-3}$

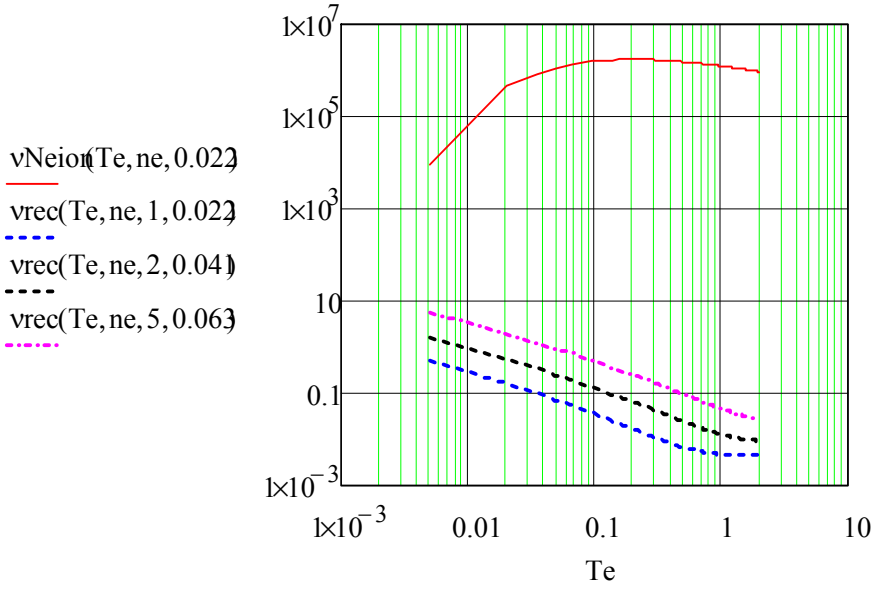

Ar

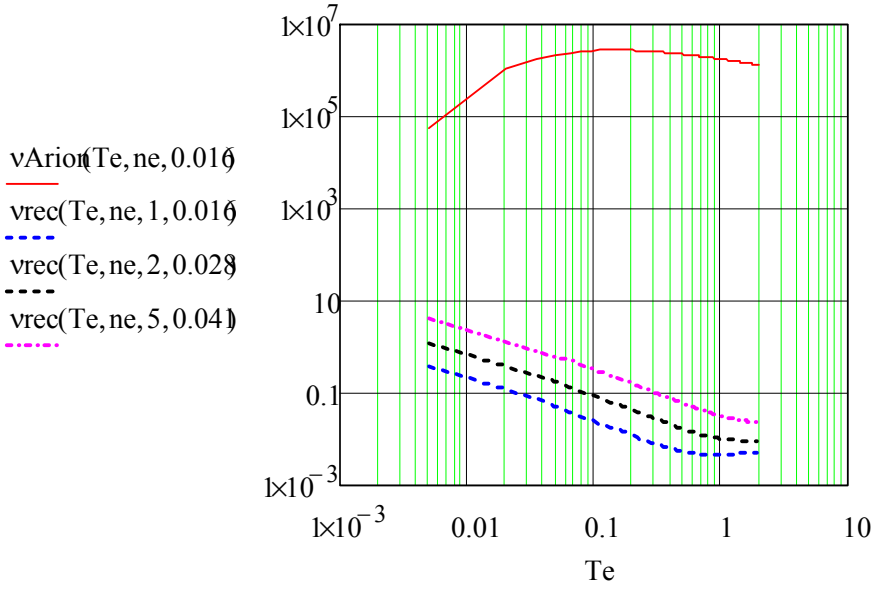

- **Comparison of Ar ionization, radiation and recombination frequencies,**

(1/sec,Te in KeV)

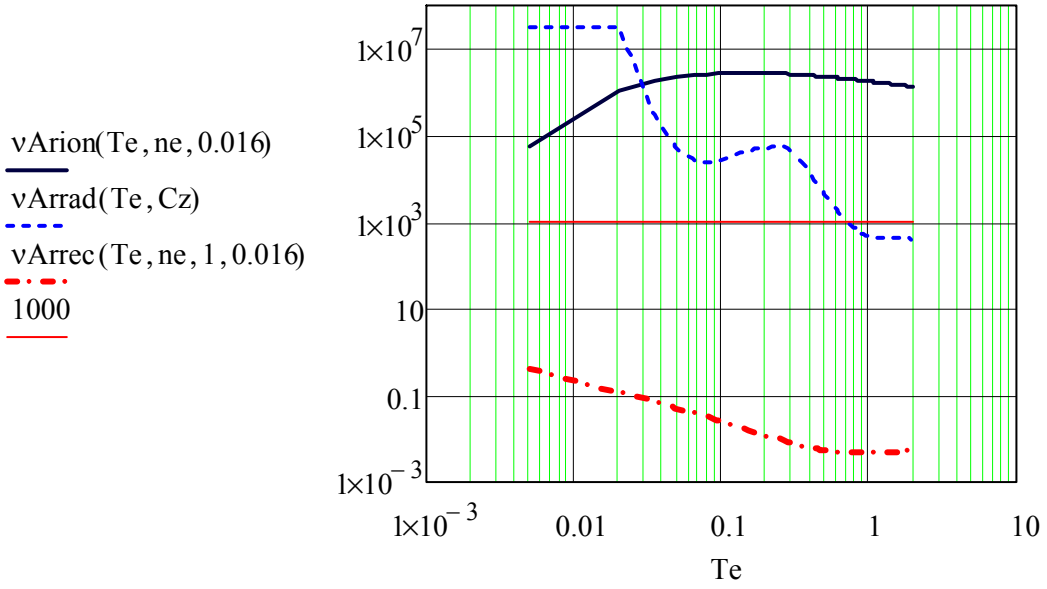

- **Comparison of Ne ionization, radiation and recombination frequencies**

(1/sec,Te in KeV)

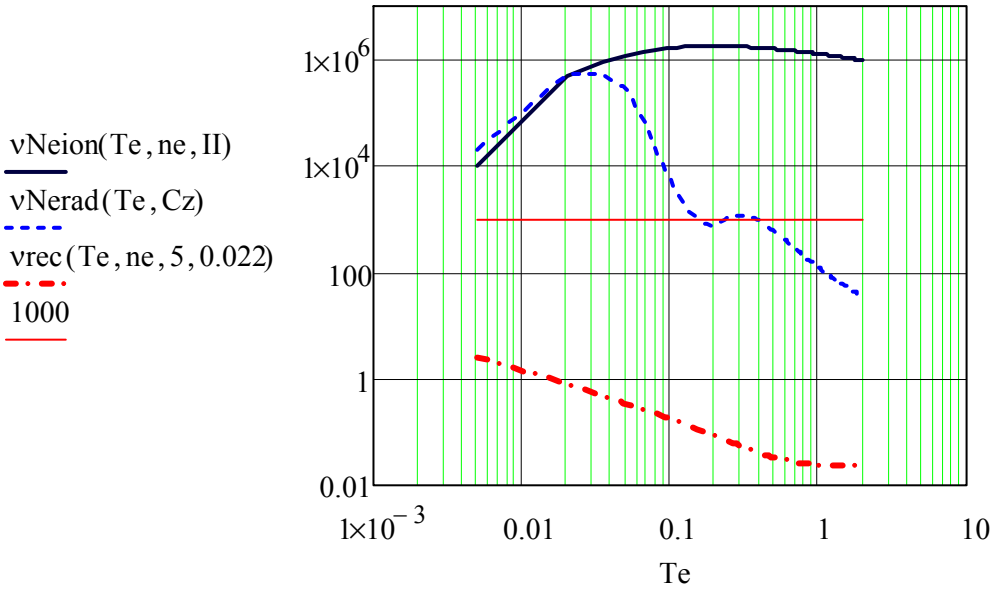

Appendix VI The quasi-dynamic transport across B

The drifts and magnetically induced current provide a mechanism for the pressure transfer across the B field even in rarefied plasma. This is so called quasi-hydrodynamic description, which is justified in drift approximation. The transport equation across the magnetic field can be written by using the Ampere's law where the current is substituted by all drift currents including the magnetically induced current and the inertial drift:

$$\mathrm{j}_\perp = \frac{c}{B^2}\left(\frac{P_\perp}{B}[\mathrm{B}\nabla B] + \frac{P_{//}}{R^2}[\mathrm{RB}] - \rho\left[\frac{d\mathrm{V}}{dt}\mathrm{B}\right]\right) - c\,\mathrm{rot}\left(\frac{P_\perp}{B^2}\mathrm{B}\right) \tag{AVI.1}$$

This equation can be written as:

$$\mathrm{j}_\perp = \frac{c}{B^2}\left(\frac{P_\perp}{B}[\nabla B\cdot\mathrm{B}] + \frac{P_{//}}{R^2}[\mathrm{RB}] - \rho\left[\frac{d\mathrm{V}}{dt}\mathrm{B}\right] - P_\perp\mathrm{rot}(\mathrm{B}) - [\nabla P_\perp\cdot\mathrm{B}]\right) \tag{AVI.2}$$

Above we used the expression:

$$\mathrm{rot}\left(\frac{P_\perp}{B^2}\mathrm{B}\right) = \frac{P_\perp}{B^2}\mathrm{rotB} + \frac{1}{B^2}[\nabla P_\perp\mathrm{B}] - \frac{2P_\perp}{B^3}[\nabla\mathrm{B}\cdot\mathrm{B}] \tag{AVI.3}$$

and also that:

$$\mathrm{rot}(u\mathrm{V}) = u\mathrm{rotV} + [\nabla u\mathrm{V}],\ \text{and}\ (\mathrm{B}\nabla B) = -[\nabla B\cdot\mathrm{B}] \tag{AVI.4}$$

Substituting current (AVI.2) in Ampere's law, one gets

$$[\mathrm{FB}] = \left(\frac{B^2}{8\pi} + P_\perp\right)\mathrm{rotB} \tag{AVI.5}$$

where

$$\mathrm{F} = \frac{P_\perp}{B}\nabla B + \frac{P_{//}}{R^2}\mathrm{R} - \nabla P_\perp - \rho\frac{\partial\mathrm{V}}{\partial t} \tag{AVI.6}$$

Here

$$\mathrm{V} = \sum_k \rho_k \mathrm{V}_k \Big/ \sum_k \rho_k \tag{AVI.7}$$

is an average velocity and summation goes over all species, ***R*** is the major radius.

From equations (AVI.4-5) it follows that,

$$B^2\mathrm{F}_\perp = \left(P_\perp + \frac{B^2}{8\pi}\right)\left(\frac{\nabla B^2}{2} - (B\nabla)\mathrm{B}\right) \tag{AVI.8}$$

or

$$\rho\frac{\partial\mathrm{V}_\perp}{\partial t} = -\nabla_\perp\left(P_\perp + \frac{B^2}{8\pi}\right) + \frac{2P_\perp}{B}\nabla B + \frac{P_{//}}{R^2}\mathrm{R} - (B\nabla\mathrm{B})\left(1 + \frac{4\pi P_\perp}{B^2}\right) \tag{AVI.9}$$

This equation differs from the hydrodynamic equation in two last terms, describing the forces due to the variation of magnetic field. After averaging over the Maxwellian distribution,

when $\langle P_{//} \rangle = mn\langle V_{//}^2 \rangle = nT$, and $\langle P_{\perp} \rangle = mn\langle V_{\perp}^2 \rangle = 2nT$:

$$mn\frac{\partial \mathrm{v}_{\perp}}{\partial t} = -\nabla_{\perp}\left(2nT + \frac{B^2}{8\pi}\right) + \frac{4nT}{B}\nabla B + \frac{nT}{R^2}\mathrm{R} - (B\nabla\mathrm{B})\left(1 + \frac{8\pi nT}{B^2}\right) \qquad \text{(AVI.10)}$$

If the magnetic field varies only in radial direction, then $(\mathrm{B}\nabla)\mathrm{B} = 0$

$$\rho\frac{\partial \mathrm{v}_{\perp}}{\partial t} = -\nabla_{\perp}\left(2nT + \frac{B^2}{8\pi}\right) + \frac{nT}{R^2}\mathrm{R} \qquad \text{(AVI.11)}$$

$$\rho\frac{\partial \mathrm{v}_{r}}{\partial t} = -\frac{B}{4\pi}\frac{\partial B}{\partial r} + \frac{nT}{R^2}r - \frac{\partial}{\partial r}nT \qquad \text{(AVI.12)}$$

$$\rho\frac{\partial \mathrm{v}_{\theta}}{\partial t} = -\frac{B}{4\pi r}\frac{\partial B}{\partial \theta} - \frac{1}{r}\frac{\partial}{\partial \theta}nT \qquad \text{(AVI.13)}$$

These are the transport equations for the entire plasma cloud**.**

Appendix VII Discretisation of transport equations: Belocerkovsky step

- In the first discretization step we are considering the following equations:

$$\frac{\partial}{\partial t}(n_a)+\frac{1}{\sqrt{g}}\frac{\partial}{\partial y}\left\{\frac{b_y\sqrt{g}}{h_y}n_aV_a\right\}=0 \qquad \text{(AVII.1)}$$

$$\frac{\partial}{\partial t}(m_an_aV_a)+\frac{1}{\sqrt{g}}\frac{\partial}{\partial y}\left\{\frac{b_y\sqrt{g}}{h_y}m_an_aV_a^2\right\}=-\frac{b_y}{h_y}\frac{\partial p_a}{\partial y}+z_a\cdot n_aE_{//} \qquad \text{(AVII.2)}$$

$$\frac{\partial\varepsilon_a}{\partial t}+\frac{1}{\sqrt{g}}\frac{\partial}{\partial y}\left\{\frac{\sqrt{g}b_y}{h_y}\varepsilon_aV_a\right\}=-\frac{1}{\sqrt{g}}\frac{\partial}{\partial y}\left\{\frac{\sqrt{g}b_y}{h_y}p_aV_a\right\}+z_an_aV_aE_{//} \qquad \text{(AVII.3)}$$

$$\frac{\partial\varepsilon_e}{\partial t}+\frac{1}{\sqrt{g}}\frac{\partial}{\partial y}\left\{\frac{\sqrt{g}b_y}{h_y}\varepsilon_eV_e\right\}=-\frac{1}{\sqrt{g}}\frac{\partial}{\partial y}\left\{\frac{\sqrt{g}b_y}{h_y}p_eV_e\right\}-n_eV_eE_{//} \qquad \text{(AVII.4)}$$

$$\frac{\partial\varepsilon_t}{\partial t}+\frac{1}{\sqrt{g}}\frac{\partial}{\partial y}\left\{\frac{\sqrt{g}b_y}{h_y}\left(\varepsilon_eV_e+\sum\varepsilon_aV_a\right)\right\}=-\frac{1}{\sqrt{g}}\frac{\partial}{\partial y}\left\{\frac{\sqrt{g}b_y}{h_y}\left(p_eV_e+\sum p_aV_a\right)\right\} \qquad \text{(AVII.5)}$$

where: $\sqrt{g}=rh_xh_y$

$$\varepsilon_t=\varepsilon_e+\sum\varepsilon_z\,, \qquad \text{(AVII.6)}$$

$$\varepsilon_e=\frac{3}{2}n_eT_e\,, \qquad \text{(AVII.7)}$$

$$\varepsilon_a=\frac{3}{2}n_aT_a+\frac{m_an_a}{2}V_a^2\,, \qquad \text{(AVII.8)}$$

V_a and V_e are the *a*-species and electron velocities along $\vec{B}$, $E_{//}$ the electric field along $\vec{B}$, and

$$p_e=n_eT_e\,,\quad p_a=n_aT_a \qquad \text{(AVII.9)}$$

- To discretizais equation we have to consider the integral operators in curvilinear coordinate system. We use the definitions:

$$dl^2=dl_x^2+dl_y^2+dl_z^2=g_{xx}dx^2+g_{yy}dy^2+g_{zz}dz^2 \qquad \text{(AVII.10)}$$

$$dl_y=\sqrt{g_{yy}}dy=h_ydy \qquad \text{(AVII.11)}$$

$$dV=dl_ydS_y=\sqrt{g}dydxdz=dl_y\sqrt{\frac{g}{g_{yy}}}\cdot dxdz=h_ydydS^{cross} \qquad \text{(AVII.12)}$$

$$d\vec{S}_y=\left[\vec{l}_z\vec{l}_x\right]=\left[\vec{e}_z\vec{e}_x\right]dzdx=\sqrt{g}\cdot\nabla\vec{y}\cdot dzdx=\vec{e}_y\sqrt{\frac{g}{g_{yy}}}dzdx\,; \qquad \text{(AVII.13)}$$

$$[\vec{e}_z \vec{e}_x] = \nabla\vec{y} \cdot \sqrt{g}\,; \qquad |\nabla\vec{y}| = \sqrt{g^{yy}} = 1/h_y \tag{AVII.14}$$

then $dS_y = \sqrt{\frac{g}{g_{yy}}} \cdot dxdz = \frac{\sqrt{g}}{h_y} \cdot dxdz$ (AVII.15)

$N_a \equiv \int n_a \sqrt{g} dxdydz = \int n_a dV$ is the total number of particles; (AVII.16)

$$\int \nabla f \cdot dV = \int_s f d\vec{S}_n = \int_s \left(f d\vec{S}_y + f d\vec{S}_x + f d\vec{S}_z \right) \approx \frac{1}{2} \int_s f dS_y = \frac{1}{2} \int_s f \frac{\sqrt{g}}{h_y} \cdot dxdz \tag{AVII.17}$$

$$f \equiv \frac{\sqrt{g}}{h_y} n_a \left(b_y V_a \right) \qquad dS_y = \frac{\sqrt{g}}{h_y} \cdot dxdz \tag{AVII.18}$$

$$\int_V \frac{\partial}{\partial y} \left\{ \frac{\sqrt{g}}{h_y} n_a \left(b_y V_a \right) \right\} dydxdz = \int_V \frac{\partial}{\partial y} \left\{ n_a \left(b_y V_a \right) \frac{\sqrt{g}}{h_y} dxdz \right\} dy =$$

$$= \int_V \frac{\partial}{\partial y} \left\{ n_a \left(b_y V_a \right) dS_y \right\} dy = \left(S_y n_a b_y V_a \right) \Big|_-^+ \tag{AVII.19}$$

After interaction over a sell volume G for *continuity equations*:

- $$\frac{\partial}{\partial t} \int n_a dV = \int n_a \sqrt{g} dxdydz = N \tag{AVII.20}$$

$$\frac{\partial}{\partial t} (N_a) + \left\{ S^{cross} n_a b_y V_a \right\}_-^+ = 0 \quad \text{with} \quad S^{cross} = r h_x = \frac{\sqrt{g}}{h_y} \quad , \quad h_y = \sqrt{g_{22}}$$

$$N_a \equiv \int n_a \sqrt{g} dxdydz = \int n_a dV \tag{AVII.21}$$

- $$\int \frac{1}{\sqrt{g}} \frac{\partial}{\partial y} \left\{ \frac{\sqrt{g}}{h_y} n_a \left(b_y V_a \right) \right\} dV = \int \frac{\partial}{\partial y} \left\{ \frac{\sqrt{g}}{h_y} n_a \left(b_y V_a \right)_a \right\} dxdydz = \int \frac{\sqrt{g}}{h_y} n_a \left(b_y V_a \right)_a \Big|_-^+ \frac{h_y}{\sqrt{g}} dS_y =$$

$$= \frac{\sqrt{g}}{h_y} n_a \left(b_y V_a \right)_a \Big|_-^+ \int \frac{h_y}{\sqrt{g}} dS_y = \frac{\sqrt{g}}{h_y} n_a \left(b_y V_a \right)_a \Big|_-^+ \int dxdz = S_y \cdot n_a \left(b_y V_a \right)_a \Big|_-^+ \tag{AVII.22}$$

For momentum equations

- $$\frac{\partial}{\partial t} \left(m_a n_a V_a \right) + \frac{1}{\sqrt{g}} \frac{\partial}{\partial y} \left\{ \frac{b_y \sqrt{g}}{h_y} m_a n_a V_a^2 \right\} = - \frac{b_y}{\sqrt{g} h_y} \frac{\partial p_a}{\partial y} + z_a \cdot n_a E \tag{AVII.23}$$

$$\int_V \frac{1}{\sqrt{g}} \frac{\partial}{\partial y} \left\{ \frac{b_y \sqrt{g}}{h_y} m_a n_a V_a^2 \right\} dV =$$

$$\int_V \frac{\partial}{\partial y} \left\{ \frac{b_y \sqrt{g}}{h_y} m_a n_a V_a^2 \right\} dxdydz = \int_S \frac{\sqrt{g}}{h_y} m_a n_a b_y V_a^2 \Big|_-^+ dxdz \approx S_y m_a n_a b_y V_a^2 \Big|_-^+ \tag{AVII.24}$$

$$\frac{\partial}{\partial t}\left(m_a N_a V_a\right)+\left\{S^{cross}\, m_a n_a V_a^2\right\}_-^+ = -b_y \frac{S_+^{cross}+S_-^{cross}}{2}\left(p_a\right)_-^+ + G\cdot z_a\cdot n_a E \qquad \text{(AVII.25)}$$

For energy equations

- $$\sqrt{g}\frac{\partial \varepsilon_a}{\partial t}+\frac{\partial}{\partial y}\left\{\frac{\sqrt{g}b_y}{h_y}\varepsilon_a V_a\right\} = -\frac{\partial}{\partial y}\left\{\frac{\sqrt{g}b_y}{h_y}p_a V_a\right\}+\sqrt{g}z_a n_a V_a E \qquad \text{(AVII.26)}$$

$$E_a \equiv \sqrt{g}\varepsilon_a$$

$$\frac{\partial E_a}{\partial t}+\left\{S^{cross}\varepsilon_a V_a\right\}_-^+ = -\left\{S^{cross}p_a V_a\right\}_-^+ + G z_a n_a V_a E \qquad \text{(AVII.27)}$$

$$\frac{\partial \varepsilon_t}{\partial t}+\frac{1}{\sqrt{g}}\frac{\partial}{\partial y}\left\{\frac{\sqrt{g}b_y}{h_y}\left(\varepsilon_e V_e+\sum \varepsilon_a V_a\right)\right\} = -\frac{1}{\sqrt{g}}\frac{\partial}{\partial y}\left\{\frac{\sqrt{g}b_y}{h_y}\left(p_e V_e+\sum p_a V_a\right)\right\} \qquad \text{(AVII.28)}$$

$$\frac{\partial E_t}{\partial t}+\left\{S^{cross}\left(\varepsilon_e V_e+\sum \varepsilon_a V_a\right)\right\}_-^+ = -\left\{S^{cross}\left(p_e V_e+\sum p_a V_a\right)\right\}_-^+ \qquad \text{(AVII.29)}$$

- Altogether:

$$\frac{\partial}{\partial t}\left(N_a\right)+\left\{S^{cross}n_a V_a\right\}_-^+ = 0 \qquad \text{(AVII.30)}$$

$$\frac{\partial}{\partial t}\left(m_a N_a V_a\right)+\left\{S^{cross}\, m_a n_a V_a^2\right\}_-^+ = -b_y \frac{S_+^{cross}+S_-^{cross}}{2}\left(p_a\right)_-^+ + G\cdot z_a\cdot n_a E \qquad \text{(AVII.31)}$$

$$\frac{\partial}{\partial t}\sum m_a N_a V_a+\left\{S^{cross}\sum m_a n_a V_a^2\right\}_-^+ = -b_y \frac{S_+^{cross}+S_-^{cross}}{2}\left(\sum p_a\right)_-^+ \qquad \text{(AVII.32)}$$

$$\frac{\partial E_a}{\partial t}+\left\{S^{cross}\varepsilon_a V_a\right\}_-^+ = -\left\{S^{cross}p_a V_a\right\}_-^+ + G z_a n_a V_a E \qquad \text{(AVII.33)}$$

$$\frac{\partial E_e}{\partial t}+\left\{S^{cross}\varepsilon_e V_e\right\}_-^+ = -\left\{S^{cross}p_e V_e\right\}_-^+ - G n_e V_e E \qquad \text{(AVII.34)}$$

$$\frac{\partial E_t}{\partial t}+\left\{S^{cross}\left(\varepsilon_e V_e+\sum \varepsilon_a V_a\right)\right\}_-^+ = -\left\{S^{cross}\left(p_e V_e+\sum p_a V_a\right)\right\}_-^+ \qquad \text{(AVII.35)}$$

These are the equations, which we solve at the first Belocerkovsky's step. In the next (Euler) step, thermo-conductivity and diffusive terms are taken into account.

.

Appendix VIII Program for neutral atoms

```
c version: 31.02.2010 16:56
c
      parameter(nxi=67,nt=50)
      implicit real*8(a-h),real*8(o-z)
      real*8 nold(nxi),vold(0:nxi),told(nxi)
      real*8 nnew(nxi),vnew(0:nxi),tnew(nxi),vtmp(nxi)
      real*8 a(nxi),b(nxi),c(nxi),d(nxi),k(nxi)
      real*8 xi(nxi),eta(nxi),pnl(nxi),qnl(nxi),nx
      real*8 te(nt),rad(nt)
      common/param/ dens,ts,denneu,aln,tau0,cz0
      common/post/te,rad,hlg,tlg1,ifile
c
      f52(x) = x**2*dsqrt(x)
      dmf(y) = dmax1(y,0.d0)
c
c constants & parameters:
      ame = 9.1d-28
      amu = dsqrt(2.5d0*1836./2.)
      smime = dsqrt(2.5d0*1836.)
      Ami = 2.5d0*1836.*AME
      qe = 4.8d-10
      pi = 3.141592653589d0
      sp = dsqrt(pi)
      poti=13.6d0
      vold(0)=0.d0
      vnew(0)=0.d0
```

```
c-----------------------------------------------------
      open(1,file='input/input.hyd')
      read(1,*)tau,nend
      read(1,*)nout
      read(1,*)isbou
      read(1,*)al
      read(1,*)slal
      read(1,*)trl
      read(1,*)dtr
      read(1,*)denneu
      read(1,*)delta
      read(1,*)aln
      read(1,*)qq
      read(1,*)flux
      read(1,*)sq
      read(1,*)ifile
      read(1,*)cz0
      read(1,*)flf
      close(1)
c-----------------------------------------------------
c atomic data from Post(in Wm**3 E40)
         if( ifile .eq. 1 ) then
         open(1,file='input/l.dat')
         read(1,*)
         do 555 i=1,nt
          read(1,*)te(i),rad(i)
```

```
            rad(i) = rad(i)*6.25d-16
c           (conversion to eV*cm**3/s)
555     continue
        close(1)
        hlg = dabs( dlog(te(1)) - dlog(te(2)) )
        tlg1 = dlog(te(1))
        endif
c-----------------------------------------------------
c (source length = al*slal)
      nxi1=nxi-1
      nxi2=nxi-2
      nxi3=nxi-3
      na = int(nxi1*slal)
      ts=6.25d24*qq/3/flux
      dens=trl*flux/2./dtr/sq
      poti = poti/ts
      tserg = ts*1.6d-12
      h = 1.d0/dfloat(nxi1)
      vs =1.38d6*dsqrt(2.5*ts)
      tau0 = al/vs
      aa = 2.d12*ts**2/dens/al
      aKn=aa
      taus = trl**2/2./dtr/tau0
      taue=taus
      taup=taue
      write(*,*)'aKn= ',sngl(aKn),'  taus=',sngl(taus),
     ,          '  tau0=',sngl(tau0), '  ts=',sngl(ts),
```

```
     , '  dens=',sngl(dens)
      a1 = 2.d0*0.96/3.*aa
      a2 = a1
      a3 = 0.8*smime*aa
c=====================================================
c  first step:
      open(1,file = 'input/hydra0.dat')
      do 1 i=1,nxi1
      read(1,*)tmp,nold(i),vold(i),told(i)
c     nnew(i)=nold(i)
c     vnew(i)=vold(i)
1     continue
      close(1)
c=====================================================
c
      icount = 0
1000  continue
      icount = icount + 1
c
      if (isbou .ne. 1) then
            dddd = nold(nxi1)*dens
            vvvv = vold(nxi1)*vs
            tttt = told(nxi1)*tserg
            call bound(dddd,vvvv,tttt
     ,                 ,tttt,ame,ami,pixx,qex,qix)
            qeiz = (qex + qix)/2.d0/(dens*vs*tserg)
```

```
            pixx = pixx/(dens*tserg)
      else
            qeiz = 8.*nold(nxi1)*told(nxi1)
     ,                  *dsqrt(told(nxi1)/2.)/2.d0
            vlast = dsqrt(told(nxi1)/2.d0)
      endif
c=======================================================
c                        density block
c     go to 115
c   first volume:
      nnew(1) = (tau/taup - tau/h*
     ,          (nold(1)*dmf(vold(1))- nold(2)*dmf(-vold(1)))
     ,          + nold(1)+pln(0.5*h)/tauion(nold(1),told(1))*tau)
     ,          /(1.+tau/taus+tau/taurec(nold(1),told(1)))
c
c-------------------------------------------------------
c   standard volume:
c
c with source
      do 2 i=2,na
      nnew(i) = (tau/taup - tau/h*(nold(i)*dmf(vold(i))
     ,          - nold(i+1)*dmf(-vold(i))
     ,          - (nold(i-1)*dmf(vold(i-1)) - nold(i)*dmf(-vold(i-1))))
     ,          + nold(i)+pln(h*(i-0.5))/tauion(nold(i),told(i))*tau)
     ,          /(1.+tau/taus+tau/taurec(nold(i),told(i)))
2     continue
c without source
```

```
      do 3 i=na+1,nxi2
      nnew(i) = (- tau/h*(nold(i)*dmf(vold(i))
     ,         - nold(i+1)*dmf(-vold(i))
     ,         -(nold(i-1)*dmf(vold(i-1)) - nold(i)*dmf(-vold(i-1))))
     ,         + nold(i)+pln(h*(i-0.5))/tauion(nold(i),told(i))*tau)
     ,         /(1.+tau/taus+tau/taurec(nold(i),told(i)))
3     continue
c-----------------------------------------------------
c   last volume:
      nnew(nxi1) =(-tau/h*(nold(nxi1)*dmf(vold(nxi1))
     ,         - nold(nxi2)*dmf(vold(nxi2))
     ,         + nold(nxi1)*dmf(-vold(nxi2)))
     ,         + nold(nxi1)
     ,         +pln(h*(nxi1-0.5))/tauion(nold(nxi1),told(nxi1))*tau)
     ,         /(1.+tau/taus+tau/taurec(nold(nxi1),told(nxi1)))
c=====================================================
c       go to 114
c                          velocity block
c                        coefficients for v
c-----------------------------------------------------
c  standard volume:
      do 4 i=1,nxi2
      tx = (told(i)+told(i+1))/2.
      nx = (nnew(i)+nnew(i+1))/2.
      coor=h*i
      a(i) = - a1*f52(told(i))/h*tau
```

```
      b(i) =  -((nnew(i)+nnew(i+1))/2.*h +
     ,       a1/h*tau*(f52(told(i+1)) + f52(told(i)))
     ,       +nx*(1./taus+delta/taucx(coor,tx)+1./taurec(nx,tx))*h*tau)
      c(i) = -a1*f52(told(i+1))/h*tau
c
            vv = (vold(i)+vold(i+1))/2.
            v = vold(i)
            if(vv.lt.0.d0) v=vold(i+1)
            vv1 = (vold(i)+vold(i-1))/2.
            v1 = vold(i-1)
            if(vv1.lt.0.d0) v1=vold(i)
c
      d(i) = (nold(i) + nold(i+1))/2.*h*vold(i)
     ,       -tau*(nnew(i+1)*vv*v-nnew(i)*vv1*v1
     ,      -nnew(i)*told(i) + nnew(i+1)*told(i+1))
     ,      +(1-delta)*pln(coor)*vold(i)/tauion(nx,tx)*h*tau
4     continue
      a(1)=0.0
c-----------------------------------------------------
c  last volume:
c
      if (isbou .ne. 1) then


Boundary conditions
            tx = told(nxi1)
            nx = nnew(nxi1)
            coor=h*nxi1
```

```
          a(nxi1) = -2*a1*f52(told(nxi1))/h*tau
          b(nxi1) = -(nnew(nxi1)*h +
     ,               2*a1/h*tau*f52(told(nxi1))
     ,              +    nnew(nxi1)*
     ,           (1./taus+delta/taucx(coor,tx)+1./taurec(nx,tx))*h*tau)
          c(nxi1) = 0.
                vv = vold(nxi1)+vold(nxi2)
                v = vold(nxi2)
                if(vv.lt.0.d0) v=vold(nxi1)
c
          d(nxi1) = nold(nxi1)*vold(nxi1)*h -
     ,               tau*(pixx - nnew(nxi1)*vv*v
     ,               - 2.*nnew(nxi1)*told(nxi1))
     ,          +(1-delta)*pln(coor)*vold(nxi1)/tauion(nx,tx)*h*tau
c
       else
c Braams' version of the boundary conditions:
          a(nxi1) = 0.d0
          b(nxi1) = -1.d0
          c(nxi1) = 0.d0
          d(nxi1) = vlast
       endif
c-----------------------------------------------------
c
       call tdmad(nxi1,a,b,c,d,vtmp,xi,eta)
       do 41 i=1,nxi1
```

```
 41   vnew(i)=vtmp(i)
c
c=====================================================
115    continue
c                 temperature block
c
c  heat conductivities (full-explicit variant):
      do 5 i=1,nxi1
      avt=(told(i)+told(i+1))/2.
      avn=(nold(i)+nold(i+1))/2.
      gradt=dabs(told(i)-told(i+1))/h
      if(gradt.le.1.d-10) gradt=1.d-10
      dgradt=avt/gradt
c  flux-limit factor flf:
      if (dgradt.gt.1.d0) dgradt=1.d0
      gq=1.d0/(1.d0+3.2d0*sp/8.d0/flf*aKn*avt**2/avn/dgradt)
c      gq=1.d0
      k(i) = f52(avt)*gq
5     continue
c-------------------------------------------------------
c              coefficients for temperature
c
c  first volume:
      tx = told(1)
      nx = nnew(1)
      coor = h/2.
      a(1) = 0.
```

```
      b(1) = -(1.5 *nnew(1)*h + tau*(2.5*nnew(1)*dmf(vnew(1))
     ,      + a3*k(1)/h
     ,      + nnew(1)*h*(1.5/taus+0.5/taurad(coor,nx,tx)
     ,      +1.5*delta/taucx(coor,tx)+0.5/tauexc(coor,tx)
     ,      +vnew(1)**2/8./told(1)*(1./taus + delta/taucx(coor,tx))
     ,      +0.5*pln(coor)*poti/told(1)/tauion(nx,tx))))
      c(1) = -tau*(2.5*nnew(2)*dmf(-vnew(1)) + a3*k(1)/h)
      d(1) = (1.5*nold(1)*told(1)-nnew(1)*vnew(1)**2/8.
     ,      +nold(1)*vold(1)**2/8.)*h
     ,      +(1.5/taue+0.5*(1.-delta)*pln(coor)*(3*told(1)
     ,      +vnew(1)**2/4.)/tauion(nx,tx))*h*tau
     ,      -tau*(nnew(1)*vnew(1)**2/8.*dmf(vnew(1))
     ,           -nnew(2)*(vnew(2)+vnew(1))**2/8.*dmf(-vnew(1))
     ,           -a2/h*(f52(told(1))*vnew(1)*dmf(vnew(1))
     ,            -f52(told(2))*(vnew(2)-vnew(1))*dmf(-vnew(1))))
c-----------------------------------------------------
c  standard volume:
c  with source
      do 6 i=2,na
      tx = told(i)
      nx = nnew(i)
      vx = (vnew(i-1)+vnew(i))/2.
      coor = h*(i-0.5)
      a(i) = -tau*(2.5*nnew(i-1)*dmf(vnew(i-1)) + k(i-1)*a3/h)
      b(i) = -(1.5*nnew(i)*h + tau*(2.5*nnew(i)*(dmf(vnew(i)) +
     ,      dmf(-vnew(i-1))) + a3/h*(k(i)+k(i-1))
```

```
     ,      + nnew(i)*h*(1.5/taus+0.5/taurad(coor,nx,tx)
     ,      +1.5*delta/taucx(coor,tx)+0.5/tauexc(coor,tx)
     ,      +vx**2/told(i)*(1./taus + delta/taucx(coor,tx))/2.
     ,      +0.5*pln(coor)*poti/told(i)/tauion(nx,tx))))
      c(i) = -tau*(2.5*nnew(i+1)*dmf(-vnew(i)) + k(i)*a3/h)
      d(i) =  1.5*h*tau/taue - h*(nnew(i)*vx**2/2.
     ,      -nold(i)*(vold(i)+vold(i-1))**2/8.- 1.5*nold(i)*told(i))
     ,      -tau*(nnew(i)*(vnew(i)+vnew(i-1))**2/8.*dmf(vnew(i))
     ,          -nnew(i+1)*(vnew(i)+vnew(i+1))**2/8.*dmf(-vnew(i))
     ,          -nnew(i-1)*(vnew(i-2)+vnew(i-1))**2/8.*dmf(vnew(i-1))
     ,          +nnew(i)*(vnew(i)+vnew(i-1))**2/8.*dmf(-vnew(i-1))
     ,      -a2*(f52(told(i))*(vnew(i)-vnew(i-1))/h*dmf(vnew(i))
     ,        -f52(told(i+1))*(vnew(i+1)-vnew(i))/h*dmf(-vnew(i))
     ,        -f52(told(i-1))*(vnew(i-1)-vnew(i-2))/h*dmf(vnew(i-1))
     ,        +f52(told(i))*(vnew(i)-vnew(i-1))/h*dmf(-vnew(i-1))))
     ,      +(0.5*(1.-delta)*pln(coor)*(3*told(i)
     ,      +vx**2)/tauion(nx,tx))*h*tau
6     continue
c without source:
      do 8 i=na+1,nxi2
      tx = told(i)
      nx = nnew(i)
      vx = (vnew(i-1)+vnew(i))/2.
      coor = h*(i-0.5)
      a(i) = -tau*(2.5*nnew(i-1)*dmf(vnew(i-1)) + k(i-1)*a3/h)
      b(i) = -(1.5*nnew(i)*h + tau*(2.5*nnew(i)*(dmf(vnew(i)) +
     ,      dmf(-vnew(i-1))) + a3/h*(k(i)+k(i-1))
```

```
     ,      + nnew(i)*h*(1.5/taus+0.5/taurad(coor,nx,tx)
     ,      +1.5*delta/taucx(coor,tx)+0.5/tauexc(coor,tx)
     ,      +vx**2/told(i)*(1./taus + delta/taucx(coor,tx))/2.
     ,      +0.5*pln(coor)*poti/told(i)/tauion(nx,tx))))
      c(i) = -tau*(2.5*nnew(i+1)*dmf(-vnew(i)) + a3*k(i)/h)
      d(i) = - h*(nnew(i)*vx**2/2.
     ,      -nold(i)*(vold(i)+vold(i-1))**2/8.- 1.5*nold(i)*told(i))
     ,      -tau*(nnew(i)*(vnew(i)+vnew(i-1))**2/8.*dmf(vnew(i))
     ,          -nnew(i+1)*(vnew(i)+vnew(i+1))**2/8.*dmf(-vnew(i))
     ,          -nnew(i-1)*(vnew(i-2)+vnew(i-1))**2/8.*dmf(vnew(i-1))
     ,          +nnew(i)*(vnew(i)+vnew(i-1))**2/8.*dmf(-vnew(i-1))
     ,      -a2*(f52(told(i))*(vnew(i)-vnew(i-1))/h*dmf(vnew(i))
     ,        -f52(told(i+1))*(vnew(i+1)-vnew(i))/h*dmf(-vnew(i))
     ,        -f52(told(i-1))*(vnew(i-1)-vnew(i-2))/h*dmf(vnew(i-1))
     ,        +f52(told(i))*(vnew(i)-vnew(i-1))/h*dmf(-vnew(i-1))))
     ,      +(0.5*(1.-delta)*pln(coor)*(3*told(i)
     ,      +vx**2)/tauion(nx,tx))*h*tau
8     continue
c-----------------------------------------------------
c  last  volume:
      tx = told(nxi1)
      nx = nnew(nxi1)
      vx = (vnew(nxi2)+vnew(nxi1))/2.
      coor = h*(nxi1-0.5)
      c(nxi1) = 0.
      b(nxi1) = -(1.5 *nnew(nxi1)*h + tau*(2.5*nnew(nxi1)
```

```
     ,       *dmf(-vnew(nxi2))
     ,      + a3*k(nxi2)/h
     ,      + nnew(nxi1)*h*(1.5/taus+0.5/taurad(coor,nx,tx)
     ,      +1.5*delta/taucx(coor,tx)+0.5/tauexc(coor,tx)
     ,      +vx**2/2./told(nxi1)*(1./taus+delta/taucx(coor,tx))
     ,      +0.5*pln(coor)*poti/told(nxi1)/tauion(nx,tx))))
      a(nxi1) = -tau*(2.5*nnew(nxi2)*dmf(vnew(nxi2)) + a3*k(nxi2)/h)
      d(nxi1) = (1.5*nold(nxi1)*told(nxi1)
     ,   -nnew(nxi1)*(vnew(nxi1)+vnew(nxi2))**2/8.
     ,   +nold(nxi1)*(vold(nxi1)+vold(nxi2))**2/8.)*h
     ,   +tau*(-qeiz
     ,   +nnew(nxi2)*(vnew(nxi2)+vnew(nxi3))**2/8.*dmf(vnew(nxi2))
     ,   -nnew(nxi1)*(vnew(nxi1)+vnew(nxi2))**2/8.*dmf(-vnew(nxi2)))
      d(nxi1)=d(nxi1)+tau*(
     ,   -a2/h*(f52(told(nxi2))*(vnew(nxi2)-vnew(nxi3))
     ,   *dmf(vnew(nxi2))
     ,   -f52(told(nxi1))*(vnew(nxi1)-vnew(nxi2))*dmf(-vnew(nxi2))))
     ,   +(0.5*(1.-delta)*pln(coor)*(3*told(nxi1)
     ,   +vx**2)/tauion(nx,tx))*h*tau
c-------------------------------------------------
c
      call tdmad(nxi1,a,b,c,d,tnew,xi,eta)
c=================================================
114   continue
      do 10 i=1,nxi1
      nold(i)=nnew(i)
      vold(i)=vnew(i)
c
```

```
c
c
      told(i)=tnew(i)

10    continue

      if( (icount/nout)*nout - icount .eq. 0 )

     ,      write(*,*)icount,sngl(tnew(nxi1)),sngl(nnew(na))

c-----------------------------------------------------

      if(icount .lt. nend)go to 1000

      open(2,file = 'output/result.dat')

      write(2,*)'     aKn=   ,','     nnew=   ,', '     vnew =   ,',
     ,   '     tnew ='

      do 9 i=1,nxi1

      write(2,*)float(i-1)/float(nxi2),sngl(nnew(i))

     ,      ,sngl(vnew(i)),sngl(tnew(i))

9     continue

      close(2)

c=========================================================

c integral balances:

      open(3,file='output/balance.dat')

c-----------------------------------------------------

c particles flow through the separatrix

      sepj =   h/taup*na

c heat flow through the separatrix

      sepq = h/taue*1.5*na

c-----------------------------------------------------

c particles flow to the wall

      sumn = 0.

      do 14 i=1,nxi1
```

```
14    sumn = sumn + nnew(i)
      wallj =  h*sumn/taus
c heat flow to the wall
      sumq = 0.
      do 15 i=1,nxi1
15    sumq = sumq + nnew(i)*tnew(i)*1.5 + nnew(i)
     ,*(vnew(i) + vnew(i-1))**2/8.
      wallq = h/taus*sumq
c momentum flow to the wall and separatrix
      sump = 0.
      do 16 i=1,nxi2
16    sump = sump + vnew(i)*(nnew(i)+nnew(i+1))/2.
      pws = h/taus*sump
c-------------------------------------------------------
c neutral source/sink:
c particles
      sumn = 0.
      do 12 i=1,nxi1
12    sumn = sumn + pln(h*(i-0.5))/tauion(nnew(i),tnew(i))
     ,  - nnew(i)/taurec(nnew(i),tnew(i))
      sneuj =  h*sumn
c momentum
      sumnlp = 0.
      do 17 i=1,nxi2
      tx = (tnew(i)+tnew(i+1))/2.
      nx = (nnew(i)+nnew(i+1))/2.
```

```
      coor=h*i
      pnl(i)= nx*vnew(i)*
     ,        (delta/taucx(coor,tx)+1./taurec(nx,tx))*h
     ,       - (1-delta)*pln(coor)*vnew(i)/tauion(nx,tx)*h
      sumnlp = sumnlp + pnl(i)
17    continue
      if( isbou .ne. 1) then
      tx = tnew(nxi1)
      nx = nnew(nxi1)
      coor=h*nxi1
      sumnlp=sumnlp
     ,     + 0.5*nnew(nxi1)*vnew(nxi1)*
     ,        (delta/taucx(coor,tx)+1./taurec(nx,tx))*h
     ,        -(1-delta)*pln(coor)*vnew(nxi1)/tauion(nx,tx)*h*0.5
      endif
c heat
      sumnlq=0.0
      do 18 i=1,nxi1
      tx = told(i)
      nx = nnew(i)
      vx = (vnew(i-1)+vnew(i))/2.
      coor = h*(i-0.5)
      qnl(i)=  nnew(i)*tnew(i)*h*(0.5/taurad(coor,nx,tx)
     ,      +1.5*delta/taucx(coor,tx)+0.5/tauexc(coor,tx)
     ,      +vx**2/told(i)*delta/taucx(coor,tx)/2.
     ,      +0.5*pln(coor)*poti/told(i)/tauion(nx,tx))
```

```
     ,       -0.5*(1.-delta)*pln(coor)*(3*told(i)
     ,       +vx**2)/tauion(nx,tx)*h
          sumnlq = sumnlq + qnl(i)
18    continue
c-----------------------------------------------------
          vv =  vnew(1)/2.
           v = vnew(1)
          if(vv .gt. 0.d0) v = 0.d0
          pfirst = nnew(1)*tnew(1) - a1*f52(tnew(1))*vnew(1)/h
     ,   + nnew(1)*vv*v
          if( isbou .ne. 1) then
             pws = pws + 0.5*h/taus*nnew(nxi1)*vnew(nxi1)
            plast = pixx/2.
          else
            vv = (vnew(nxi1) + vnew(nxi2))/2.
            v = vnew(nxi2)
            if(vv .lt. 0.d0) v = vnew(nxi1)
            plast = nnew(nxi1)*vv*v
     ,           + nnew(nxi1)*tnew(nxi1)
     ,           - a1*f52(tnew(nxi1))*(vnew(nxi1) - vnew(nxi2))/h
          endif
c-----------------------------------------------------
c common balances:
          baln = (sepj + sneuj - wallj - nnew(nxi1)*dmf(vnew(nxi1)))
     ,       /sepj*100
          balp = (pfirst - pws - sumnlp - plast)
```

```
     ,       /nnew(1)/tnew(1)*100
      balq = (sepq - wallq - sumnlq - qeiz)
     ,      /sepq*100
c-----------------------------------------------------
      dmp =  sq*trl/al/slal*dens*vs
      write(3,*)'j separatrix = ',sngl(sepj*dmp)
      write(3,*)'j neutrals = ',sngl(sneuj*dmp)
      write(3,*)'j wall = ',sngl(wallj*dmp)
      write(3,*)'j plate= ',sngl(nnew(nxi1)*dmf(vnew(nxi1))*dmp)
      write(3,*)' '
      write(3,*)'p separatrix & wall = ',sngl(pws)
      write(3,*)'p neutrals = ',sngl(sumnlp)
      write(3,*)'p plate = ',sngl(plast)
      write(3,*)'p midplane = ',sngl(pfirst)
      write(3,*)' '
      dm=2*sq*trl/al/slal*dens*ts*vs/6.25d24
      write(3,*)'q separatrix = ',sngl(dm*sepq)
      write(3,*)'q neutrals = ',sngl(sumnlq*dm)
      write(3,*)'q wall = ',sngl(wallq*dm)
      write(3,*)'q plate = ',sngl(qeiz*dm)
      write(3,*)' '
      write(3,*)'common disbalances, %:'
      write(3,*)baln,balp,balq
c     write(3,*)'neutral losses, p & q:'
c     do 19 i=1,nxi
c     write(3,*)i,'   ',pnl(i),'   ',qnl(i)
```

```
c19    continue
       close(3)
c=====================================================
       stop
       end
c=====================================================
       real*8 function tauion(den,te)
       implicit real*8(a-h),real*8(o-z)
       common/param/ dens,ts,denneu,aln,tau0,cz0
       t = te*ts
       d = den*dens
       x = dlog10(t)
       if(t.le.20.)then
          svl= -3.054*x - 15.72*dexp(-x) + 1.603*dexp(-x**2)
       else
          svl= -.5151*x -2.563/x - 5.231
       endif
       sv = (1.d1)**svl
       tauion = 1.d0/(d*sv)/tau0
c      tauion = 1.d40
       return
       end
c=====================================================
       real*8 function taucx(x,te)
       implicit real*8(a-h),real*8(o-z)
       common/param/ dens,ts,denneu,aln,tau0,cz0
```

```
      tt = te*ts
      den0 = pln(x)*denneu*dens
      if(tt.gt.0.d0 .and. den0.gt.0.d0) then
         scx = 7.8d-9*dsqrt(tt)*(1.d0 - .16*dlog10(tt))**2
         taucx = 1.d0/scx/den0/tau0
      else
         taucx = 1.d40
      endif
      return
      end
c=====================================================
      real*8 function tauexc(x,te)
      implicit real*8(a-h),real*8(o-z)
      common/param/ dens,ts,denneu,aln,tau0,cz0
      tt = te*ts
      den0 = pln(x)*denneu*dens
      if(tt.gt.0.d0 .and. den0.gt.0.d0) then
         y = 10.2/tt
         exc = 49.d-8/(.28 + y)*dexp(-y)*dsqrt(y*(1. + y))
         tauexc = 1.d0/exc/den0/tau0*tt
      else
         tauexc = 1.d40
      endif
      return
      end
c=====================================================
```

```
      real*8 function taurec(d,te)
      implicit real*8(a-h),real*8(o-z)
      common/param/ dens,ts,denneu,aln,tau0,cz0
      den = d*dens
      tt = te*ts
c     recr = den*2.7d-13/dsqrt(tt)
c     rec3 = den**2*8.75d-27/tt**4/dsqrt(tt)
c     taurec = 1.d0/(recr + rec3)/tau0
      taurec = 1.d80
      return
      end
c=======================================================
      real*8 function taurad(x,dd,tt)
      implicit real*8(a-h),real*8(o-z)
      common/param/ dens,ts,denneu,aln,tau0,cz0
      if(tt .le. 0.d0 .or. cz(x). le.0.d0) then
         taurad = 1.d40
      else
         t = tt*ts
         taurad = 1.d0/(cz(x)*dd*flin(t)/tt*dens*tau0/ts)
      endif
      return
      end
C=======================================================
      real*8 function cz(x)
      parameter(nt=501)
```

```
      implicit real*8(a-h),real*8(o-z)
      real*8 te(nt),rad(nt)
      common/param/ dens,ts,denneu,aln,tau0,cz0
      common/post/te,rad,hlg,tlg1,ifile
      cz = cz0
      return
      end
C=======================================================
      real*8 function flin(x)
      parameter(nt=501)
      implicit real*8(a-h),real*8(o-z)
      real*8 te(nt),rad(nt)
      common/param/ dens,ts,denneu,aln,tau0,cz0
      common/post/te,rad,hlg,tlg1,ifile
      data af/7.54d-7/,bf/4.83d-1/,cf/5.65d-2/,ef/5.48d0/
C
      if( ifile .eq.  1 ) then
C-------------------------------------------------
c
         if( x .le. 0.d0) then
           flin = 0.d0
           return
         endif
c
         if( x .ge. te(nt) ) then
           flin = rad(nt)
```

```
            return
          endif
c
          if( x .le. te(1) ) then
            a = rad(1)/te(1)
            flin = a*x
            return
          else
            i = int( (dlog(x) - tlg1)/hlg ) + 1
            a = (rad(i+1) - rad(i))/(te(i+1) - te(i))
            b = rad(i) - a*te(i)
            flin = a*x + b
            return
          endif
C-------------------------------------------------
      else
C-------------------------------------------------
          flin = af*dsqrt(x)*dexp( -ef/x )/
     ,           ( 1.d0 + bf*dsqrt(x) + cf*x )
          return
C-------------------------------------------------
      endif
      end
C=======================================================
      real*8 function pln(x)
      implicit real*8(a-h),real*8(o-z)
```

```
      common/param/ dens,ts,denneu,aln,tau0,cz0
        pln = dexp( (x-1.)/aln)*denneu
c     pln=denneu
c     pln = 0.d0
      return
      end
c=======================================================
      subroutine tdmad(n,a,b,c,d,y,xi,eta)
      real*8 a(n+1),b(n+1),c(n+1),d(n+1),y(n+1),xi(n+1),eta(n+1),ccc
      xi(1) = 0.0
      eta(1) = 0.0
      do 1 i=1,n
        ccc =  b(i) - a(i)*xi(i)
        xi(i+1) = c(i)/ccc
        eta(i+1) = ( a(i)*eta(i) - d(i) )/ ccc
1     continue
      y(n) = eta(n+1)
      do 2 i=n-1,1,-1
        ip1 = i+1
        y(i) = xi(ip1)*y(ip1) + eta(ip1)
2     continue
      return
      end
c=======================================================
      function erfd(x)
      implicit real*8(a-h),real*8(o-z)
```

```
c
c  version : 18.11.88
c
c=======================================================
      parameter  ( a1 = 0.07052 30784, a2 = 0.04228 20123,
     ,             a3 = 0.00927 05272, a4 = 0.00015 10143,
     ,             a5 = 0.00027 65672, a6 = 0.00004 30638 )
c=======================================================
c
      f(t) = 1./((1.+t*(a1+t*(a2+t*(a3+t*(a4+t*(a5+t*a6))))))**4)**4
c
      w = 1. - f(dabs(x))
      erfd = sign(w,x)
      return
c=======================================================
      entry erfcd
c=======================================================
      w = 1.- f(dabs(x))
      erfd = 1. - sign(w,x)
c=======================================================
      end
C  VERSION : 15.10.93 15:40
C
C Version for orthogonal mesh,
C pure plasma, zero net current
C-----------------------------------------------------
```

```
C  INPUT VALUES (all in the last mesh interval):
C
C  DEN - plasma density
C  VEL - plasma velocity
C  TE - electron temperature
C  TI - ion temperature
C  AME - electron mass
C  AMI - ion mass
C  ---------------- all in units used in the main program
C-------------------------------------------------------
C OUTPUT VALUES (fluxes trough the last mesh bound):
C
C PIXX - momentum flux (summarized electrons & ions)
C QEX - total heat flux in the electron component
C QIX - total heat flux in the ion component
C  ---------------- all in units used in the main program
C
C=======================================================
      SUBROUTINE BOUND(DEN,VEL,TE,TI,AME,AMI,PIXX,QEX,QIX)
      IMPLICIT REAL*8(A-H),REAL*8(O-Z)
      COMMON/FPS/CPSI
      COMMON/FSH/CSVTI
      EXTERNAL FPSID,FSHIFT
      DATA SP,GAMMA,TOL/1.7724539D0,1.6666667D0,1.D-5/
C
      CSVTI = DSQRT((GAMMA*TI + TE)/2./TI)
```

```
      IF(VEL.LE.0.) VEL = 0.
      XMACH = VEL/DSQRT(2.*TI/AMI)
C-----------------------------------------------------
C Potential drop
C
C Presheath:
      IF(XMACH.GE.CSVTI) THEN
         PSIPS = 0.
      ELSE
         PSIPS = -TI/TE*(XMACH**2 - CSVTI**2)
      ENDIF
C Sheath:
      A = 0.
      B = 5.
      CPSI = DLOG(DSQRT(TE*AMI/(TI*AME))/SP/CSVTI)
      PSID = ZEROIN(A,B,FPSID,TOL)
      IF(DABS(FPSID(PSID)).GT.1.E-4)
     ,WRITE(*,*)'WARNING! IN PSI,  PSID =',PSID
C
      PSIT = PSID + PSIPS
C Shift velocity:
C
      IF(XMACH.GE.CSVTI) THEN
         VSHIFT = XMACH
      ELSE
         A = 0.
```

```
          B = 3.
          VSHIFT = ZEROIN(A,B,FSHIFT,TOL)
          IF(DABS(FSHIFT(VSHIFT)).GT.1.E-4)
     ,   WRITE(*,*)'WARNING! IN VSHIFT, VSHIFT =',VSHIFT
      ENDIF
C-----------------------------------------------------
C  Boundary fluxes:
C
      EVSH = ERFD(VSHIFT)
      ESPSI = ERFD(DSQRT(PSIT))
      GVSH = G(VSHIFT)
C
      FE = 2.+ PSIT
      FI = 2.+ XMACH*(XMACH + 0.5/CSVTI) - TE/TI*PSIPS
      FPI = 2.*SP*XMACH/GVSH*( VSHIFT/SP*DEXP(-VSHIFT**2)
     ,     + (VSHIFT**2 + 0.5)*(1.+ EVSH) )
      FPE = 2.*SP*XMACH/GVSH*(1.+ EVSH)/(1.+ ESPSI)
     ,     *( (1.+ESPSI)/2.- DSQRT(PSIT)/SP*DEXP(-PSIT) )
c     write(*,*)'fpe= ',fpe,' fpi = ',fpi
      QEX = FE*DEN*VEL*TE
      QIX = FI*DEN*VEL*TI
      PIXX = FPI*DEN*TI + FPE*DEN*TE
C
      RETURN
      END
C=======================================================
      FUNCTION FPSID(X)
```

```
      IMPLICIT REAL*8(A-H),REAL*8(O-Z)
      COMMON/FPS/CPSI
      FPSID = X - CPSI - DLOG(1.+ ERFD(DSQRT(X)))
      RETURN
      END
C=====================================================
      FUNCTION FSHIFT(X)
      IMPLICIT REAL*8(A-H),REAL*8(O-Z)
      COMMON/FSH/CSVTI
      DATA SP/1.7724539D0/
      FSHIFT = CSVTI - G(X)/SP/(1.+ ERFD(X))
      RETURN
      END
C=====================================================
      FUNCTION G(X)
      IMPLICIT REAL*8(A-H),REAL*8(O-Z)
      DATA SP/1.7724539D0/
      G = DEXP(-X**2) + X*SP*(1.+ ERFD(X))
      RETURN
      END
C=====================================================
       REAL*8 FUNCTION ZEROIN(AX,BX,F,TOL)
       IMPLICIT REAL*8(A-H),REAL*8(O-Z)
       REAL*8 AX,BX,TOL
       REAL*8 A,B,C,D,E,EPS,FA,FB,FC,TOL1,XM,P,Q,R,S
       EPS=1.0D0
10     EPS=EPS/2.0
```

```
      TOL1=1.0+EPS
      IF(TOL1.GT.1.0) GO TO 10
      A=AX
      B=BX
      FA=F(A)
      FB=F(B)
20    C=A
      FC=FA
      D=B-A
      E=D
30    IF(DABS(FC).GE.DABS(FB)) GO TO 40
      A=B
      B=C
      C=A
      FA=FB
      FB=FC
      FC=FA
40    TOL1=2.0*EPS*DABS(B)+0.5*TOL
      XM=0.5*(C-B)
      IF(DABS(XM).LE.TOL1) GO TO 90
      IF(FB.EQ.0.0) GO TO 90
      IF(DABS(E).LT.TOL1) GO TO 70
      IF(DABS(FA).LE.DABS(FB)) GO TO 70
      IF(A.NE.C) GO TO 50
      S=FB/FA
      P=2.0*XM*S
```

```
      Q=1.0-S
      GO TO 60
50    Q=FA/FC
      R=FB/FC
      S=FB/FA
      P=S*(2.0*XM*Q*(Q-R)-(B-A)*(R-1.0))
      Q=(Q-1.0)*(R-1.0)*(S-1.0)
60    IF(P.GT.0.0) Q=-Q
      P=DABS(P)
      IF((2.0*P).GE.(3.0*XM*Q-DABS(TOL1*Q))) GO TO 70
      IF(P.GE.DABS(0.5*E*Q)) GO TO 70
      E=D
      D=P/Q
      GO TO 80
70    D=XM
      E=D
80    A=B
      FA=FB
      IF(DABS(D).GT.TOL1) B=B+D
      IF(DABS(D).LE.TOL1) B=B+DSIGN(TOL1,XM)
      FB=F(B)
      IF((FB*(FC/DABS(FC))).GT.0.0) GO TO 20
      GO TO 30
90    ZEROIN=B
      RETURN
      END
```

ISSN 1869-9669